IOWA STATE UNIVERSITY
Digital Repository

Graduate Theses and Dissertations

Iowa State University Capstones, Theses and Dissertations

2014

Two integral girder connections for precast concrete bridges in seismic regions utilizing extended prestressing strands

Robert Peggar
Iowa State University

Follow this and additional works at: https://lib.dr.iastate.edu/etd

 Part of the Civil Engineering Commons

Recommended Citation
Peggar, Robert, "Two integral girder connections for precast concrete bridges in seismic regions utilizing extended prestressing strands" (2014). *Graduate Theses and Dissertations*. 14233.
https://lib.dr.iastate.edu/etd/14233

This Thesis is brought to you for free and open access by the Iowa State University Capstones, Theses and Dissertations at Iowa State University Digital Repository. It has been accepted for inclusion in Graduate Theses and Dissertations by an authorized administrator of Iowa State University Digital Repository. For more information, please contact digirep@iastate.edu.

www.manaraa.com

Two integral girder connections for precast concrete bridges in seismic regions utilizing extended prestressing strands

by

Robert Peggar

A thesis submitted to the graduate faculty

in partial fulfillment of the requirements for the degree of

MASTER OF SCIENCE

Major: Civil, Construction and Environmental Engineering (Structural Engineering)

Program of Study Committee:
Sri Sritharan, Major Professor
Jon Matthew Rouse
David Jeong

Iowa State University

Ames, Iowa

2014

www.manaraa.com

TABLE OF CONTENTS

www.manaraa.com

www.manaraa.com

www.manaraa.com

LIST OF FIGURES

www.manaraa.com

www.manaraa.com

www.manaraa.com

www.manaraa.com

www.manaraa.com

LIST OF TABLES

www.manaraa.com

ACKNOWLEDGEMENTS

I would like to thank my committee chair, Dr. Sritharan, and my committee members, Dr. Rouse, and Dr. Jeong, for their guidance and support throughout the course of this research. I would also like to thank Justin Vandewerff and Zhao Cheng for their work on this project along with Doug Wood and Owen Steffens.

In addition, I would also like to thank the department faculty and staff for making my time at Iowa State University worthwhile and productive. I want to also offer my appreciation to my family for their encouragement and to my wife Elyse for her support throughout this process.

www.manaraa.com

ABSTRACT

Accelerated Bridge Construction (ABC) utilizing precast components continues to be used as an effective tool for bridge construction due to time and cost saving techniques as well as the reduction of environmental impacts. However, in seismic regions, the use of precast members and ABC methods are limited due to concerns about poor performance of connections primarily between cap beam and girders. With sponsorship from the California Department of Transportation (Caltrans), two alternative connections between precast bulb tee girders and bridge cap were designed utilizing extended girder prestressed strands. The connections were designed to resist positive moments at the girder to cap connection. Positive moments occur at the connection when seismic forces cause upward deflection of the precast girders resulting in tension forces along the bottom of the girder to cap connection. The tension forces cause damage to the connection and can also unseat or disconnect the girders from the cap beam resulting in span collapse. The two connections were designed to minimized connection damage and prevent unseating of the girders. In one connection the extended strands were curved and relied on bond strength for anchorage along the 60 in. embedment length. The other connection consisted of spliced strands with anchor plates and chucks which relied on the transfer of forces through strand splices. Both connections also included three grouted dowel bars placed through the girder web. The connections were designed to provide adequate seismic moment resistance up to a combined load of gravity, horizontal ground acceleration corresponding to the column overstrength moment, as well as shear and moment values up to 0.5g vertical acceleration. A 40% scale test unit was constructed in the Iowa State University structures laboratory and the two connections were tested. An analytical model was formulated to analytically quantify the behavior of each connection. The results of the tests showed that both connections had adequate capacity to resist horizontal and vertical ground acceleration forces as specified in current Caltrans seismic design criteria. Adjustments were made to the analytical model based on results of the test to improve the accuracy of the model. The overall results of

www.manaraa.com

the test demonstrate that ABC methods can be safely implemented in high seismic regions and be relied upon for dependable performance.

www.manaraa.com

CHAPTER 1 - INTRODUCTION

1.1 General

The design and repair of bridges across the United States is a continual process. Currently, one in nine bridges in the U.S. is rated as structurally deficient by the American Society of Civil Engineers (ASCE). Many of the bridges within in the U.S. will need to receive significant repairs or be replaced in the next ten years (ASCE, 2014). A large number of these bridges are highway bridges which represent a vital part of the transportation and economic systems. Current onsite construction practices are not able to accommodate the rate at which bridges must be repaired or replaced. New construction practices and techniques must be implemented to ensure the reliability and durability of the nation's infrastructure.

1.2 Accelerated Bridge Construction

In an effort to improve the efficiency of building bridges, accelerated bridge construction (ABC) practices have been developed and deployed across the U.S. ABC uses prefabricated bridge members that are manufactured offsite in a controlled environment and then shipped to the construction site and assembled (Culmo, 2011). This reduces onsite construction time, avoids long traffic detours, and minimizes environmental impacts. The goal of ABC construction is to close the gap between the number of new bridges needed and the number of bridges actually being built.

Prefabricated members used in ABC systems can be made of concrete or steel and the size of the members varies according the design of the project. One option that is widely implemented is the use of precast concrete beams combined with a precast or cast-in-place deck as shown in Figure 1.1. A benefit of this design is that only a small amount of concrete to connect the beams is poured at the construction site. Concrete is a versatile material that can be conformed to meet the constraints of multiple projects, and precast plants are usually located in close proximity to major cities to allow for easy transportation to the work site. For the construction of highway bridges, precast concrete is a viable solution. Challenges have occurred when using precast concrete bridges in

www.manaraa.com

certain areas, however, especially in seismic regions such as the state of California where earthquakes are common.

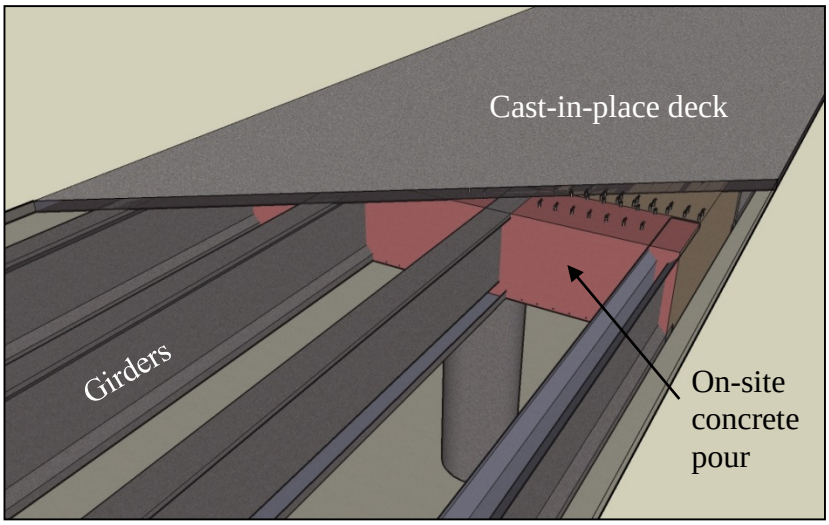

Figure 1.1: Concrete precast bridge members (Snyder, 2010)

1.3 ABC in California

The state of California has a long history of earthquakes and seismic activity. In the past 25 years, California has experienced two major earthquakes: the Northridge earthquake of 1994 and the Loma Prieta earthquake of 1989. Both caused significant structural damage to bridges as shown in Figure 1.2 and 1.3, billions of dollars in economic loss, and resulted in a combined 120 fatalities (USGS 2010). Seismic damage to bridges causes loss of life, endangers public safety, and also causes many economic issues. Damaged bridges must be repaired or replaced and traffic must be rerouted which challenges the traffic capacity of alternate roadways. California has recognized the benefits that ABC provides to recover quickly from earthquakes and also to replace deteriorating bridges to prevent future seismic damage. However, due to the requirements of design for bridges in seismic regions, the benefits of ABC are not able to be fully realized.

www.manaraa.com

Figure 1.2: Bridge collapse during Northridge earthquake (USGS, 2010)

Figure 1.3: Damage to Cypress Street Viaduct in Oakland California (USGS, 1999)

The California Department of Transportation (Caltrans) has developed guidelines known as the Seismic Design Criteria (SDC) to ensure that bridges can adequately resist seismic forces (Caltrans, 2010). The requirements outlined in Caltrans SDC are specifically determined for what is defined as an "Ordinary Bridge" built either by traditional onsite construction techniques or ABC. A specific definition of an Ordinary Bridge can be found in Caltrans SDC, but for the purposes of this thesis it will be assumed that the concepts and designs discussed fall within the proper criteria and

www.manaraa.com

therefore must meet SDC requirements. In order to better understand the SDC and how the requirements relate to ABC methods, a brief overview of seismic design philosophy for bridges is needed.

1.3.1 Seismic Design Philosophy

The design philosophy with which many of the existing California bridges were built was based on ensuring an entirely elastic structural response to seismic forces. However, performance of bridges during earthquakes as well as experimental research has shown that seismic forces were often underestimated resulting in a high damage rate (Priestley, 1996). In many cases, elastic design utilizing correct seismic forces would have resulted in a bridge that was not economical to build. For this reason, others design philosophies were developed including one known as capacity design. Capacity design allows for a region of flexural inelastic response (also known as a plastic hinge) within a structural member at predetermined locations and prevents plastic hinges from forming in other locations by use of an appropriate strength margin (Priestley, 1996).

1.3.1.1 Plastic Hinges

The development of plastic hinges as an inelastic response mechanism enables the structure to dissipate energy caused by the ground motion of an earthquake. In the capacity design of bridges, plastic hinges are usually developed at the bottom and /or top of bridge columns to allow for easy inspection and repair of the structure after an earthquake. Plastic hinges can be developed in the superstructure of a bridge as well. The superstructure usually consists of the bridge girders and deck with a bent cap connecting the girders to the columns as shown in Figure 1.4. However, developing hinges in the superstructure is often discouraged due to the difficulty of assessing damage and making repairs.

www.manaraa.com

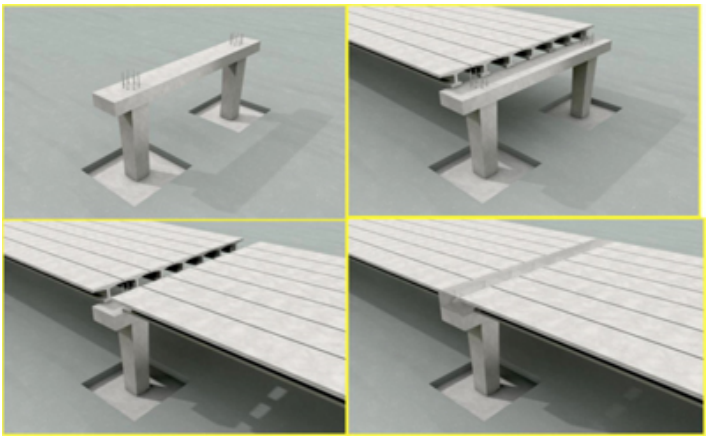

Figure 1.4: Typical superstructure construction (Federal Highway Administration, 2013)

1.3.1.2 Superstructure Classification

A superstructure can be classified according to its ability to transfer moments. If the connection between the girders and cap beam is able to resist an applied moment it is known as a fixed connection or integral superstructure. If the connection has no moment resistance it is referred to as a pinned connection or non-integral superstructure. A benefit of an integral superstructure in seismic design is that the moment resistance provided by the fixed connection allows for an additional plastic hinge to form at the top of the bridge column. The second plastic hinge facilitates additional energy dissipation which allows a designer to use a smaller column cross-section as well as a smaller footing; it is also possible to have a plastic hinge develop at the top of the column and have a pinned base resulting in reduced foundations costs (Priestley, 1996). These benefits can make the structure more economical but is not possible with a non-integral superstructure.

1.3.1.3 Positive and Negative Moments

At an integral girder to cap connection, both positive and negative moments are generated in the superstructure. Negative moments are caused by dead and live loads, result in downward deflection of the bridge girders, and are increased by seismic ground motion. Positive moments are caused by earthquake ground motion, live loads, and volumetric changes in the concrete and result in upward deflection of a bridge girder. Negative moments at precast connections have been traditionally resisted by reinforcement placed in the bridge deck which runs continuously over the girder to cap

www.manaraa.com

connection. Designing for positive moment resistance is more difficult due to a lack of continuity over the bottom region of the girder to cap connection. Cast-in-place bridges are able to provide positive moment resistance by placing standard mild steel reinforcement at the bottom of the cap to girder interface during construction. However, ABC construction does not readily provide this opportunity since the beams are precast.

1.3.2 SDC Requirements

The SDC requirements established by Caltrans state that for precast girders the superstructure should be considered pinned or non-integral based on the assumption that under seismic activity adequate positive moment capacity cannot be developed (Caltrans, 2010). This means that by following the SDC guidelines the column of a bridge built with precast girders can only develop a single plastic hinge at its base and designers cannot take advantage of the smaller members and economy provided by an integral superstructure.

Another issue addressed by SDC is vertical acceleration. Positive and negative moments generated in a bridge superstructure by seismic ground motion are caused by two components: horizontal and vertical ground acceleration. SDC guidelines require that all bridges account for horizontal ground acceleration. It also requires vertical acceleration to be accounted for if the site where the bridge is to be built has a peak rock acceleration of 0.6g or greater. Vertical acceleration is measured as a percentage of gravity. For example, a vertical acceleration noted as 0.25g means that the bridge experiences an additional 25% of the load due to gravity or a 125% gravity load. If vertical acceleration must be accounted for per SDC, then longitudinal side reinforcement in the girders must be added and be capable of resisting 125% of the dead load shear, by means of shear friction, at the girder to cap connection. SDC also requires that the added side reinforcement extend continuously beyond the face of the cap by 2.5 times the depth of the superstructure. The added requirements for vertical acceleration are difficult to include in precast members and also make the connection region very congested and costly. The added reinforcement is easier to install with traditional cast-in-place construction than with ABC methods.

www.manaraa.com

When current SDC guidelines are considered, ABC methods become less advantageous. First, the pinned superstructure requires larger members and prevents the designer from utilizing cost savings available from an integral superstructure. Secondly, if vertical acceleration is considered the extra longitudinal steel becomes harder to place than in traditional cast-in-place construction. These two requirements prevent the state of California from fully exercising the benefits of ABC methods and make traditional cast-in-place construction more economical despite savings in the time of construction for ABC methods. In order to fully utilize the benefits of ABC, adequate positive moment resistance and sufficient shear capacity to resist vertical acceleration must be developed for precast members in seismic regions.

1.4 Precast Positive Moment Connections

Different solutions have been tested to adequately resist positive moments at the girder to cap connection for precast members. These solutions include extending mild steel reinforcement from the end of a precast girder (Figure 1.5), extending the prestressed strands in a girder (Figure 1.5), placing ducts through the girder and cap and then grouting unstressed prestressing strands inside the ducts, and also using dowel bars which are placed through the web of the girder and embedded in the cap beam (Figure 1.5).

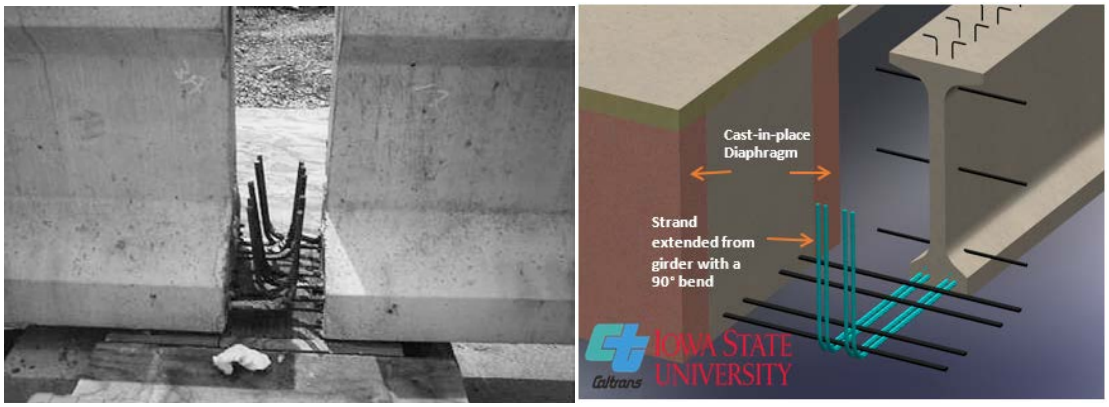

Figure 1.5: Extended mild steel reinforcing bars (left) (NCHRP, 2004); extended strands and dowel bars placed through the girder web (right)

Extending mild steel reinforcement from precast girders is not favorable for precast plants. Special formwork must be made and protruding rebar makes moving and

www.manaraa.com

storing the member more challenging. Extended strands are a viable option to form this connection and do not require any changes to standard formwork. For normal precast girders, strands are typically cut at the girder face after the concrete has cured but it is fairly simple to leave a length of strand extending from the girder. However, the protruding strands can cause the movement and storage of the girder to be more cumbersome. Installing ducts in the girders and strands is another good option as strands can be placed inside the ducts and grouted into place. However, there must be room for the ducts to be placed in the girders and the grout must be pumped through the ducts for an extended length. It is possible for the grout to leave gaps or voids along the strand when a long pumping length is required. The placement of dowel bars through the web of the girder are fairly easy to install. Pipe inserts are placed through the girder web before casting and the dowel bars are then inserted through the pipes and grouted in place. The only drawback from this option is that no steel is extending longitudinally from the bottom of the girder into the cap beam. However, the location of the dowel bars allows them to be combined with any of the other methods discussed for resisting positive moment.

1.5 Scope of Research

The scope of the following research, with sponsorship provided by Caltrans, was to develop ABC girder to bent cap connections that create an integral superstructure by resisting positive moments at the girder to cap connections. Positive moments are caused by horizontal and vertical acceleration ground motion. Development of fixed superstructure connections for ABC precast girders will allow implementation of smaller column and/or footing members just as for traditional cast-in-place construction. The two connection details presented use prestressing strands extended from the girders and anchored in the bent cap along with dowel bars to provide positive moment resistance. Extended strands were chosen for ease of construction because they do not require changes in formwork or the addition of ducts at the precast plant. To provide further advantage in using ABC precast members, the target value for vertical acceleration was selected to be 0.5g which well exceeds current Caltrans SDC requirements and provides

www.manaraa.com

an alternative solution to adding longitudinal girder side reinforcement for resisting vertical acceleration. Successful design and testing of the connections would enable the benefits of ABC to be fully utilized in areas that experience high seismic forces.

A prototype bridge was developed using the current Caltrans bridge design approach using California bulb-tee girders with a cast-in-place bent cap. Negative moment resistance was provided by a cast-in-place deck while positive moment resistance was provided by the combination of extended strands and dowel action. After development of the prototype, a 40% test unit was designed and tested at the Iowa State University (ISU) structures laboratory. Analysis of the girder to cap connection was also conducted prior to testing to adequately predict the behavior of the connection region and highlight any potential problems that might be encountered during testing.

As a part of testing, the connections were loaded to target shear and moment values in order to fully quantify the capacity of each design. Upon completion of the test, conclusions and recommendations were formulated to assist Caltrans in analyzing and implementing the connections details. Adjustments were also made to the analysis process for predicting the connection behavior in order to benefit future analytical work.

1.6 Thesis Layout

A literature review of past research regarding positive moment resistance by use of extended strands for both seismic and non-seismic applications is provided in Chapter 2. Chapter 3 provides details regarding the prototype as well as the design, construction, and instrumentation of the test unit. Chapter 3 also provides the test unit loading protocol and details regarding the analysis conducted to predict connection behavior. Testing and performance of each connection is included in Chapter 4 along with comparisons to the predicted connection behavior. Finally, Chapter 5 provides conclusions drawn from the project and recommendations both for implementation in the field as well as further testing.

www.manaraa.com

CHAPTER 2 - LITERATURE REVIEW

2.1 Introduction

To better evaluate the use of extended strands to form a positive moment girder to cap connection, a review of literature on the subject was performed. Current design practices are discussed first, followed by research regarding both seismic positive moment resistance of precast girders and extended strand moment resistance. It was found that limited amount of research has been conducted in relation to the use of extended strands to resist seismic forces. Much of the previous research conducted focused on resisting positive moments with other mechanisms or solely focused on the use of extended strands to resist forces due to creep, shrinkage, and temperature differentials but not seismic loading. Details of each topic will be discussed in the following sections.

2.2 Current Design Practice

2.2.1 California Department of Transportation

The California Department of Transportation (Caltrans) follows the SDC guidelines (Caltrans, 2010) described earlier, as well as Caltrans Bridge Design Aids (BDA) (Caltans, 2012) when designing precast concrete girder bridges with positive moment connections. In the current Caltrans design, the girder to cap connection is treated as pinned and dowel bars are placed transversely through the web of the girder as shown in Figure 2.1. This provides some positive moment resistance but no other positive moment mechanisms are currently specified in Caltrans SDC. The lack of positive moment design details is a result of treating the precast girder connections as pinned and also likely due to the limited amount of research and testing regarding specific positive moment mechanisms such as extended strands and reinforcing bars.

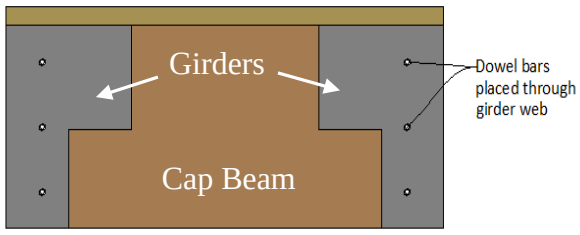

Figure 2.1: Current Caltrans connection detail

www.manaraa.com

2.2.2 Washington State Department of Transportation

The Washington State Department of Transportation (WSDOT) is currently designing bridges using extended strands to form positive moment connections. These connections are designed for use at intermediate piers of bridges with prestressed girders (Khaleghi, 2012). Three methods of design for connection details are specified by WSDOT design policy as shown in Figure 2.2, Figure 2.3, and Figure 2.4.

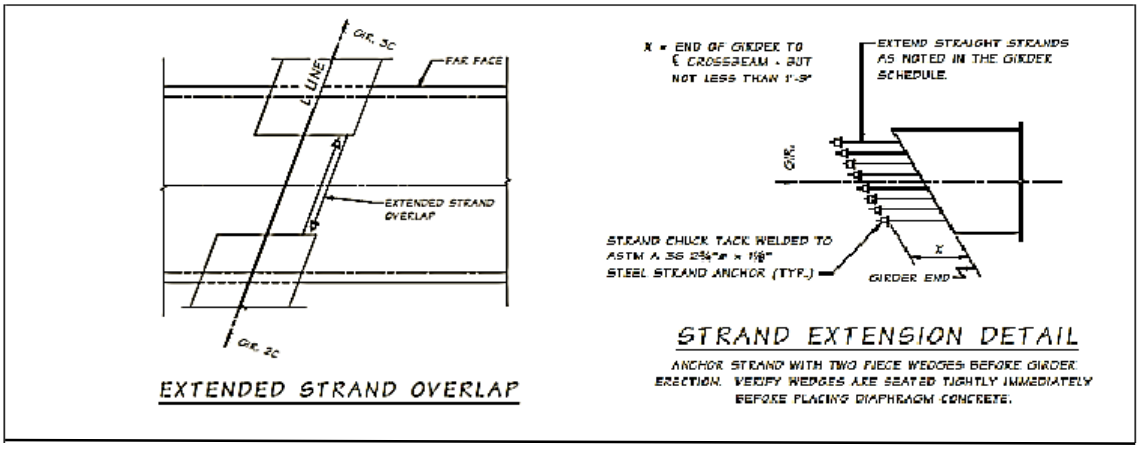

Figure 2.2: Extended Strand Overlap Detail (Khaleghi, 2012)

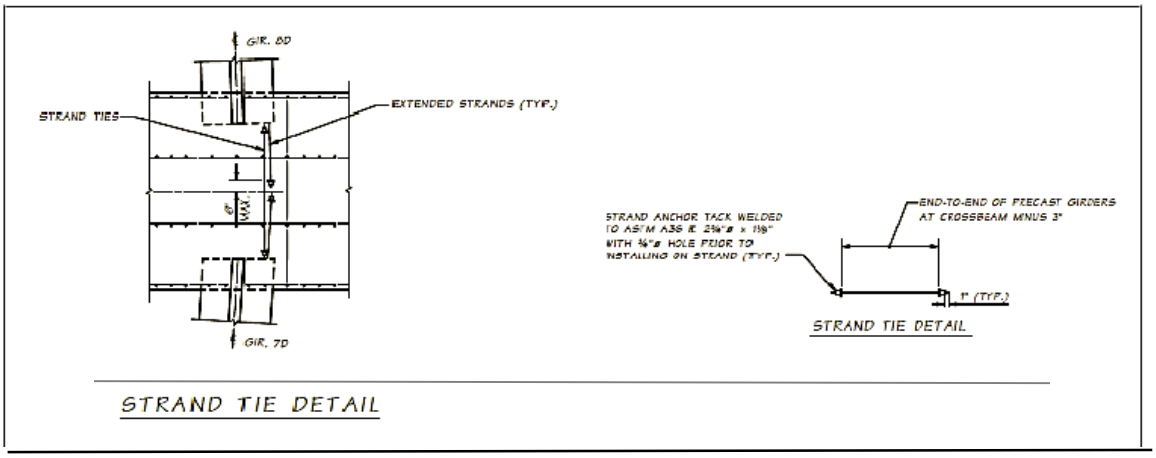

Figure 2.3: Strand Tie Detail (Khaleghi, 2012)

www.manaraa.com

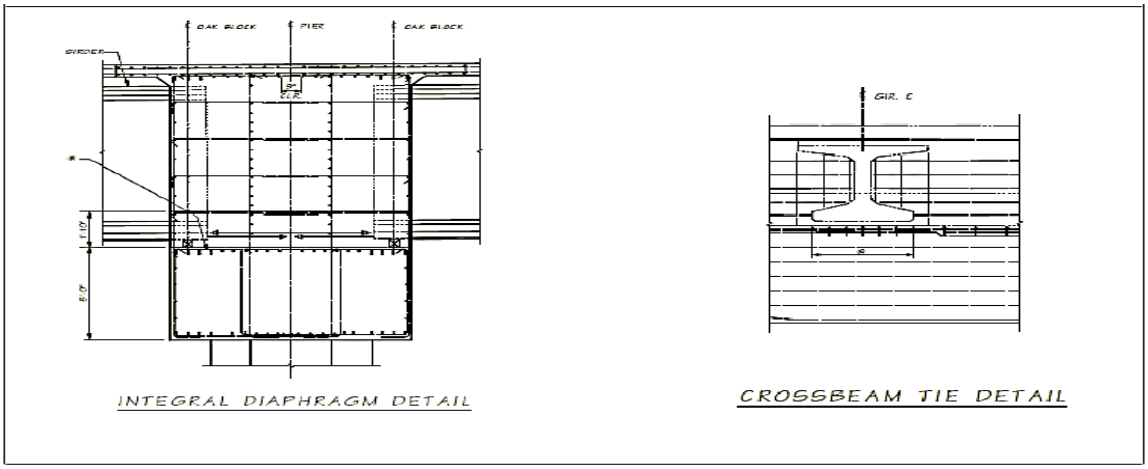

Figure 2.4: Integral diaphragm and crossbeam detail (Khaleghi, 2012)

The first method utilizes extended strands that overlap strands from the girders on the opposite side of the cap beam. This detail is allowed for any width of cap beam and for bridges without skew or horizontal curvature. The second method uses strand ties for cases in which bridge skew or horizontal curvature would cause the strands to cross. Strand ties require a cap beam that is at least six feet wide. If the width of the cap beam is less than six feet, strand ties are allowed as long as a minimum of 8 in. of lap is provided between the strand tie and extended strand. If 8 in. of lap is not provided the effectiveness of the tie is reduced in proportion to the reduction in lap length. The third method specifies that any additional design forces beyond the capacity of the strand ties used in the second method must be carried by crossbeam ties. A maximum area of crossbeam ties that can be considered effective for carrying strand forces is specified by Equation 2.1. An increase in the width of the crossbeam is required if sufficient resistance cannot be developed using crossbeam ties (Khaleghi, 2012).

$$A_s = \frac{1}{2}\left(\frac{A_{ps} f_{py} n_s}{f_{ye}}\right) \qquad (2.1)$$

where:

A_{ps} = area of strand ties, in^2

n_s = number of extended strands that are spliced with strand and crossbeam ties

f_{py} = yield strength of extended strands, ksi

f_{ye} = expected yield strength of reinforcement, ksi

www.manaraa.com

If crossbeam ties are used, two-thirds of the A_s value calculated in Equation 2.1 must be placed directly below the girder and the remaining reinforcement must be placed outside the width of the bottom flange. These design details have not been experimentally tested but are currently used in practice by the Washington DOT.

2.3 Seismic Positive Moment Research

2.3.1 Spliced girder test

In 1999, Caltrans funded a research project at UCSD to develop precast spliced girder bridges in which the girders and connection diaphragms are post-tensioned together (Holombo, 1999). Two prototypes were developed with one utilizing bulb-tee girders and the other bathtub girders. A schematic of the prototypes is shown in Figure 2.5. Spliced girders were viewed as a possible alternative to traditional precast girder bridges because the self-weight of the superstructure was able to be supported continuously across the bent cap.

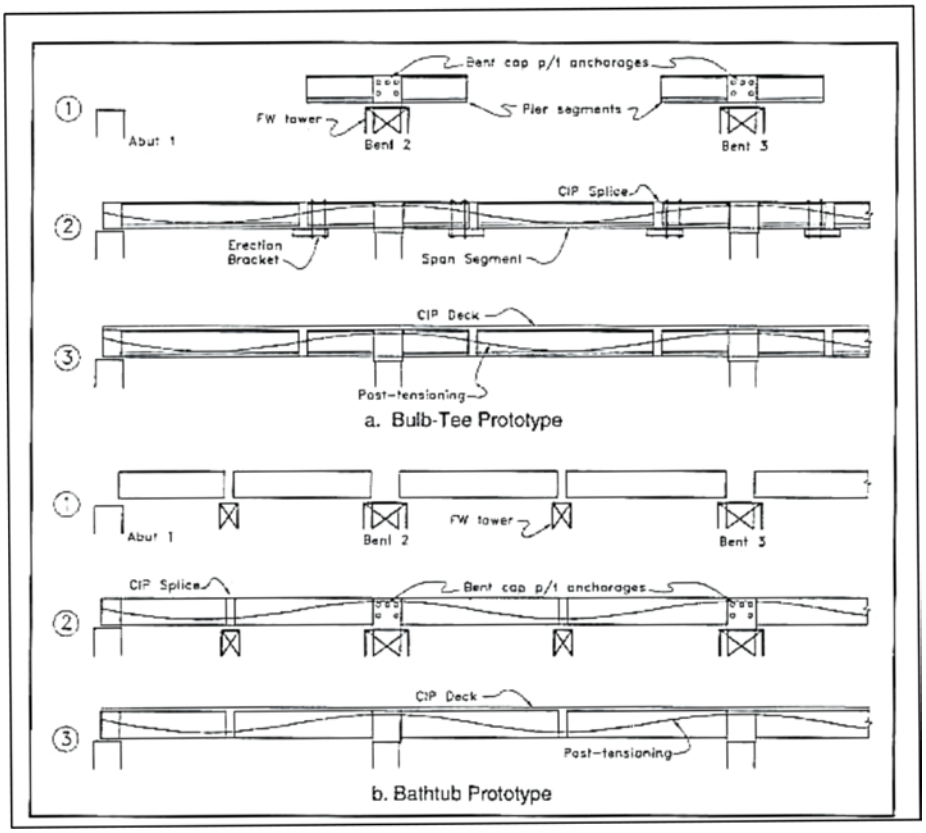

Figure 2.5: Schematic of prototype bridges (Holombo, 1999)

www.manaraa.com

The use of spliced girders changes the moment profile of the bridge and results in a higher negative moment at the girder to cap connection due to the dead load. The redistribution of dead load also results in a smaller positive moment demand due to seismic activity as shown in Figure 2.6. The increased negative moment demand can then be resisted with reinforcement in the bridge deck while less resistance is needed for positive moment (Holombo, 1999). Other benefits of using spliced girder bridges include longer span lengths, since the girders are spliced on site and therefore not limited by hauling limits, and reduced cost since the sections can be made continuous for self-weight moments reduces the superstructure depth (Holombo, 1999).

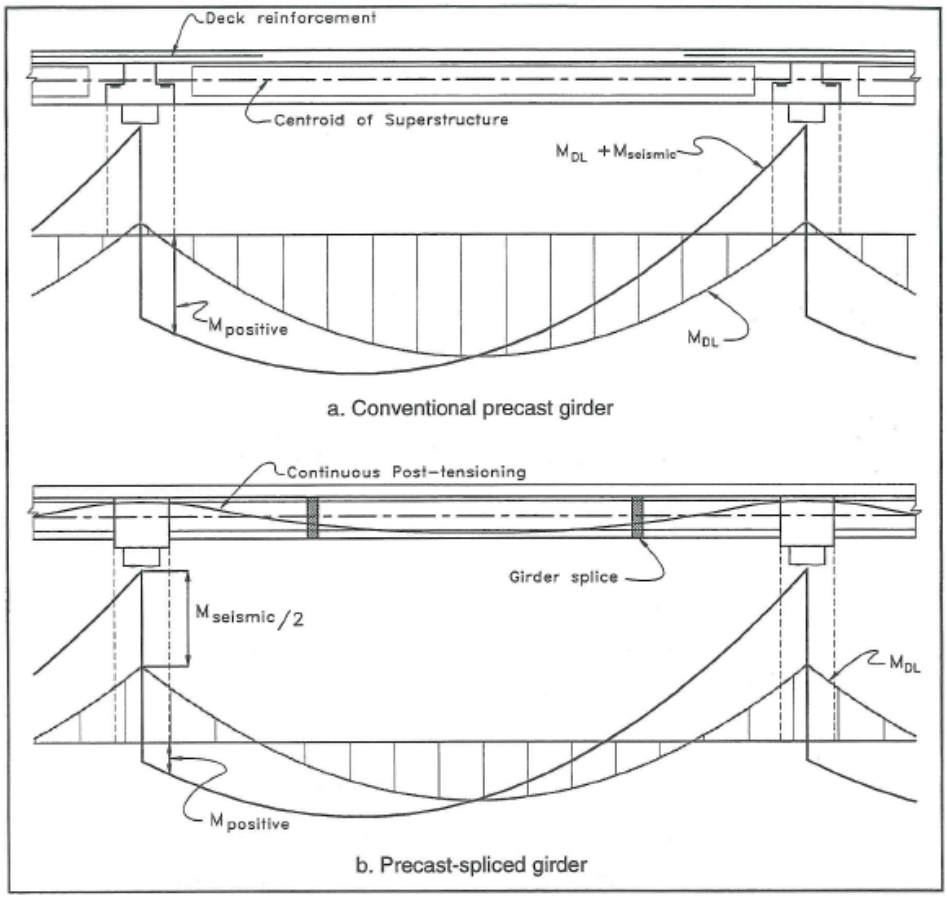

Figure 2.6: Moment profile comparison

Two 40% scale test units were constructed and tested at the structures lab of UCSD. One unit used Modified Florida bulb-tee girders while the second unit was built using bathtub girders. After construction was complete, both units were subject to

www.manaraa.com

horizontal displacement cycles. Horizontal actuators applied the push and pull forces to generated target connection moments while vertical actuators provided the appropriate shear forces as shown in Figure 2.7. As the test units approached failure due to horizontal displacement, the testing was stopped and the location of the actuators was changed to determine the capacity of the superstructure by pushing and pulling vertically as shown in Figure 2.8.

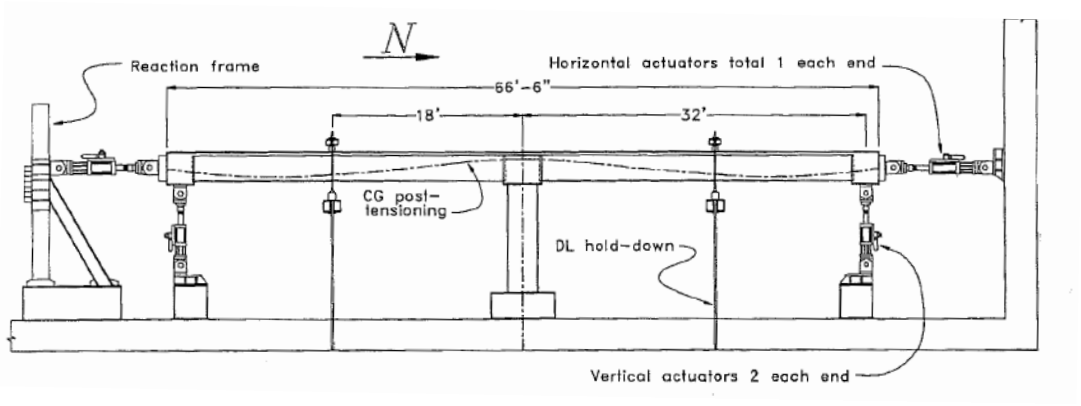

Figure 2.7: Spliced girder test setup (Holombo, 1999)

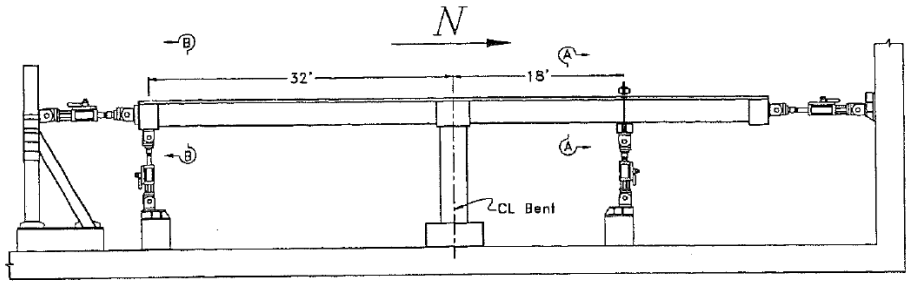

Figure 2.8: New location of actuators (Holombo, 1999)

In the horizontal displacement cycles, both the bathtub and bulb-tee units were able to reach a higher displacement ductility than the design ductility of μ_Δ=4. The bulb-tee reached a ductility of μ_Δ=8 while the bathtub unit reached a ductility of μ_Δ=6. Only minor cracking was observed at the girder to cap interface and many of the cracks closed after the testing loads were removed. When the actuators were moved to the vertical position and the capacity of the superstructure was tested, the bulb-tee reached the actuator displacement limits of μ_Δ=2.5 and μ_Δ=1.5 in the push and pull directions without spalling any concrete around the section (Figure 2.9). The maximum positive

www.manaraa.com

moment reached by the connection was around 243 k-ft as shown in Figure 2.10. The bathtub unit experienced plastic hinge failure at a ductility of μ_Δ=2.4 in the pull direction with spalling around the girder to cap interface as shown in Figure 2.11 and Figure 2.12. The maximum positive moment reached was 300 k-ft as shown in Figure 2.13. Results from both of the horizontal and vertical displacement show that the spliced girders were adequate to resist design level earthquakes.

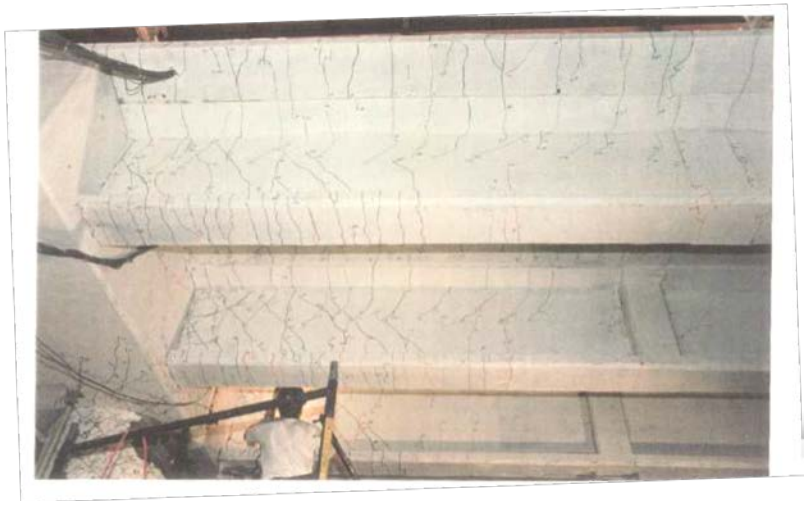

Figure 2.9: Bulb-tee test unit (Holombo, 1999)

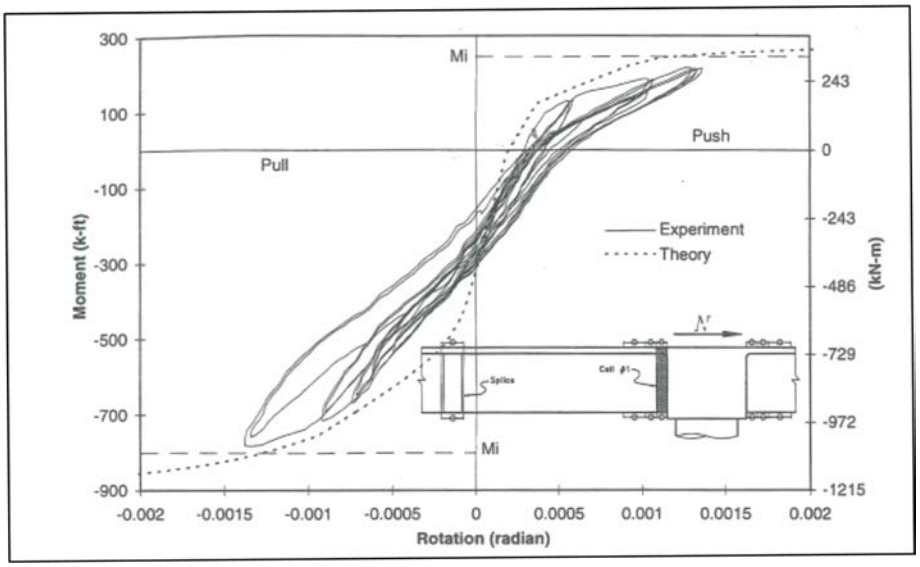

Figure 2.10: Moment-rotation response of bulb-tee girder (Holombo, 1999)

www.manaraa.com

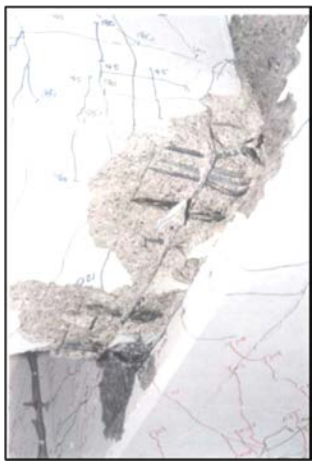

Figure 2.11: Spalling of bathtub girder at cap interface (Holombo, 1999)

Figure 2.12: Bathtub test unit (Holombo, 1999)

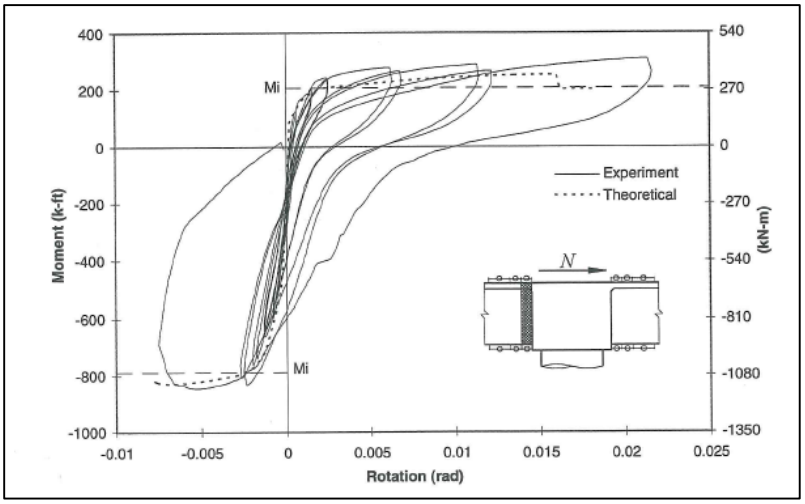

Figure 2.13: Moment-rotation response of bathtub girder (Holombo, 1999)

www.manaraa.com

2.3.1 Caltrans system test

In 2010, a joint project between ISU and the University of California San Diego (UCSD) was sponsored by Caltrans for the purpose of verifying that girder to cap positive moment connections could be established to create an integral superstructure and allow plastic hinge formation in both the top and bottom of bridge columns. This project, known as the system test, was conducted at UCSD and included the design, construction, and testing of a bridge column and five girder superstructure. A prototype structure was developed to accurately represent existing Caltrans bridges as shown in Figure 2.14. Dapped end California I-girders were used in the design as well as an inverted tee cap beam. The deepest I-girder was chosen to create the largest possible demand at the girder to cap beam connection. A 50% scale test unit was then designed to adequately capture the behavior of the girder to cap connections and identify whether the superstructure would remain integral under high loads. The test unit consisted of a single column, cap beam, five girders on each side of the cap, and a deck overlaying the entire superstructure. Only a single section of the prototype structure was represented, as outlined in Figure 2.15 because it was determined that the highest moment and shear values experienced by the bridge would occur at this section.

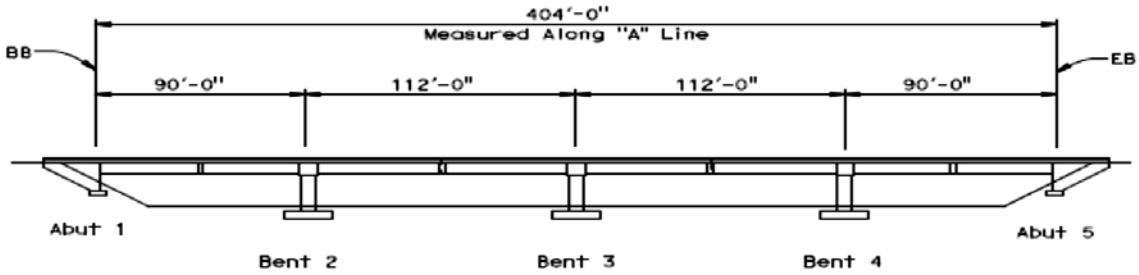

Figure 2.15: System test prototype (Snyder, 2010)

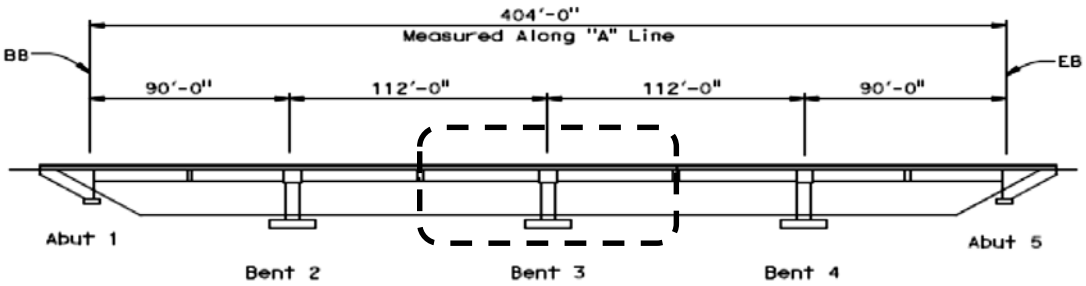

Figure 2.14: Test unit section for the system test (Snyder, 2010)

www.manaraa.com

The test unit constructed at UCSD consisted of two different girder to cap connection details. One detail was the current connection used by Caltrans which was expected to behave as a pinned connection and labeled the “as-built” connection, and the other was an experimental connection utilizing grouted unstressed strands and labeled as the “improved” connection. The as-built connection consisted of three dowel bars placed transversely through the girder web. The improved connection had the same dowel bars as the as-built but also had four unstressed strands that ran along the bottom of the cap and girder. Two ducts were placed in the members prior to casting of the girders and cap and two strands were then run through each duct and grouted in place. Simplified details of the connections are shown in Figure 2.16.

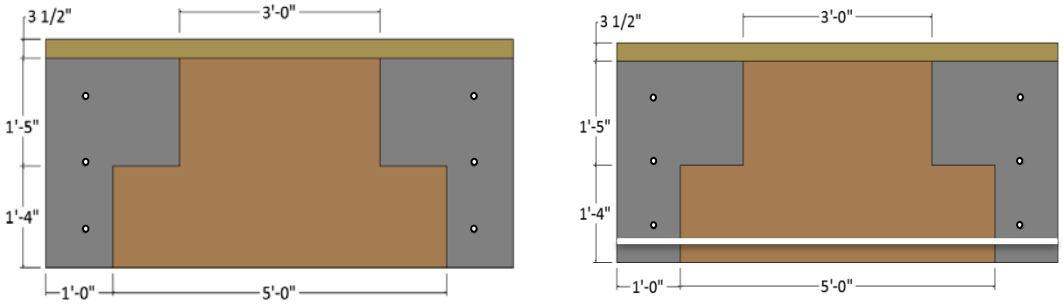

Figure 2.16: Simplified system test details: as-built (left); grouted strand (right)

The test unit was then subject to dead loads and loads generated by horizontal ground motion. The results of the test showed that both connections details behaved as fixed connections resulting in an integral superstructure which allowed a plastic hinge to form in both the top and bottom of the column with a maximum displacement ductility of 10. The fixed behavior of the as-built connection was not expected since it had been designed to behave as a pinned connection. Both connections were damaged after reaching a displacement ductility of 10, but the full capacity of the connections had not yet been reached. In order to fully quantify the connection, vertical forces were applied to each set of girders in increments. In this manner, the capacity of the as-built connection was fully quantified; however, the improved connection was not able to be fully quantified because of instability developed within the test unit. Final condition of

www.manaraa.com

the test unit is shown in Figure 2.17 along with the final capacity of each connection in Figure 2.18 and Figure 2.19. More detailed results as well as information regarding the design of the prototype and test unit can be found in “Seismic Performance of an I-Girder to Inverted-T Bent Cap Connection” by R Snyder et. al (R. Snyder, 2011).

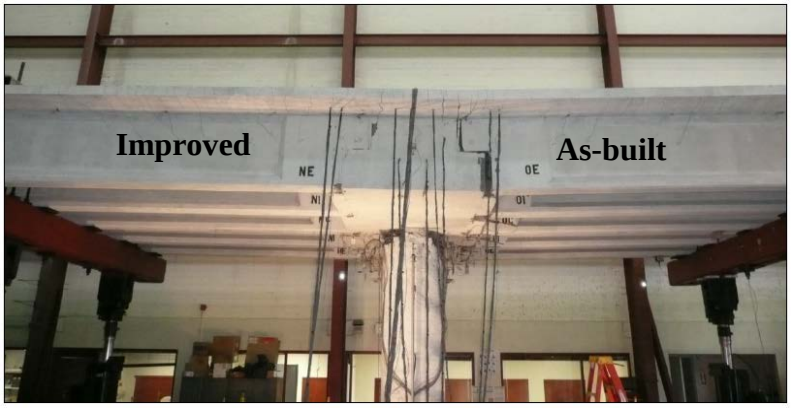

Figure 2.17: Test unit for system test (Snyder, 2010)

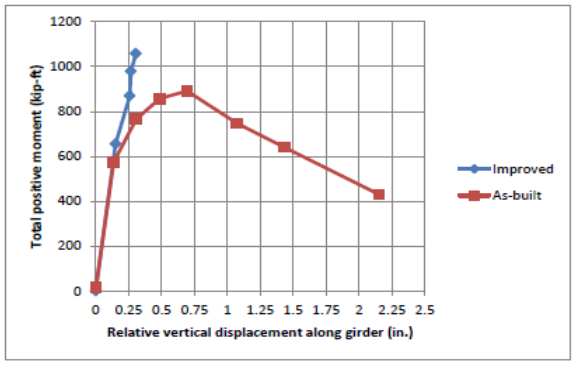

Figure 2.18: Positive moment response of connections established from vertical disp. test (R. Snyder, 2011)

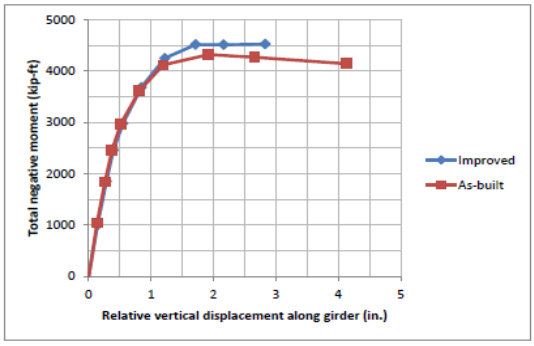

Figure 2.19: Negative moment response of connections established from vertical disp. test (R. Snyder, 2011)

www.manaraa.com

2.3.2 Connection tests

The system test showed that the superstructure of the prototype bridge will remain integral and elastic allowing for the formation of two plastic hinges at the ends of the bridge column during seismic loading. However, the full capacity of the grouted strand connection was not able to be determined. With support from Caltrans, it was determined that ISU would conduct further testing to quantify this connection and also develop new connection details. A total of six positive moment connections, including the improved connection, were designed in order to help understand the best way to create positive moment continuity for precast girders. The resistance of each connection to forces generated by vertical acceleration effects was also examined. This series of tests will be referred to as the connection tests. One goal of the connection tests was to fully quantify the shear and moment capacity of individual girder to cap connections to ensure that each connection remained elastic well beyond the formation of plastic hinges developed in the system test. The second goal was to demonstrate that each connection had adequate shear and moment capacity when subjected to 0.5g vertical acceleration in addition to horizontal ground acceleration. Meeting the second goal would eliminate the need for added side longitudinal girder mild steel reinforcement currently required by Caltrans SDC. Full quantification of the connections would also allow for improved design of integral bridge superstructures.

Since the goal of the tests was to quantify the behavior of the connections, the formation of column plastic hinges was not necessary. Therefore a short square column was designed which would remain elastic throughout the test to enable the connections to be fully quantified. In order to perform individual testing of the connections, each girder had its own bridge deck. The width of each bridge deck was determined based on the percentage of the entire bridge load that a single girder would carry.

The first test unit was designed using a 50% scale model of the same prototype used in the system test (Figure 2.20) and consisted of a footing, column, cap beam, and two girders with individual decks shown in Figure 2.21. An inverted cap beam and California I-girders were used to duplicate the system test.

www.manaraa.com

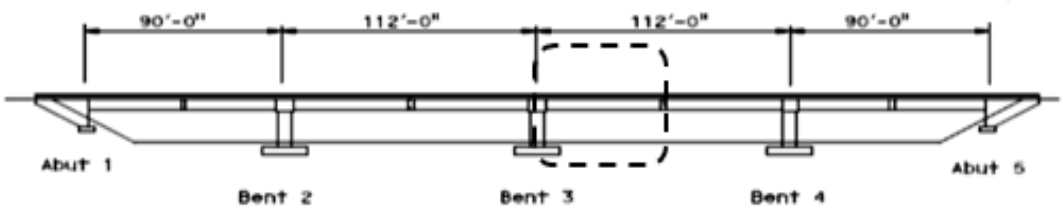

Figure 2.20: Test unit section for CT1

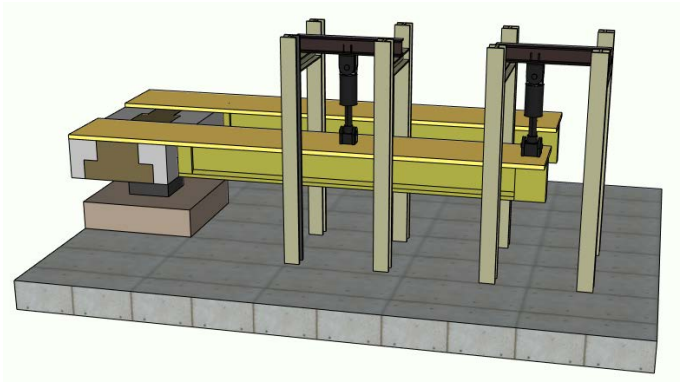

Figure 2.21: CT1 test setup

The two connection details designed for CT1 were the grouted unstressed strand connection (GUSC) or improved connection from the system test and the looped unstressed strand connection (LUSC) which was designed by Caltrans. The LUSC connection had unstressed strand loops cast inside the girders and also protruding from the corbel of the cap beam. The loops overlapped when the members were placed and four dowel bars were run transversely through the loops as shown in Figure 2.22. The loops confined the concrete around the dowel bars in order to provide positive moment resistance.

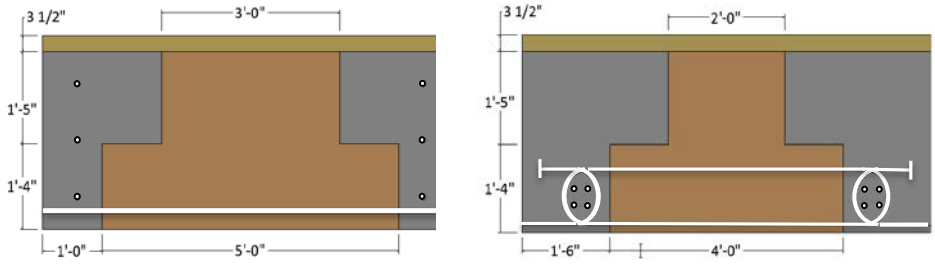

Figure 2.22: GUSC (left) and LUSC (right) connections tested in CT1

www.manaraa.com

The CT1 test unit was constructed in the ISU structures lab and utilized ABC components including a precast cap beam and precast I-girders. The precast cap beam contained ducts that slid over extended column reinforcement and then were filled with grout to establish a secure column to cap connection. A diaphragm was then poured to attach the I-girders to the cap beam. After pouring the individual bridge decks and setting up the necessary instrumentation, the CT1 test unit was tested according to a loading protocol that included dead loads, horizontal ground acceleration, and vertical ground acceleration.

Both connections for CT1 performed well and provided adequate positive moment resistance beyond the as-built connection from the system test. Comparison of the moment values and corresponding deflections near the center of the girder are shown in Figure 2.23 and Figure 2.24. The performance of the connections ensured that the superstructure of the bridge would remain elastic well beyond the moment necessary to form a plastic hinge in the top of the column. Further details regarding specifics of design, construction, and results are detailed in “Integral precast girder-to-cap connections for accelerated bridge construction in seismic region” by Justin Vanderwerff, 2014.

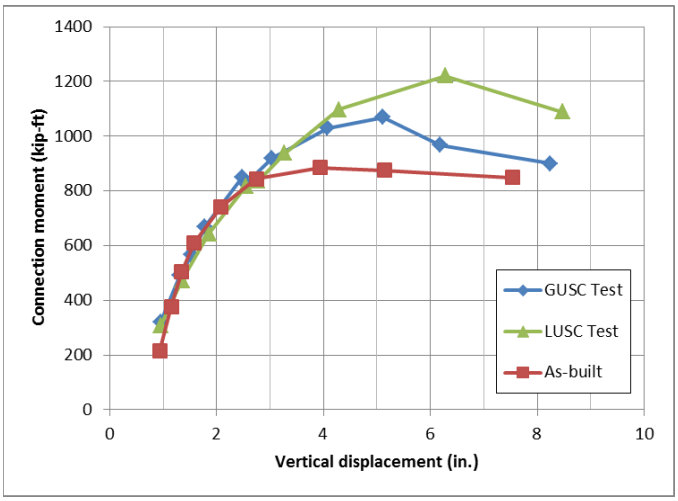

Figure 2.23: Negative moment vs. displacement performance of GUSC and LUSC connections compared to system test

www.manaraa.com

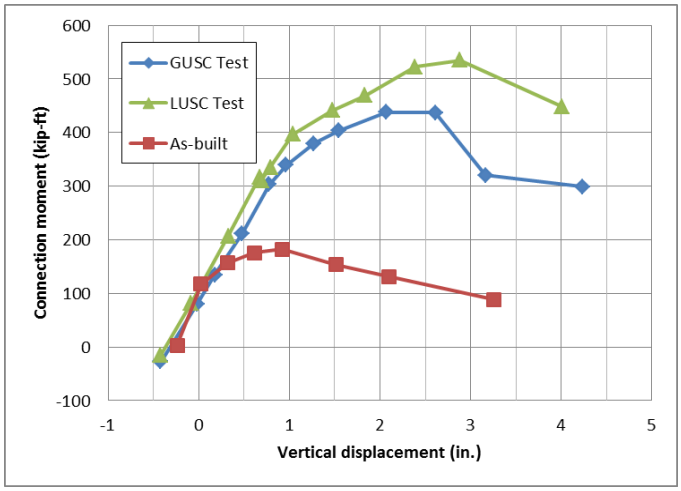

Figure 2.24: Positive moment vs. displacement performance of GUSC and LUSC connections compared to system test

2.4 Extended Strand Research

While the previously discussed research focused on seismic moment resistance of precast girders by various mechanisms, the following two tests examine the capacity of extended strands to resist positive moments due to volume changes caused by creep, temperature shrinkage, and loading in spans away from the supports.

One of the first tests was conducted by Salmons at the University of Missouri in 1974 to provide reinforcement to resist volume changes at precast girder to cap connection regions. The test had two phases, the first phase investigated the bond of untensioned prestressing strands in concrete and the second phase specifically looked at using extended strands at the girder to cap connection. In the first phase, 69 specimens were tested with consideration given to the configuration of embedded strands, embedment length, diameter of the strand, and strength of concrete (Salmons, 1974).

Pull out tests were conducted after the strands were cast into the concrete. The study tested strands with three different end conditions: strand bent at 90° over a reinforcing bar, straight strand, and frayed strand. The 90° strand was found to be the strongest followed by the straight strand and then the frayed strand. It was found for the sizes of strand tested (3/8”, 7/16”, 1/2”, and 0.6”) that the strand diameter had no effect on the slip of the strand in relation to the stress in the steel. The study also concluded that concrete strength (3,750-6,900 psi) had no effect on the bond of the strand in

www.manaraa.com

relation to slip (Salmons, 1974). Phase 1 of the test provided recommendations for embedment length of the strands to prevent slip:

90° bent strand:

$$L_e = 0.163f_s + 8.25 \text{ in.} \quad (2.2)$$

Straight strand:

$$L_e = 0.337f_s + 8.00 \text{ in.} \quad (2.3)$$

Frayed strand:

$$L_e = 0.552f_s + 5.50 \text{ in.} \quad (2.4)$$

f_s = loaded end steel stress in ksi

L_e = total embedment length in inches

The second phase of the test involved testing of short I-girder sections which were placed end to end and embedded in a diaphragm.A total of six test specimens were constructed, three utilized a slab over the girders and diaphragm, while the other three were tested without a slab as shown in Figure 2.25 and Figure 2.26. The diaphragm was 2 ft. 6 in. wide and 8 ft. long, while the slab was 6.5 in. deep.

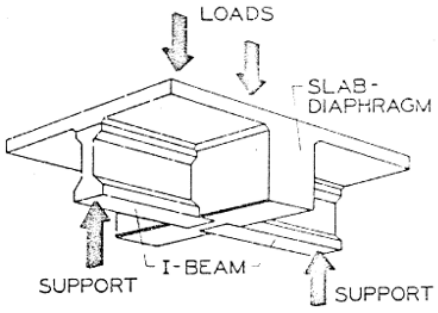

Figure 2.25: I-girder with slab extended strand test specimen (Salmons, 1974)

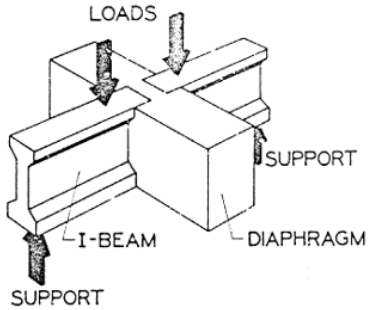

Figure 2.26: I-girder without slab extended strand test specimens (Salmons, 1974)

www.manaraa.com

Each specimen contained a different number of 0.5 in. diameter, 270 ksi relaxed prestressing strands which were embedded at different lengths as shown in Table 2-1. Test specimens S1-S3 are I-girder sections that were tested with slabs while O1-O3 are I-girder sections tested without slabs. Each girder specimens was subjected to flexural loading and it was found that the specimens with more strands were able to carry higher moments due to increased stiffness values. The ultimate moments established from the flexural loading of the test specimens are shown in the M_{act} column of Table 2-2.

Table 2-1: Number of strands and embedment length for each girder specimen (Salmons, 1974)

Specimen	No. of Strand	Embedment Length (in.)
S1	4	30
S2	2	30
S3	2	24
O4	2	30
O5	4	30
O6	7	24

Table 2-2: Cracking and ultimate moment values for each girder specimen (Salmons, 1974)

Specimen	No. of Strand	Embedment Length (in.)	Cracking Moment (k-ft)	Ultimate Moment (k-ft)
S1	4	30	252	489
S2	2	30	238	349
S3	2	24	252	369
O4	2	30	135	207
O5	4	30	150	327
O6	7	24	180	442

Other notable observations included that a larger number of strands in the connection region was not detrimental to the integrity of the connection and that tension forces transferred into the diaphragm tended to dimish rapidly as the loads were increased (Salmons, 1974). In all the tests, failure occurred when the I-girder and diaphragm split and the girder was pulled away from the specimen. It was also noted that the slab caused a notable change in the compressives strain distribution with the slab distributing the strain over a larger width. Overall, the test showed that extended strands

www.manaraa.com

were able to be adequately resist positive moments caused by volume change at the girder to cap connection (Salmons, 1974).

Another set of tests of positive moment connections to resist creep, shrinkage, and temperature effects was performed by the Transportation Research Board in 2004 and published in the NCHRP 519 report. The first part of the study included a survey about continuous superstructure connections with positive moment reinforcement used by state DOTs and private contractors, fabricators, and designers (NCHRP, 2004). The survey found that the majority of positive moment connections built consisted of bent bars or extended bent strands as shown in Figure 2.27 and Figure 2.28. The most common types of girders used in the survey were I-girders and bulb-tee girders.

Figure 2.27: Bent reinforcing bar connection (NCHRP, 2004)

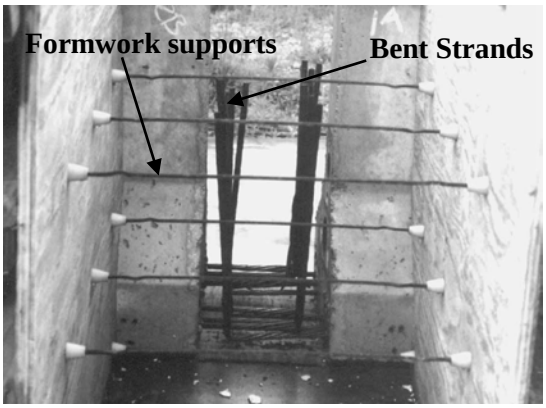

Figure 2.28: Bent strand connection with diaphragm formwork (NCHRP, 2004)

The second part of the test included the construction and testing of six short specimens which consisted of two 16-ft long I-girders joined by a diaphragm as well as two 50-ft specimens (NCHRP, 2004). For each specimen, the ends of the girders were

www.manaraa.com

always ten inches apart but the width of the diaphragm was varied in order to investigate its effect on the connection.

Two of the 16-ft long girders used 0.5 in. diameter, 270 ksi relaxed strands that were extended from the girders and bent with one specimen having a 10 in. diaphragm and the other having a 22 in. diaphragm. The bent strands had a total length of 26 in. with 8 in. before the 90° bend and 18 in. after the bend. A total of six strands were used in each connection and the strand was bent in the field using a hydraulic hand tool. The other four 16-ft connections used bent bars with various diaphragm widths and reinforcement details. For each specimen, a deck slab was cast over the beams and diaphragm. The 16-ft specimens were tested as cantilever beams and subjected to cyclic loading as shown in Figure 2.29 (NCHRP, 2004). The loading was made up of three distinct phases. In the first phase the girders were cycled between the positive and negative live load moments without considering time dependent effects. The second phase considered creep, shrinkage, and temperature change and cycled the girder to the positive cracking moment (M_{cr}) of the girder (NCHRP, 2004). The third phase took into account the maximum positive and negative moments generated by live loads combined with the maximum positive moment generated by creep, shrinkage, and temperature change. The girders were cycled to these combined maximum moment values until failure. The total number of cycles at the combine maximum moment was then compared for each specimen and is shown in Table 2-3.

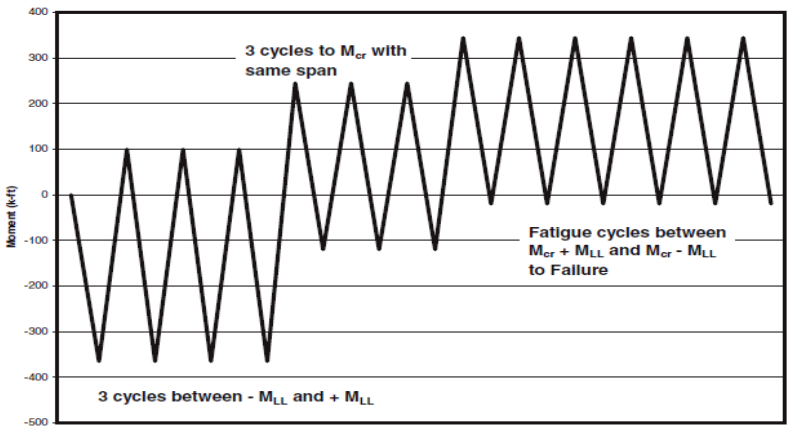

Figure 2.29: Cyclic loading cycle used to test strand or bar capacity in 16-ft specimens (NCHRP, 2004)

www.manaraa.com

Table 2-3: Results and descriptions of 16-ft specimens (NCHRP, 2004)

Specimen Number	Type of Specimen	Diaphragm Width (in.)	Girder End Embedment (in.)	Special Feature	Cycles to Failure
1	Bent strand	10	0	None	16,000
2	Bent bar	10	0	None	25,000
3	Bent strand	22	6	None	55,000
4	Bent bar	22	6	None	11,600
5	Bent bar	22	6	Extra Stirrups in diaphragm	56,000
6	Bent bar	26	8	Web bars	133,000

The 50-ft specimens were constructed using the bent strand detail and bent bar detail. Both specimens had a standard 10 in. diaphragm and a deck slab. The bent strand connection consisted of ten 0.5 in. diameter strands with the same 26 in. length as the 16-ft specimens. The 50-ft specimens were loaded in a similar manner to the 16-ft. However, instead of cycling the loads when the maximum moment values were reached, the load was gradually increased beyond the maximum values until failure. The bent strand connection reached a maximum positive moment of approximately 1400 k-ft. One of the concerns while testing the 50-ft specimens was the loss of continuity over the connection region once positive moment cracking occurred. However, both connections did not experience any loss of continuity until failure of the connection was reached.

Many conclusions were drawn from the testing of the 16-ft and 50-ft specimens. It was observed that for both size specimens that the bent strand and bent bar connections provided adequate positive moment capacity to resist creep, shrinkage, and temperature effects in the girder. The 16-ft specimens were able to withstand over 10,000 cycles at maximum moment values and the 50-ft specimens both withstood a maximum positive moment of around two times M_{cr} (NCHRP, 2004). Considering constructability, the bent strand connections were easy to fabricate and the length of the bent strands was determined using Equations 2.2 - 2.4 from Salmon's report mentioned earlier. It was found that the bent bar connections were harder to construct and required asymmetrical spacing to allow the two girders to mesh together. The asymmetrical

www.manaraa.com

spacing resulted in asymmetrical stresses and cracking; however, this problem could be avoided if a wider diaphragm was used (NCHRP, 2004). It was also concluded that the embedment length of the girders in the diaphragm reduced the stress in the connection and allowed for higher cycling of loads in the 16-ft specimens before failure. However, the report suggests that quantifying the reduction in stress was difficult and therefore the effect of diaphragm embedment should not be considered in the design of the connections.

Finally, one of the 16-ft test specimens contained dowel bars that were placed transversely through the web of the girder and embedded in the diaphragm. It was noted that these bars significantly improved the behavior of the connections (Table 2-3). However, they also caused a large amount of cracking in the girder which may not be desirable (NCHRP, 2004). The report concluded that each connection tested was sufficient and that the selection of specific details should be left to the preference of the designer. The end of the report also discussed the application of the test results to seismic regions. The authors state that the work done in the tests may be relevant to seismic design but that proper detailing of the connection region and further testing would need to be performed. It is also observed that the bent strand connections tend to slip under cyclic loading in the 16-ft tests but specific slip values related to the applied girder force were not provided.

www.manaraa.com

CHAPTER 3 – PROTOTYPE STRUCTURE AND TEST CONFIGURATION

3.1 Introduction

Following the review of previously conducted research, an experimental investigation was performed to design and test two positive moment connections for ABC girders using prestressed extended strands and dowel bars. A prototype structure was first designed, followed by the design, construction, and instrumentation of a 40% scale test unit. A loading protocol was then developed along with an analytical model to predict the behavior of each connection. Details of each component of the investigation are discussed in the following sections.

3.2 Prototype Design

3.2.1 General

The current connection test is an extension of the system test performed at UCSD which was discussed in a previous section. The system test, as outlined in Snyder et al. 2011, provided overall superstructure behavior and column response of a single column bent. It showed that the superstructure would remain fixed under high seismic loads and allow a second plastic hinge to develop at the top of the bridge column. The connection tests were developed to further understand and quantify the response of specific girder to cap connections within the superstructure. The first set of connection tests (CT1) investigated the improved detail used in the system test (known as the GUSC connection) as well as a detail designed by Caltrans (LUSC connection). The results of CT1 showed that both connections acted as fixed connections, as opposed to degrading to a pin connection, and had adequate capacity to resist shear and moment values corresponding to the combined loads of gravity, horizontal seismic, and vertical acceleration of 0.5g. For both the system test and CT1, the same prototype structure was used as shown in Figure 3.1.

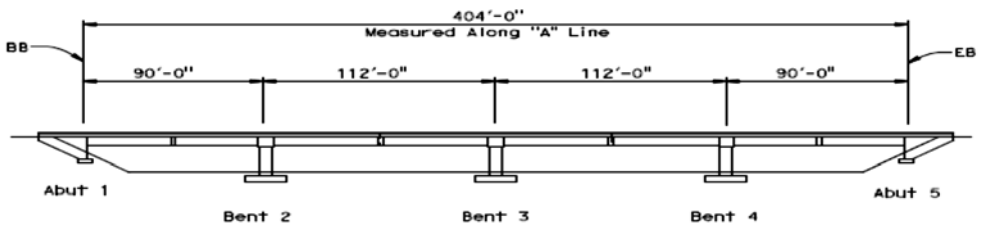

Figure 3.1: System test prototype design

www.manaraa.com

The system test prototype superstructure was designed in accordance with current Caltrans standards, had a maximum possible span length of 112 ft, and consisted of five dapped end I-girders. A five girder superstructure was used based on calculations which showed that five girders would provide the maximum bridge width allowed for a single column bent. Discussion following the completion of CT1 examined the possibility of extending the findings to bridges with longer span lengths which would in turn generate larger connection forces. The 112 ft prototype span length of the first test unit was actually longer than the preferred span length for I-girders which Caltrans specifies to be 95 ft. However, use of the 112 ft span ensured that the connections would work well for any I-girder bridge (Caltans, 2012). Bridges using bulb-tee or wide-flange girders with span lengths of up to 150 ft are not uncommon in California. Therefore it was decided to use bulb-tee girders for the second connection test with a 150 ft prototype span length in order to accurately investigate the connection behavior for longer bridge spans.

The 150 ft span length required use of California Bulb-Tee 85 girders (CA-BT85) which are the largest bulb-tee girders currently used in the state of California. To replicate the system test, a single column bent was used for the bulb-tee prototype along with the maximum superstructure width which again corresponded to five girders. The maximum girder size and span length generated the maximum moment possible at the girder to cap connection region for a single column bent, bulb-tee girder bridge. Since the system test provided a fully designed prototype structure, the design of the bulb-tee prototype followed the system test design. In order to adequately design the bulb-tee prototype, the scale factors listed in Table 3-1 were formulated to appropriately increase the dimensions of the system test. The scale factors provided very close approximation for superstructure length and depth as well as the appropriate section areas.

Table 3-1: System test prototype scale factors

Parameter	Scale Factor
Length	1.34
Area	1.8
Stress	1
Force	1.8
Moment	2.41

www.manaraa.com

Using details from the system test, along with the appropriate scale factors shown above, the bulb-tee prototype structure was developed as shown in Figure 3.2. Specific design considerations for sections of the bridge including the column, girders and deck, bent cap, and connection regions are discussed in the following sections.

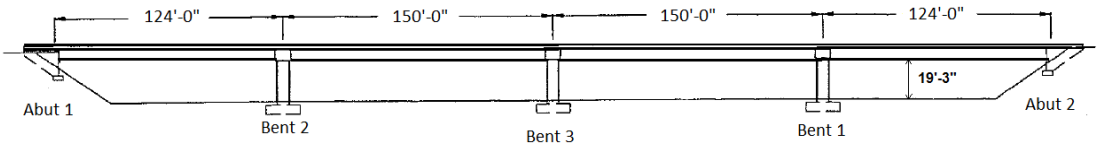

Figure 3.2: Bulb-tee prototype structure

3.2.2 Column Design

In the system test, a circular column was designed with plastic hinge locations at both the top and bottom of the column and a column overstrength moment of 17,662 k-ft (Thiemann, 2009). The scale factors listed in Table 3-1 and the overstrength moment from the system test were used to determine the overstrength moment for the bulb-tee prototype. The overstrength moment was found to be 42565 k-ft. It was not necessary to scale the column height from the system test, therefore the bulb-tee prototype had a clearance height of 19 ft 3 in. Scaling of the column section area resulted in a possible column diameter ranging from 6-8 ft depending on the reinforcement detail and plastic hinge design method. A specific column detail was not necessary for this connection test since the column overstrength moment and clearance height would be sufficient to adequately design the test unit.

3.2.3 Bent Cap Design

The main goal of the connection tests was to investigate different girder to cap connections in order to identify the best options for ABC construction. The system test used a precast inverted tee bent cap while the CT1 test unit utilized a precast inverted-tee bent cap. Both cap details provided a bearing surface for dapped end I-girders. To better understand how the bearing surface affected the cap connection and to further evaluate the benefits of the inverted-tee, the bulb-tee prototype was designed with a cast-in-place, square bent cap and girders without dapped or end blocks. The square bent cap

www.manaraa.com

eliminated the bearing surface provided by the inverted-tee and the girders without end blocks provided an opportunity to investigate the effectiveness of the girder to cap connections excluding end blocks. Due to the cast-in-place cap beam, a set of reference drawings was provided by Caltrans and were used to supplement the system test reinforcement details. The drawings contained details for a proposed widening project of interstate I-215/I-10 in California. The widening project used a square cap that would be added to an existing multi-column bent. By scaling the system test cap beam and referencing the provided Caltrans drawings, the dimensions and details of the cap beam were determined. The depth of the cap was 7 ft 0-5/8 in. to correspond with the CA-BT85 girders, and the cap length was set to 34 ft 5 in. to accommodate five girders with 8 ft center-to-center spacing. The ends of the bulb-tee girders were extended into the cap beam a length of 1 ft 4 in.

3.2.4 Girder and Deck Design

The CA-BT85 girders were designed according to dimensions specified in Caltrans Bridge Design Aids (BDA) (Caltans, 2012) and did not include an end block as mentioned previously. The details of the girder reinforcement were slightly different then the system test due to the change from an I-girder to the bulb-tee. The reference drawings provided by Caltrans included details of bulb-tee girder reinforcement for CA-BT73 girders and were able to be used in combination with the system test drawings to correctly detail reinforcement for the CA-BT85 girders. The deck dimensions from the system test were not scaled since a typical 8 in. thick deck was used for the bulb-tee prototype in order to follow current Caltrans design standards.

3.2.5 Connection Design

3.2.5.1 General

The design of the connections was completed based on a combination of current field practices and research results. Each connection would experience both positive and negative moments and needed to be designed accordingly. The magnitudes of the positive and negative design moments are normally calculated based on the distribution

www.manaraa.com

of moment generated by horizontal seismic forces at the connection region. In the report by Snyder et. al., percentages of the column overstrength moment were used with 45% corresponding to the positive moment and 55% to the negative moment. These percentages however, do not account for the effects of vertical seismic acceleration. Results from CT1 were examined and it was found through a force based approach that the percentages changed to 30% for positive moment and 70% for negative moment if vertical acceleration was considered. The shift in percentage of moment can be attributed to the vertical acceleration in the positive moment direction being counteracted by the mass of the structure. However, it is important to note that the overstrength moment value increases if vertical acceleration is considered. The higher overstrength moment results in the 30% moment due to vertical acceleration being higher than the 45% moment due to only horizontal forces. Equations 3.1 and 3.2 were used to calculate the positive and negative design moments of the bulb-tee prototype.

$$M_{pos} = pos\% * M_o \quad (3.1)$$

$$M_{neg} = neg\% * M_o \quad (3.2)$$

M_{pos} = positive design moment

M_{neg} = negative design moment

M_o = column overstrength moment

pos% = percentage of overstrength moment applied in positive direction

neg% = percentage of overstrength moment applied in negative direction

Applied percentages:

$$M_{pos} = 0.30 * 42565 = 12770 \text{ k-ft}$$

$$M_{neg} = 0.70 * 42565 = 29796 \text{ k-ft}$$

The connection negative moment would be resisted by the deck reinforcement. To obtain the negative moment for a single girder, the total negative design moment was multiplied by a distribution factor of 0.24. The distribution factor is a result of previous research by Vanderwerff et. al 2014, and resulted in a single girder negative design moment of 7150 k-ft. An equivalent stress block approach was then used to calculate an

www.manaraa.com

appropriate steel area and compression block depth. The girder and cap act as a composite section and therefore are assumed to be similar to a T-beam. Equation 3.3 and 3.4 were both solved for the area of steel and then set equal to each other to determine the appropriate area of steel and compression block depth. A more detailed calculation is presented in Appendix A.

$$M_{neg} = A_s f_y \left(d - \frac{a}{2}\right) \quad (3.3)$$

$$A_s f_y = 0.85 f'_c a b_f \quad (3.4)$$

M_{neg} = Negative design moment

A_s = Area of steel

f_y = yield strength of steel

d = depth from center of deck steel to bottom of girder

a = depth of compressive block

$f'c$= compressive strength of concrete

b_f = width of lower flange

Solving Equations 3.3 and 3.4 resulted in a steel area of 15.56 in.^{2} per girder and an equivalent compression block depth of 10.24 in. The total area of deck steel compares well to the system test which was not designed for vertical acceleration and had a total area of 12.7 in.^{2} per girder.

To resist positive moment, both extended 0.6 in. diameter strands and dowel bars were implemented in the connection. In the system test, as well as in the GUSC connection test from CT1, three dowel bars were placed transversely through the web of each girder. Results from the tests showed that the dowel bars provided significant positive moment capacity and therefore would reduce the required number of extended strands needed in the connection. For this reason, the same size dowel bars as the system test were included in the bulb-tee connections. By examining data from the system test and CT1, it was determined that the dowel bars would provide a moment resistance of

www.manaraa.com

1280 k-ft per girder. The positive moment requirement for a single girder was calculated by multiplying the previously calculated positive design moment (M_{pos}) by the distribution factor of 0.24 and was found to be 3065 k-ft. Equations 3.5 and 3.6 were then formulated using an equivalent stress block approach with the assumptions that the girder and deck would again act as a composite section and that the compressive area of the section would occur within the deck slab. Equations 3.5 and 3.6 were then set equal to each other and solved to provide the total number of strands required for each girder. Derivation and detailed calculations are again included in Appendix A.

$$N_s = \left(M_{pos} - M_{DA}\right)/(f_{ys} * A_{strand} * (d_s - \frac{a}{2})) \quad (3.5)$$

$$N_s = \frac{0.85\, f'_c b_d * a}{A_{strand} * f_{ys}} \quad (3.6)$$

N_s = number of strands

M_{DA} = dowel action moment resistance

f_{ys} = yield strength of strand

A_{strand} = area of single prestressing strand

d_s = depth from top of deck to centroid of strands

a = depth of compression block

b_d = effective width of bridge deck for a single girder

Solving Equations 3.5 and 3.6 resulted in the use of five 0.6 in. diameter strands per girder with a compressive block depth of 0.71 inches.

3.2.5.2 ESBF Connection

The first connection, labeled as the Extended Strand Bent with Free end (ESBF) connection, is shown in Figure 3.3. The connection utilizes extended strands bent at 90 degrees, three grouted bars placed through the girder web, and crossties which connect the dowel bars on each side of the cap beam.

www.manaraa.com

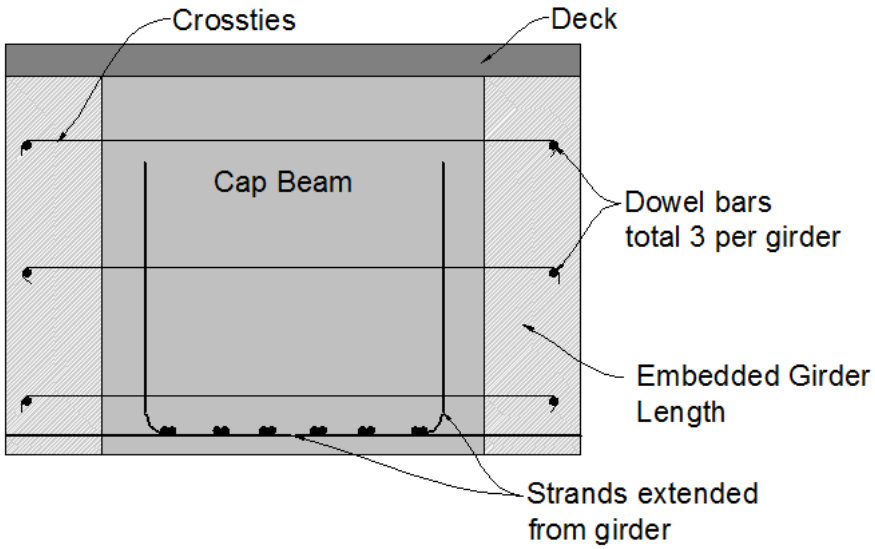

Figure 3.3: ESBF connection schematic

Precast girder connections with extended strands bent at 90 degrees have been designed and tested to resist positive moments resulting from volume changes caused by creep, temperature shrinkage, and loading in spans away from the supports. The bent strand connection performed well in these tests (NCHRP, 2004); however, the concept had not yet been tested for seismic loading. The goal of the ESBF connection design was to extend the bent strand detail to seismic applications and determine the bent strand performance under larger loads caused by seismic action. Dowel bars were also included in the design of the connection in order to decrease the number of extended strands required for positive moment resistance and thereby reduce congestion at the connection region.

The extended strands in the ESBF connection rely on development length for anchorage in the bent cap. Development length of an extended strand is the length required for proper anchorage based on the bond strength between the strands and concrete. The 90 degree bend in the strand allows for a longer development length within the cap beam and also provides tension continuity in the superstructure as the strands from girders on opposite sides of the bent cap overlap.

www.manaraa.com

Current research conducted at ISU provided recommended development lengths for different sizes and configurations of strands. The recommendations were based on a series of pull-out tests performed on strands. For the 0.6 in. diameter strands used in the prototype, the recommended development length of a curved strand was 70 in. This length is conservative when compared to the length of 52.5 in. suggested by using Equation 2.2 (Salmons, 1974). The initial placement of the strands was designed to be under the longitudinal reinforcement bars in the cap beam so that the strands could be bent around the longitudinal bars as shown in Figure 3.3. For placing the bent extended strands, strands can be bent at 90 degrees and set in place prior to assembling the cap reinforcement or the strands can also be threaded through the completed cap reinforcement.

3.2.5.3 ESSP Connection

The second connection, known as the Extended Strand with Splice and end Plate (ESSP) connection, is shown in Figure 3.4. The extended strands and addition of strand ties in this connection were designed according to details used by the Washington Department of Transportation (WSDOT) (Khaleghi, 2012).

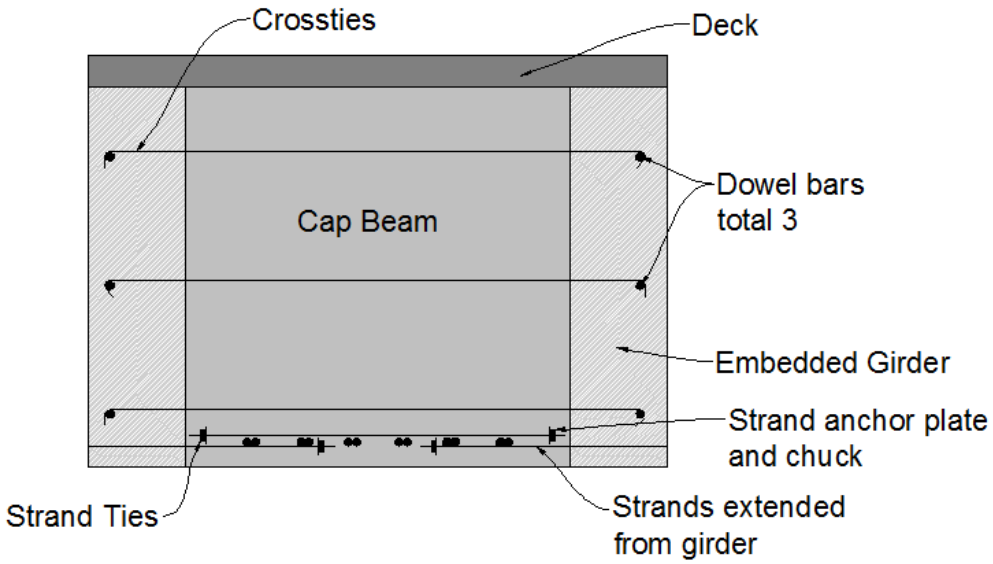

Figure 3.4: ESSP connection schematic

www.manaraa.com

For the ESSP connection, WSDOT has provided design recommendations, but the connection detail has not been experimentally verified. The detail is beneficial to bridges where congestion of cap beam reinforcement makes it difficult to extend strands further into the cap beam to provide tension continuity. Experimental verification of the capacity of the connection will validate the design guidelines specified by WSDOT and also provide a better understanding of how force would transfer through the connection.

In the ESSP connection, the prestressed strands from the girders extend a short distance into each side of the cap beam and are anchored with plates and strand chucks. Strand ties are placed to overlap the extended strands on both sides of the cap and create tension continuity along the bottom of the cap beam as shown in Figure 3.4. The strand ties are also anchored on both ends with a plate and anchor chuck. The WSDOT design does not include dowel bars, but based on the system test each girder contains three dowel bars connected with crossties in order to reduce the required number of extended strands.

The spliced strand concept relies on the idea that the tension force developed in the strand under positive moment will transfer from the extended girder strand into the strand tie through a manner similar to a strut-and-tie model as shown in Figure 3.5. The plate and anchor chuck on each end of the strand tie provide anchorage and resist the tension force generated by positive moment. The vertical component of the strut is assumed to be negligible due to the close proximity of the strands. WSDOT guidelines state that there must be at least 8 in. of overlap between the extended strands and the strand tie. It is not clarified if the 8 in. includes the plate and chuck anchorage, so it is assumed that there must be 8 in. between the anchor plates of the extended strand and strand tie. The strand ties allow for flexibility in the placement of the strands if the connection region is congested or if the girder strands cannot extend straight into the cap. In these cases, the strand ties can be moved as long as the ends remain reasonably close to the strands extending from the girder. It is likely that placement of the strands and strand ties would need to be completed prior to the completion of the cap reinforcement due to space required to place the anchor plates and chucks.

www.manaraa.com

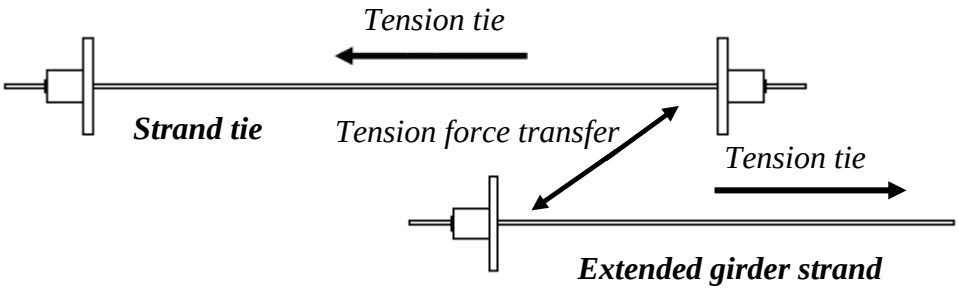

Figure 3.5: Strut and tie model

3.3 Test Unit Design

3.3.1 Introduction

Based on the prototype bridge dimensions presented in Figure 3.2, a 40% scale test unit was designed. The design was based on the region of the prototype where moments in the girder to cap connection would be the highest during seismic activity. This region was determined to be located at Bent 3 as indicated in Figure 3.7.

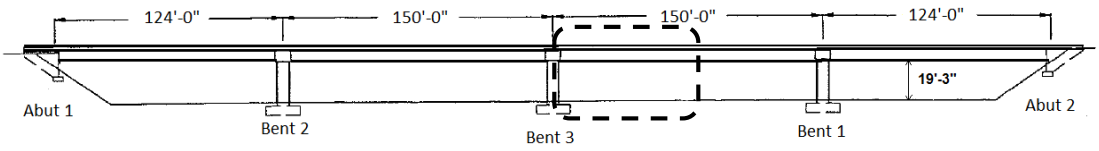

Figure 3.6: Region of highest forces during seismic activity

In designing the test unit, consideration was given to positioning girders on both sides of the cap beam or only on a single side. It was decided to place girders on only one side of the cap beam in order to simplify testing because placing girders on both sides of the cap would require simultaneous testing of opposing girders. Therefore the test unit was designed with two girders placed on one side of the cap beam. One girder would test the ESBF connection, and the other the ESSP connection. Each girder was designed with an individual deck to prevent interaction between connections. The factors shown in Table 3-2 were used to design the test unit by appropriately scaling the prototype structure. Details regarding the design of the girders, test unit connections,

www.manaraa.com

column and footing, and cap beam are discussed in the following sections. A complete set of drawings for the test unit are attached in Appendix B.

Table 3-2: Test unit scale factors

Parameter	Scale Factor
Length	0.4
Area	0.16
Stress	1
Force	0.16
Moment	0.064
Uniform Load	0.4
Displacement	0.4

3.3.2 Girder Design

The first members of the test unit to be designed were the precast girders. The scale factors listed in Table 3-2 were used to scale the girder dimensions which resulted in the scaled girder cross-section shown in Figure 3.8.

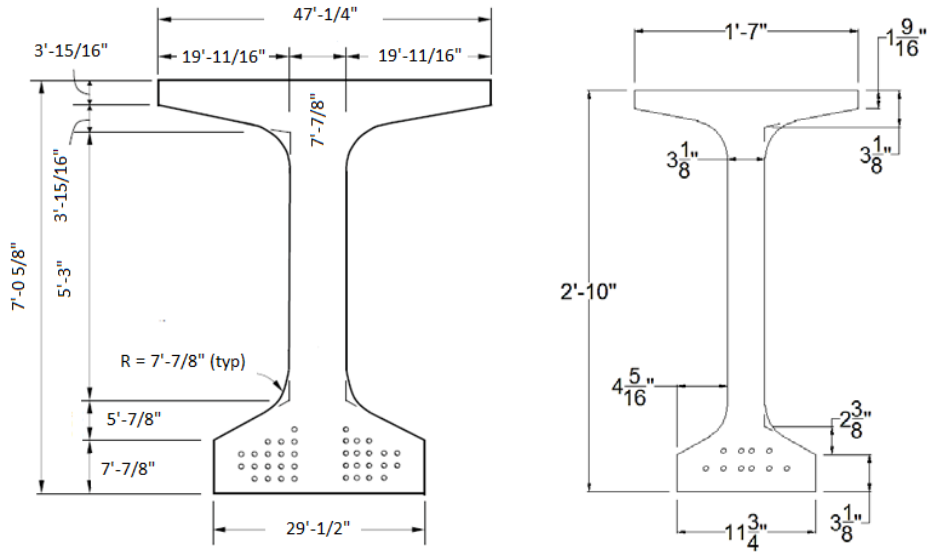

Figure 3.7: Cross-sections of prototype girder (left) and scaled test unit girder (right)

Half of the 150 ft prototype span was scaled for design of the test unit as shown in Figure 3.7 since, due to symmetry, the moment behavior of the girder could be accurately represented without considering the entire span length. Scaling half the 150 ft span length resulted in a 30 ft test unit girder, but also required the design of the

www.manaraa.com

prestressed strands in the girder to be adjusted due to the shorter girder length. The prestressing force from the prototype girder was scaled for the test unit and 3/8 in. strands were selected to provide the appropriate strand area. Next, the permissible stresses at transfer were checked and it was found that the extreme fiber stresses in tension were too high. To solve this problem, the number of strands in the girder was reduced until the stresses fell within the required range. The final design of the girder resulted in the use of ten 3/8 in. strands instead of thirteen strands in the bottom flange of the girder. The reduction in strands resulted in a decrease of approximately 18% in the overall girder moment capacity. The negative cracking moment of the girder at the connection interface was calculated to be 287 k-ft with a positive cracking moment of 158 k-ft.

Scaling of the girder reinforcement resulted in the use of wire mesh since standard rebar sizes were too large. Wire mesh was previously used in the system test girders as well as the girders for CT1 without encountering any problems. At one end of each girder, 1 in. diameter holes were placed to allow for the insertion of dowel bars.

3.3.3 Connection Design

Both the ESSP and ESBF connections were designed based on the scaled prototype positive and negative design moments using Equations 3.1-3.6. The test unit column overstrength moment was calculated using Equation 3.7.

$$M_o^t = M_o * sf * df * n \quad (3.7)$$

M^t_o = test unit column overstrength moment

sf = prototype to test unit scale factor

df = load distribution factor

n = number of girders

$$M_o^t = 42565 * 0.064 * 0.24 * 2 = 1308 \text{ k-ft}$$

Positive and negative design moments were then calculated:

$$M_{pos} = 0.30 * 1308 = 393 \text{ k-ft}$$

$$M_{neg} = 0.70 * 1308 = 916 \text{ k-ft}$$

www.manaraa.com

For the design negative moment the required amount of deck steel was calculated in the same manner as the prototype structure. The amount of deck steel that coincided to the negative design moment and allowed for even distribution across the width of the deck was calculated to be 5.26 $in.^2$, which results in a moment capacity of 940 k-ft.

Design of the connection for positive moment also followed the prototype design process using 3/8 in. strands. The moment resistance from dowel action needed to be calculated at the test unit scale and was found to be 160 k-ft for a single girder based on data from the system test and CT1. The number of strands per connection was then calculated in the same manner as the prototype structure and 5 strands were found to be required for each girder.

The embedment length of the curved strands for the ESBF connection was also based on current research at ISU and set at the recommended length of 60 inches. For the ESSP connection, the minimum overlap length of the strand ties and extended strands at the prototype level was specified by WSDOT as 8 in. For the test unit the overlap length was not scaled but instead was kept at the minimum prototype length of 8 in. to ensure integrity of the connection and facilitate force transfer from the extended strands to the strand ties.

After determining the amount of deck steel and the number of strands, the embedment length of the girder into the cap beam was scaled to 6.4 in. The embedment length of the girder has a direct impact on the amount dowel action developed for positive moments. One of the ways in which positive moment connections can be better designed is to gain an improved understanding of dowel action. Data from the CT1 GUSC test provided useful information regarding dowel action behavior, however, the GUSC connection had a larger embedment length of 12 in. In order to generate dowel action behavior comparable to the GUSC connection, the embedment length was increased to 9 in. The embedment length could have been increased to 12 in. for direct comparison. However, this would have created an unnecessarily large cap width at the prototype level. While the 9 in. embedment length corresponds to an increased prototype

www.manaraa.com

cap width, the increase was more reasonable than 12 in. and still allowed for adequate comparison of dowel action behavior.

3.3.4 Column and Footing Design

3.3.4.1 General

Since the testing focused on the connections, the column was designed to remain elastic throughout the test and the footing was then designed to resist the overstrength moment of the column. As the test unit was being designed, planning was underway for the design of a third connection test. With this in mind, the footing and column of the test unit were designed to be reused after completion of the ESBF and ESSP connection tests. A cast-in-place square column and footing were chosen and post-tensioning ducts were inserted in the column and footing for placement of 2 in. diameter, 150 ksi post-tensioning bars. As shown in Figure 3.8, the post-tensioning bars would be anchored in a pocket underneath the footing, run through the column, and be extended through the top of ducts. The bars would be post-tensioned to secure the cap to the column and also provide column moment resistance. At the completion of the test, the tension in the bars would be released, the cap beam removed, and the footing and the column reused.

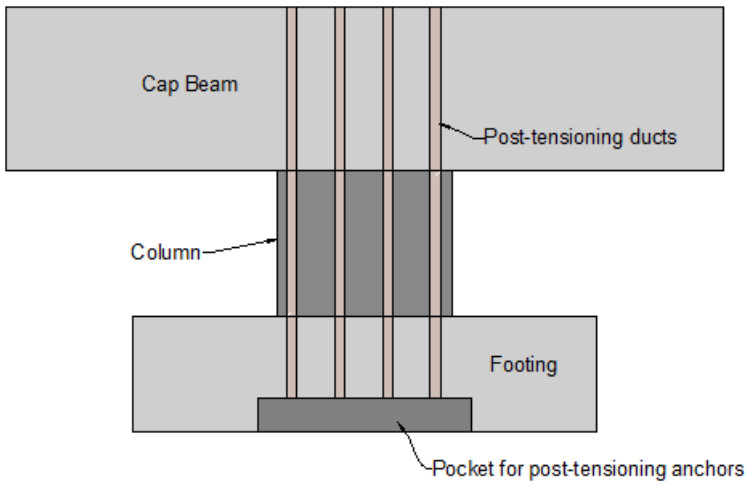

Figure 3.8: Post-tensioning bar schematic

www.manaraa.com

3.3.4.2 Column Design

The column was designed based on the expected connection positive and negative moments. The negative design moment would produce the largest force at the column cross-section and was calculated to be 940 k-ft. Inelastic behavior of the connection could cause a large negative moment with a maximum value of 1410 k-ft assuming all the deck steel reaches an ultimate stress of 99 ksi. Therefore, the column design moment was taken to be 1410 k-ft.

A 3 ft x 3 ft square column section was chosen and twelve round 2.37 in. ducts were placed in the column as shown in Figure 3.9. A check was performed for the post-tensioning force required in the bars to meet the design moment of 1410 k-ft by using stress calculations and setting Equations 3.7 and 3.8 equal to each other.

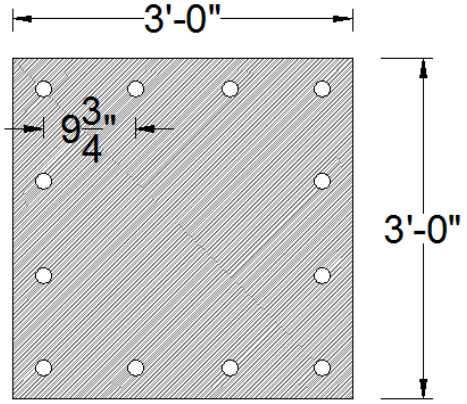

Figure 3.9: Column cross-section

Equation 3.7 assumes that the moment is applied diagonally from one corner of the column due to the girders being tested individually:

$$\sigma = (M_o^t * y)/I \qquad (3.7)$$

σ = bending stress

y = distance from centroid to point of bending (measured diagonally)

I = moment of inertia of column section

$$\sigma = (1410 * 12\ in./ft * 25.45\ in.)/139986 in.^4 = 3.07 \text{ ksi}$$

Equation 3.8 was used to check the required force in prestressing bars:

$$P = (A * \sigma)/n_b \qquad (3.8)$$

www.manaraa.com

P = force in bars
A = area of column section
n_b = number of bars

$$P = \frac{1296\ in.^2 * 3.07\ ksi}{12\ bars} = 332 \text{ kips}$$

A single 2 in. diameter, 150 ksi post-tensioning bar yields at a force of 308 kips. Therefore the post-tensioning bars would not be able to resist the design moment of 1410 k-ft. A lower force in the bars of 275 kips corresponded to a column moment resistance of 1170 k-ft. This moment resistance was above the negative design moment of 940 k-ft and also allowed for some inelastic behavior in the negative direction. It was decided that the moment of 1170 k-ft would be acceptable for the test in order to prevent yielding of the post-tensioning bars or increasing the column dimensions. Stirrups were then added to the design at 3" on center spacing.

3.3.4.3 Footing Design

The design of the footing was based on column design moment of 1410 k-ft in order to be conservative. The layout of the ISU laboratory strong floor, which has tie down locations spaced every 3 feet, was also considered in the design. The footing was designed as an 8 ft x 8 ft x 2 ft square and the reinforcement details were calculated using Equations 3.9-3.12.

Force developed at tie down locations:

$$F_c = M_o^t / s \qquad (3.9)$$

F_c = Force couple developed at tie down locations

s = largest spacing between tie downs

$$F_c = \frac{1410}{6\ ft} = 235 \text{ kips}$$

Calculation of moment at column face:

$$M_{cf} = F_c * h \qquad (3.10)$$

M_{cf} = Moment at column face due to tie down force

h = height of footing

$$M_{cf} = 235\ kips * 24\ inches = 5640 \text{ k-in.}$$

www.manaraa.com

Equivalent stress block equations were used for calculating moment capacity:

$$a = \frac{A_s f_y}{0.85 * f_c' * b} \quad (3.11)$$

$$M_{cf} = A_s f_y (d - \frac{a}{2}) \quad (3.12)$$

a = depth of equivalent stress block

A_s = area of steel

f_y = yield stress of steel

$f'c$= concrete strength

b = effective width of footing (distance between tie down locations)

d = depth from top of footing to location of tension steel

The following values were used for each variable:

M_{cf} = 5640 k-in

f_y = 60 ksi

f'_c = 4 ksi

b = 72 inches

d = 21 inches (assuming 3 in. was used for clear cover and stirrups)

Iteration of A_s was performed to reach a solution:

A_s = 4.5 in.^{2}

a = 1.21 inches

The area of steel (A_s) was then divided by the effective width (b) to provide a required amount of 0.75 in.^{2} of steel per foot. Two #6 bars spaced at 6 inches meets this requirement. Although #6 bars were specified, a miscalculation caused #7 bars to be used. This did not adversely affect the design or construction of the footing, but did provide the footing with extra moment capacity. Stirrups were added to the footing according to current Caltrans design details. A 44 in. x 44 in. x 7 in. block out was left underneath the footing to anchor the column post-tensioning bars as shown in Figure 3.10.

www.manaraa.com

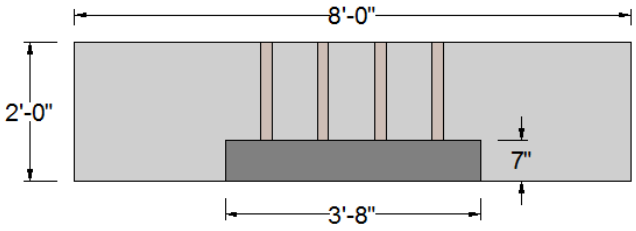

Figure 3.10: Footing block out detail

3.3.5 Cap Beam Design

The cap beam for the test unit was also scaled from the prototype structure. Post-tensioning ducts were placed at the center of the beam to allow connection to the column. The cap reinforcement was detailed to accommodate the two girders which were attached 4 feet on either side of the column centerline to allow construction of each girder with its own deck. The cap had a design width of 54 in., height of 37.25 in., and length of 12 ft 4 inches.

Design for torsional forces within the cap was required since girders were only attached to one side of the cap beam and each girder would reach full flexural capacity as a girder-deck composite member. The torsional resistance of the cap needed to be greater or equal to the design moment of the column since the moment at the connection would be roughly equivalent to the cap beam torsion. The Priestley method, based on plastic shear friction, was used to approximate the torsional capacity by dividing the cap beam into triangular quadrants as shown in Figure 3.11 (Priestley, 1996).

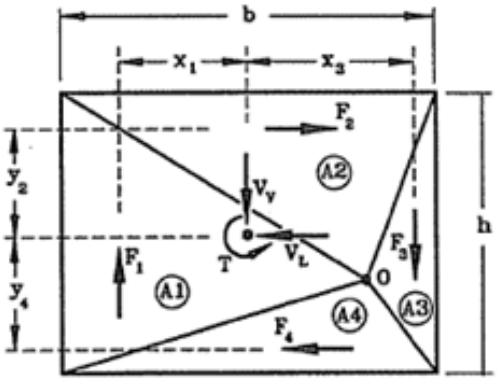

Figure 3.11: Cap beam section with triangular quadrants

www.manaraa.com

Torsional resistance of the cap beam was then calculated using the following equations:

$$T = F_1 x_1 + F_2 y_2 + F_3 x_3 + F_4 y_4 \quad (3.13)$$

T = torsional capacity

F_i = force component of triangular area (Figure 3.12)

xi,yi = distance from section centroid to triangle centroid

Equation 3.13 can also be rewritten as:

$$T = \frac{\mu P}{A} (A_1 x_1 + A_2 y_2 + A_3 x_3 + A_4 y_4) \quad (3.13a)$$

P = clamping force

μ = coefficient of friction of cap interface

A_i = triangular area of cap beam

$$P = F + V_T + 0.0006 E_s A_{st} \quad (3.14)$$

F = cap beam prestressing force

V_T = column transverse shear force

E_s = modulus of elasticity of steel

A_{st} = total area of cap beam longitudinal reinforcement

Since no prestressing force is applied to the cap and the column transverse shear is assumed to be zero:

$$P = 0.0006 E_s A_{st}$$

$$P = 0.0006(29000\ ksi)(22.88\ in.^2) = 398\ kips$$

Two more equations were then used to solve for torsion:

$$V_v = F_1 - F_3 = \frac{\mu P}{A}(A_1 - A_3) \quad (3.15)$$

$$V_L = F_2 - F_4 = \frac{\mu P}{A}(A_2 - A_4) \quad (3.16)$$

V_v = vertical shear

V_L = lateral shear

No lateral shear would be experienced by the cap beam, therefore F_2 is equal to F_4 and A_2 is equal to A_4. Equations 3.13a, 3.15, and 3.16 were then used along with the following values and iterated to calculate a cap torsional capacity of 670 k-ft.

www.manaraa.com

$\mu = 1.4$ (Priestley, 1996)

$A = 2012$ in.^{2}

$V_v = 110$ kips

x_i, y_i = calculated based on areas A_1-A_4

Since the torsional capacity of the cap was lower than the column design moment, longitudinal post-tensioning ducts were added to the design. The ducts were designed for six 1-3/8 in. diameter Diwidag bars that would be post-tensioned to 80 kips each. The post-tensioning added 480 kips to the clamping force (P) and increased the torsional capacity of the cap beam to 1537 k-ft, which was greater than the required value of the column design moment. It was determined that the post-tensioning of the Diwidag bars would not need to take place until loads higher than the combination of gravity, horizontal seismic, and 0.5g vertical acceleration were applied to the test unit.

3.4 Test Unit Construction

3.4.1 Construction sequence

Construction of the test unit took place in the ISU structures laboratory. The reinforcement cage for the footing and column were tied as a single piece and a wood insert was placed at the bottom of the footing to form a 7” pocket for the post-tensioning anchorage. Steel plates with holes at the post-tensioning bar locations were placed on top of the wood insert (Figure 3.12). The plates would be cast into the footing and provide a bearing surface for the post-tensioning anchors. Twelve 59 mm post-tensioning ducts were tied to the column stirrups and PVC tubes were inserted in the footing reinforcement to allow the footing to be secured to the strong floor of the laboratory. The column post-tensioning bars were then set in the ducts to ensure that the ducts stayed straight during the both the footing and column concrete pours.

www.manaraa.com

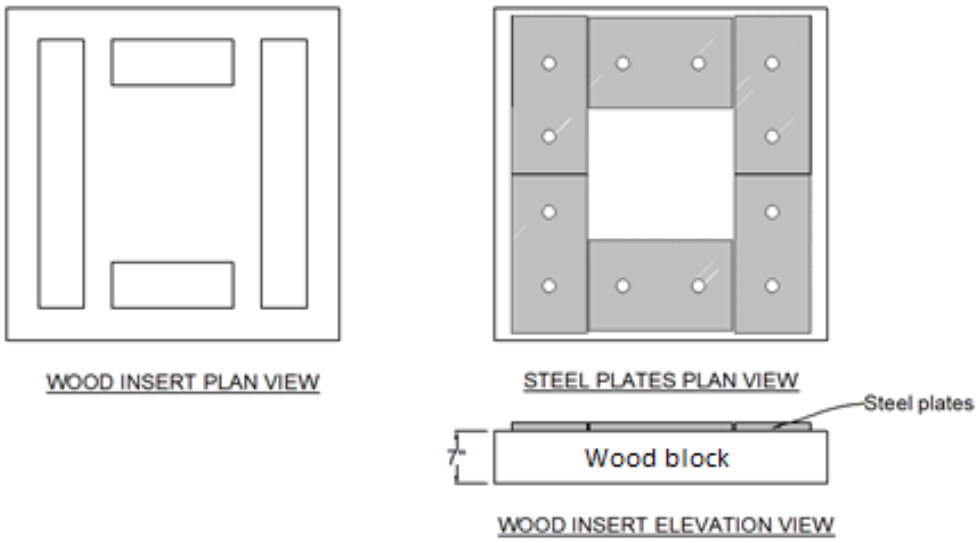

Figure 3.12: Wood insert details

The footing was poured first and a second pour was done a week later for the column (Figure 3.13). Once the concrete had cured and the formwork was removed, the footing was moved to the test location within the laboratory. The footing was lifted so that nuts and washers could be attached to anchor the post-tensioning bars inside the 7" pocket. The footing was then set in place, a layer of hydrostone was poured underneath to ensure a level bearing surface, and the footing was secured to the laboratory strong floor.

The cap beam was constructed following the completion of the footing. Most of the reinforcement cage was tied on the floor (Figure 3.14) with ducts set in place for both the column and longitudinal post-tensioning. A platform was constructed around the cap beam and the cap was then lifted and lowered into place over the column post-tensioning bars (Figure 3.15). Strain gages were attached at specific locations on the cap and a portion of the cap steel was left unfinished until the girders were set in place.

www.manaraa.com

Figure 3.13: Footing and Column pour

Figure 3.14: Cap beam reinforcement cage

Figure 3.15: Cap beam set in place on platform over column bars

www.manaraa.com

The precast girders were cast at Cretex Concrete Products in Iowa Falls, Iowa and shipped to the ISU structures lab. A visit was made to the precast plant before pouring of the girders to attach instrumentation and ensure correct placement of rebar (Figure 3.16).

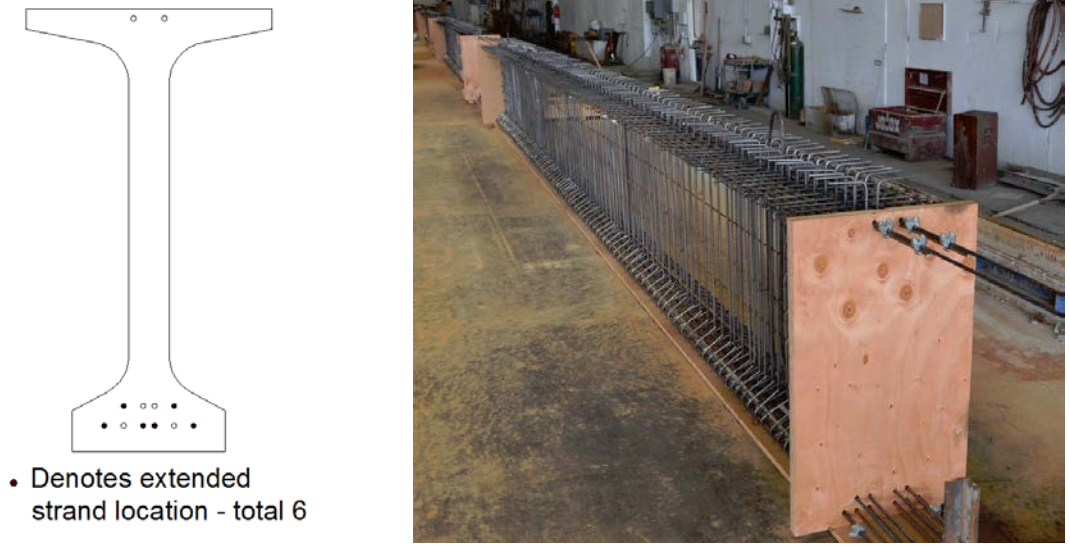

Figure 3.16: Girder strand layout and rebar cage

The girders arrived at the ISU laboratory with six of the ten strands extending 8 feet from each girder. Since six strands were extended but only five were needed for the connection, the strand in the upper row that would be located furthest away from the test unit column was cut. The girders were then placed on temporary formwork and the five remaining strands were instrumented and extended into the cap beam according to each connection detail. The bent strands from the ESBF connection were curved and threaded through the cap reinforcement (Figure 3.17). For the ESSP connection (Figure 3.18) strand chucks were welded to anchor plates and then attached to the strand ties and extended strands. Two additional strands were also added on the back side of the cap to simulate opposite girder strands as shown in Figure 3.19. The added strands were instrumented to see if any force would be transferred from the ESSP connection to the opposite side of the cap beam. If force is transferred all the way through the cap, it could result in force interaction between girders on each side of the cap beam and result in a decreased connection moment capacity.

www.manaraa.com

Figure 3.17: ESBF connection prior to cutting one strand and inserting strands into cap beam

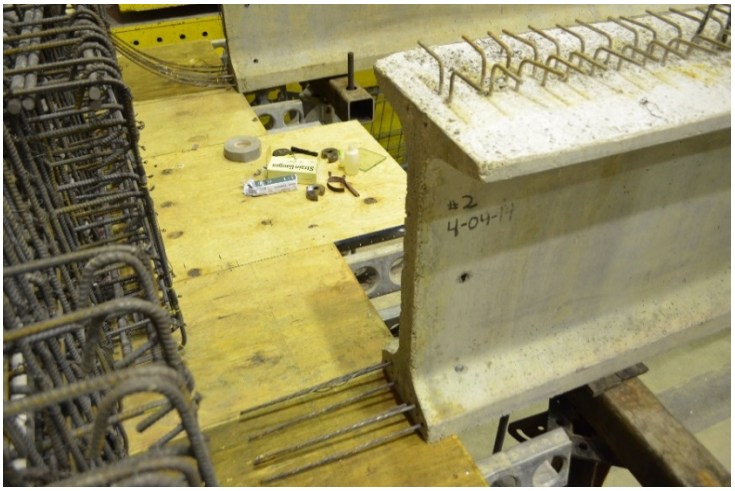

Figure 3.18: ESSP connection prior to cutting one strand and attaching anchor plates and chucks

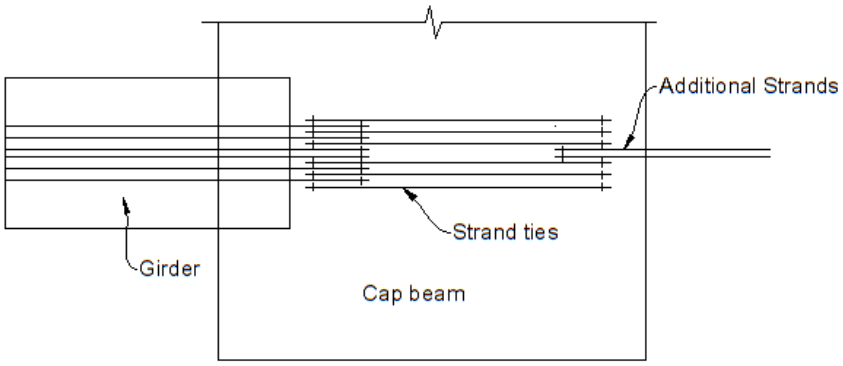

Figure 3.19: Additional strands on back side of cap beam

www.manaraa.com

Before the remainder of the cap reinforcement was added, the dowel bars were instrumented, inserted through the web of the girders, and grouted in place. The rest of the cap reinforcement was then added and the cap formwork was fabricated and set into place. The longitudinal cap post-tensioning bars were also inserted to make sure that the ducts remained straight during the concrete pour. The deck formwork was constructed with bridge hangars, brackets, and plywood. Deck reinforcement was placed over the girders and tied both along the girder and into the cap beam (Figure 3.20). The reinforcement was instrumented and plastic inserts were placed in the formwork to allow actuators to be attached to each girder. The cap and girder concrete were then placed in one continuous pour and allowed to cure (Figure 3.21).

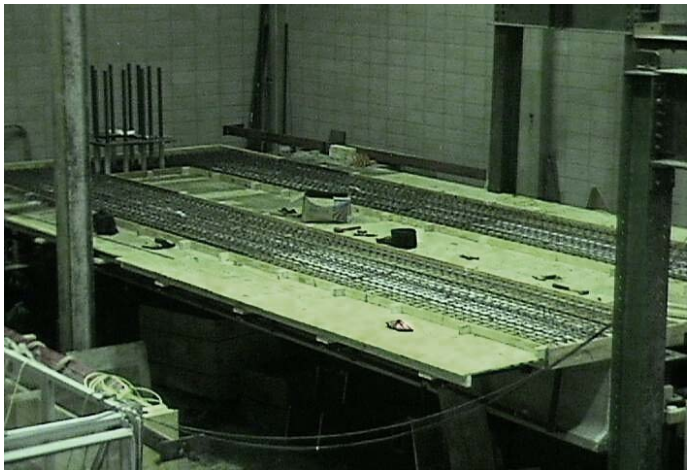

Figure 3.20: Deck formwork and rebar

Figure 3.21: Completed cap and deck concrete pour

www.manaraa.com

3.4.2 Construction challenges

A few challenges occurred during construction. One of these challenges was the placement of the strands in the ESSP connection. It was decided to place the strands after constructing the cap reinforcement cage. Once the anchor plates and chucks were attached to the strands it was difficult to slide the extended strands into place due to the tight spacing of the cap reinforcement. The cap steel spacing also made it difficult to place the strand ties. Eventually the strands were able to be placed correctly by temporarily removing some of the cap reinforcement. The problem could have been prevented by placing the strands prior to constructing the cap reinforcement.

A second challenge occurred during the concrete pour of the cap beam and deck. Two trucks were used to bring the concrete to the ISU laboratories. Plasticizer was added to the first truck, but the mix started to stiffen very quickly upon placement. The stiffness of the concrete prevented it from flowing freely through the tight cap reinforcement. A larger amount of plasticizer was added to the second truck and no problems were experienced. However, after the concrete cured, gaps and honeycombing were found in areas on the cap where the concrete from the first truck had been poured. The cap was repaired by patching the gaps with concrete and filling in the honeycomb areas with high-strength grout. To prevent this problem in the future it is recommended that a retardant be added to the concrete mix along with the plasticizer to allow proper pour time.

3.5 Instrumentation

3.5.1 General

To capture the behavior of the girder to cap beam connections in the test unit, instrumentation was attached both internally and externally. The internal instrumentation consisted of strain gages placed on rebar, extended strands, and dowel bars. The external instrumentation included DCDT's, string pots, and an Optotrak camera system.

www.manaraa.com

3.5.2 Internal Instrumentation

Strain gages were placed in specific locations to capture the response of the cap beam. On the cap longitudinal reinforcement, gages were placed to capture the torsional behavior as shown in Figure 3.22. Gage labels are shown with CTL corresponding to gages placed on the cap top longitudinal reinforcement and CBL corresponding to the cap bottom longitudinal reinforcement. At girder connection regions, gages were placed at and around the girder interface on the cap transverse reinforcement to monitor the effects of the girder movement as shown in Figure 3.23. The gage labels indicate either the spliced strand (CTSS) or curved strand (CTCS) connection.

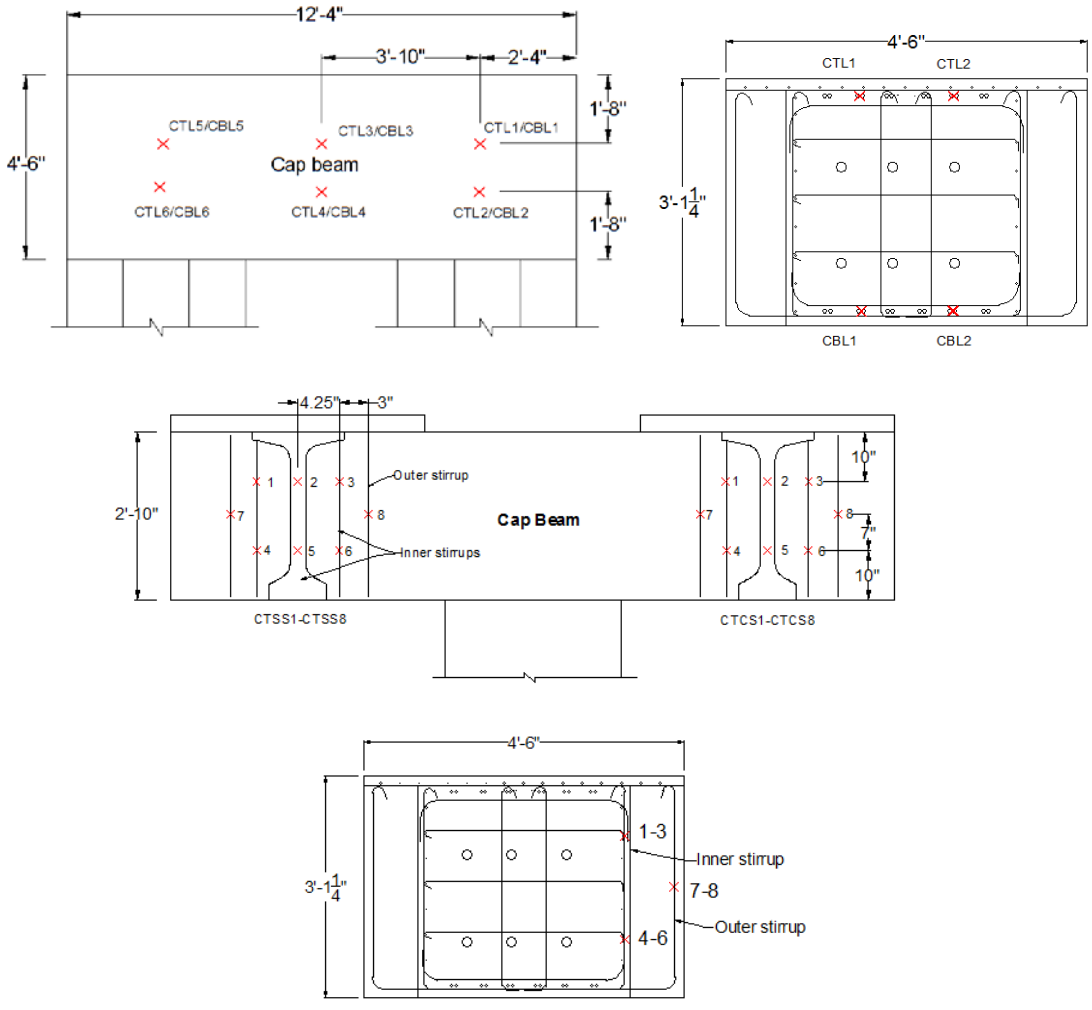

Figure 3.23: Cap stirrup gages

www.manaraa.com

For the ESBF connection, the two middle extended strands in the bottom row were instrumented. Gages were placed at the connection interface between the girder and cap and also 15 inches on either side of the bend as shown in Figure 3.24. The gage labels CS1-CS3 correspond to the middle strand closest to the column. For the ESSP connection, instrumentation was placed on the same strands as the ESBF connection. Gages were placed at the connection interface, at plate and chuck locations, and also at two additional points on the stand ties to monitor the transfer of tension force as shown in Figure 3.25. Gage labels SS1-SS2 and SS5-SS8 were located on the strand furthest from the test unit column.

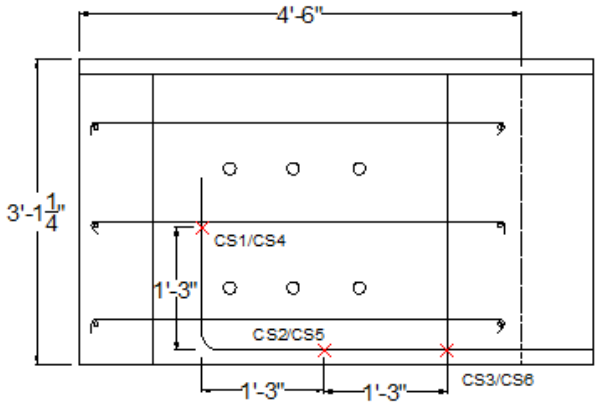

Figure 3.24: ESBF extended strand gages

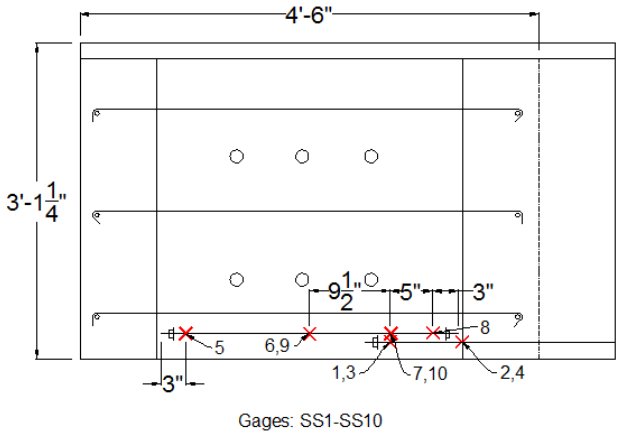

Figure 3.25: ESSP strand gages

For both connections gages were also placed on the dowel bars and crossties as shown in Figure 3.26. Gage labels are only shown for the ESBF connection (indicated

www.manaraa.com

by “CS” in label name) but gages were placed in the same locations for the ESSP connection. Three crosstie gages (CSC1-CSC3) were added with CSC1 and CSC3 placed on the column side of the connection and CSC2 placed on the lowest crosstie at the outside of the connection. A larger number of gages were placed on the lower dowel bars to better quantify the dowel resistance for positive moments.

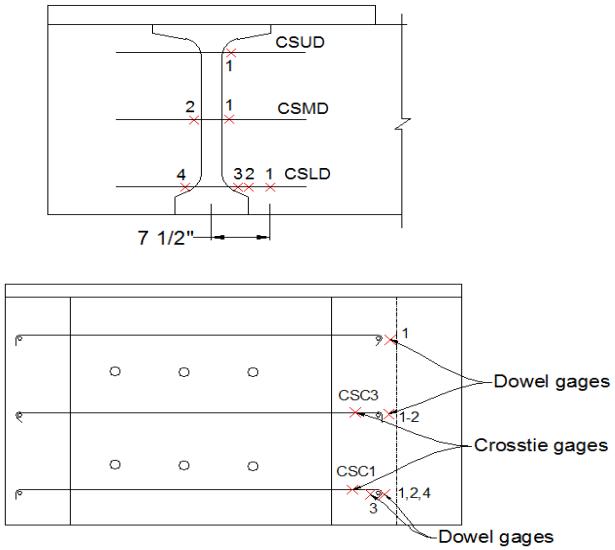

Figure 3.26: Dowel and crosstie gages

Gages were also placed on the prestressing strands inside the girders as shown in Figure 3.27. The gages were attached after the strands were pulled to the proper prestressing force but before the girder concrete was cast. Strands were placed 1, 2, 4, and 15 feet from end of the girder and were located on the center strand noted in Figure 3.28. These gages would monitor the length of strain penetration into the girder caused by tension forces under positive moments. Gages were also placed on the top layer of deck steel to monitor the condition deck reinforcement under negative moments as shown in Figure 3.29.

www.manaraa.com

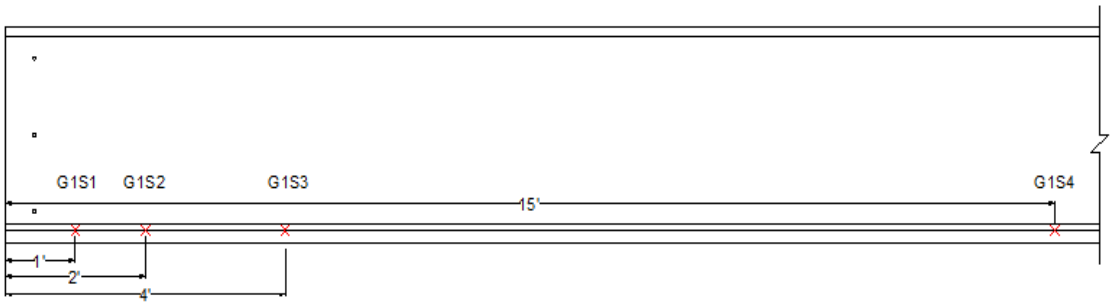

Figure 3.27: Girder strand gages

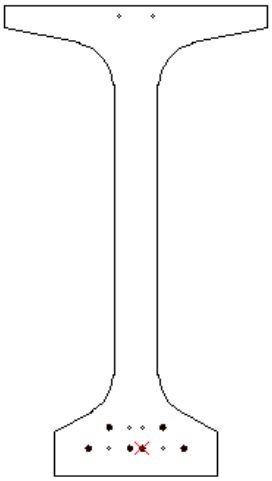

Figure 3.28: Girder cross section

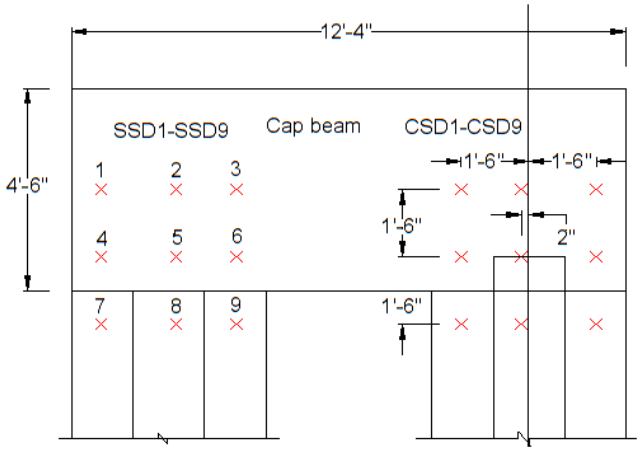

Figure 3.29: Deck steel gages

www.manaraa.com

3.5.3 External Instrumentation

To record movement of the girder at the girder to cap interface, three DCDT linear displacement transducers were used. One was located underneath the girder to cap connection as shown in Figure 3.30, another of at the top of the girder to cap connection, and a third was located on top of the deck at the edge of the cap beam (Figure 3.31). DCDT's were also placed at the column to cap connection to monitor the movement of the cap beam and ensure that the column post-tensioning bars were not overloaded. For the ESSP connection, a DCDT was placed on one of the additional strands at the backside of the cap beam (Figure 3.19) and a load cell was placed on the second in order to monitor possible load transfer from the connection region through the strand ties.

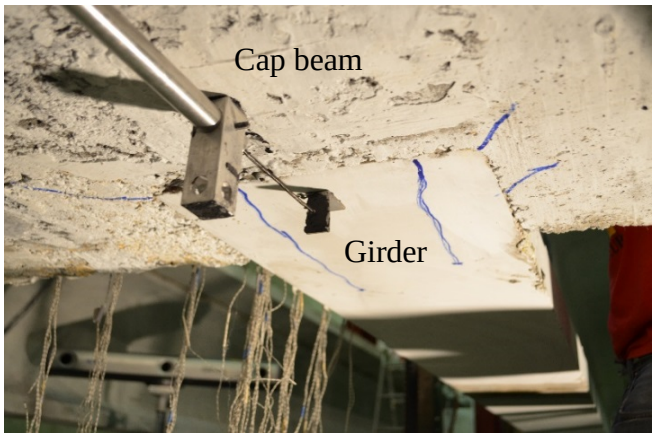

Figure 3.30: DCDT at underside of girder to cap connection

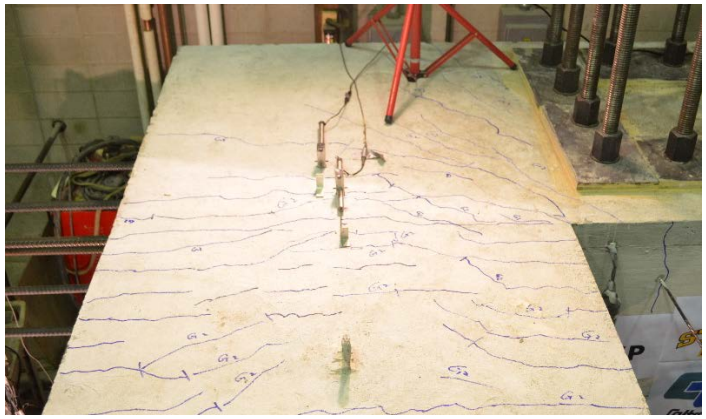

Figure 3.31: DCDT's on top of girder and deck

String pots were used to measure displacement at various points on the test unit and along the girders. Four string pots were placed horizontally on the sides of the cap beam

www.manaraa.com

along with two vertical string pots under the cap to monitor rotation. Two additional string pots were also placed horizontally at the actuator locations to monitor out-of-plane movement of the girders. Lastly, a string pot was placed vertically under the girder at each actuator location to record vertical displacements (Figure 3.32 and Figure 3.33).

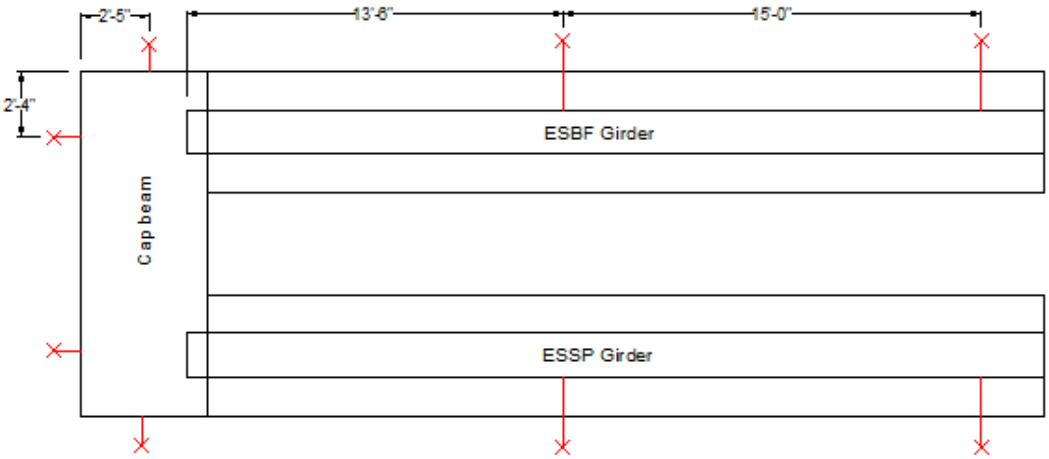

Figure 3.32: Locations of horizontal string pots

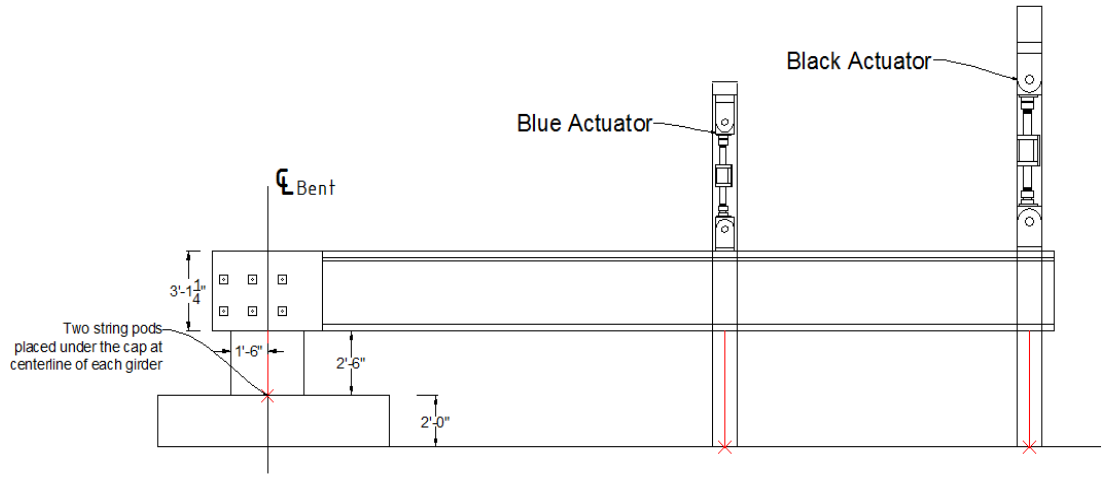

Figure 3.33: Location of vertical string pots

An Optotrak camera system was used to record 3-dimensional movement on the surface of the connection region. LED sensors were glued to the inside region of each connection as shown in Figure 3.34. During the testing of each connection, the Optotrak

www.manaraa.com

camera recorded the movement of the LED's which would allow surface displacements and cracking to be measured.

Figure 3.34: LED configuration at connection region

3.6 Material Strength

Material strengths for the members of the test unit were recorded throughout the construction process and also on the day of testing as shown in Table 3-3. The reinforcement used throughout the project is A706 steel and all the strands were 270 ksi low-relaxation strands.

Table 3-3: Material strengths

Member		Strength (psi)		
	Release	7 day	28 day	Test day
Footing	-	3093	4258	-
Column	-	3478	4302	-
Cap Beam and deck	-	3618	4319	4505
ESBF girder	6665	12410	12577	10085
ESSP girder	6665	12410	12843	11201
Dowel bar grout	-	-	-	6553
Cap and Deck Steel (A706)	yield	60000	ultimate	90000
270 ksi Relaxed Strands	yield	230000	ultimate	250000

www.manaraa.com

3.7 Loading Protocol

To test the capacity of the connections, each girder would be individually tested by pushing and pulling a pair of actuators pseudo-statically as shown in Figure 3.35. The actuator forces applied to the test unit would correspond to target shear and moment values determined by the loading protocol. The test unit was a scaled representation of the prototype structure, therefore the target moment and shear values were also scaled from the prototype level. Prototype loads resulting from gravity, horizontal ground acceleration, and vertical ground acceleration forces were calculated. Each type of load will be discussed in the following sections.

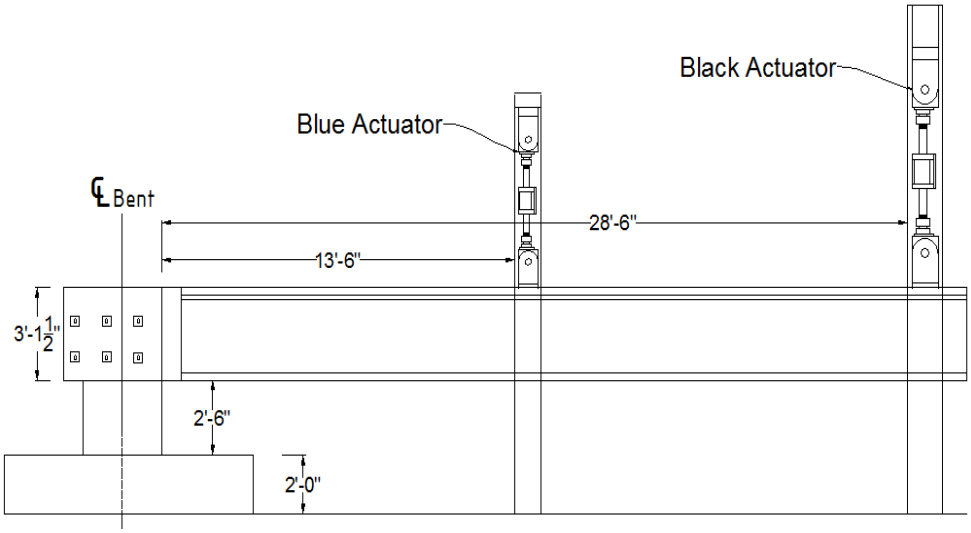

Figure 3.35: Test unit setup

3.7.1 Gravity Load

The calculation of gravity load for a bridge utilizing precast concrete girders depends on the type of cap beam selected and how the girders are supported throughout the construction process. For a cast-in-place cap beam, there are three phases of construction. In the first phase, the girders are lifted into place and supported by falsework as shown in steps 1-2 of Figure 3.36. The end condition of these girders is considered to be pinned and the self-weight of the girders does not cause any moment to be generated at the connection. In steps 3-4 the cast-in-place cap beam, abutments, and

www.manaraa.com

deck are poured. The girders will rotate a small amount due to the added weight of the deck, but it is assumed that any rotation of the girder takes place before the cap and deck fully cure. Due to this assumption the girder and deck do not create any gravity moment at the connection region because rotation took place before the connection became fixed.

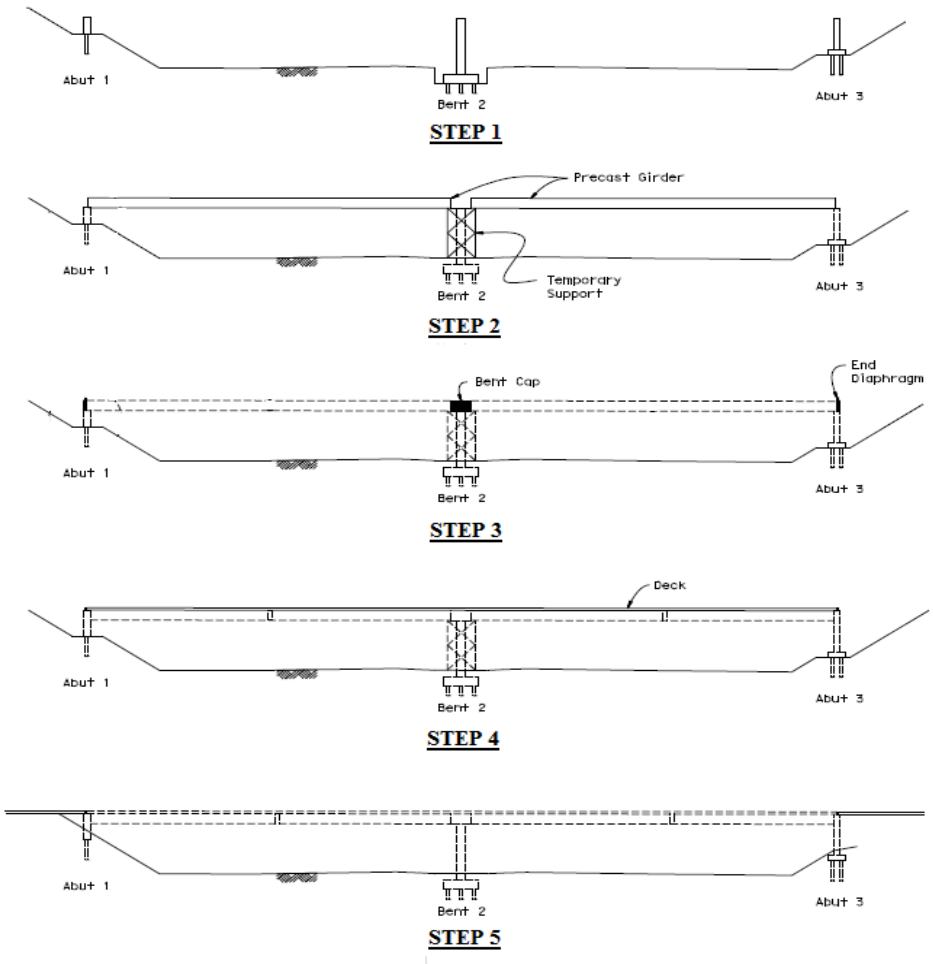

Figure 3.36: Construction sequence (California Department of Transportation, 2013)

The third phase includes step 5 in which the falsework is removed and a wearing surface and barriers are place on top of the deck. A gravity moment is generated at the connection region by the weight of the girder, deck, wearing surface and barriers. A precast cap beam follows the same construction process, but provides a permanent bearing surface for the girders which eliminates the need for falsework. The bearing surface provided by the precast cap reduces the gravity moment at the connection

www.manaraa.com

because the girder and deck self-weight continue to be supported by the cap beam and no rotation occurs due to the removal of the falsework. The gravity moment for a precast cap is produced by the weight of the bearing surface and barriers.

For the test unit a precast cap was used, however, when comparing the maximum positive moment generated for each type of cap beam, a precast cap beam is the worst case scenario. This is because in order for a connection to be subject to positive moments the gravity moment of a structure must first be overcome. A precast cap has a lower gravity moment due to the bearing surface provided for the girders and therefore requires a greater positive moment capacity. It was decided to test the ESBF and ESSP connections for the worst case possible to determine the capacity and performance of each connection. Therefore the self-weight of the wearing surface and barrier were used to produce the gravity moment and shear values for the loading protocol.

3.7.2 Horizontal Ground Motion

The previously mentioned system test was used to calculate forces caused by horizontal ground motion acting longitudinal to the bridge girders. Results of the system test gave the largest horizontal force experienced by a single girder in the system test prototype. This force was then multiplied by the appropriate scale factor to convert the force to the current prototype. The scaled force was converted to the connection moment value by multiplying by half the height of the prototype column since it was assumed that a plastic hinge would form at each end of the column. The resulting moment was then multiplied by the factor of 0.45 for the positive direction and 0.55 for the negative direction (Snyder, 2010) in order to distribute the horizontal seismic forces and then scaled for application to the test unit.

3.7.3 Vertical Ground Motion

The vertical ground acceleration forces were calculated based on the mass of the prototype structure. Target values for vertical acceleration were 0.5g and 1.0g. Since weight is mass multiplied by acceleration, the entire self-weight of the prototype girder and slab was multiplied by 1.5 and 2.0 respectively. The multiplied self-weights were

www.manaraa.com

then used to calculated moment and shear values for the connection region which corresponded to the fixed-fixed end condition of the girders and scaled to be applied to the test unit.

3.7.4 Combination of Forces for Loading Protocol

Upon determining the gravity, horizontal seismic, and vertical seismic target moment and shear values, a loading protocol was developed by combining each load. Figure 3.37-3.42 show the progression of adding horizontal and vertical seismic forces to the gravity load at the connection region. The graphs are formulated to show two 30 ft girders which meet at the connection region located where the distance equals zero. The graphs do not show forces in the cap beam, instead zero is taken to represent the end of each girder at the connection region. For the test unit, each girder was attached to two actuators and cantilevered from the bent cap. The actuators had the option of being controlled by either force or displacement input values. Force values were used to match the moment applied to the test unit with scaled loads calculated from the prototype. It is important to note that the loads applied by the actuators only matched the prototype loads in the connection region in order to simplify the testing.

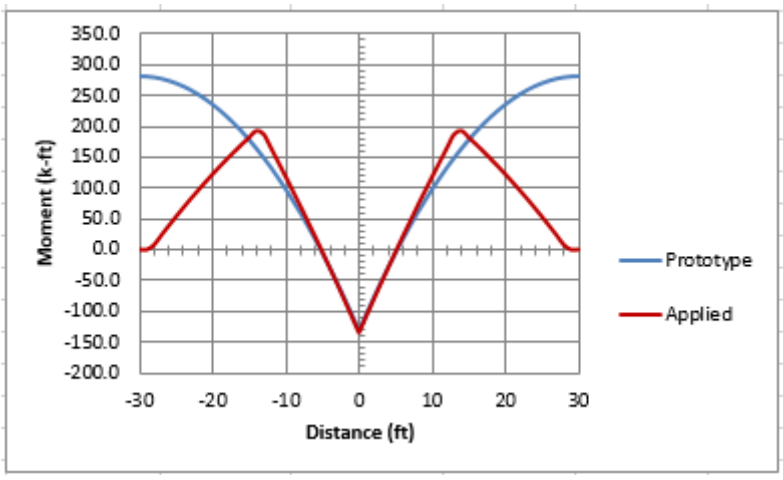

Figure 3.37: Gravity moment along the girders and at the connection

www.manaraa.com

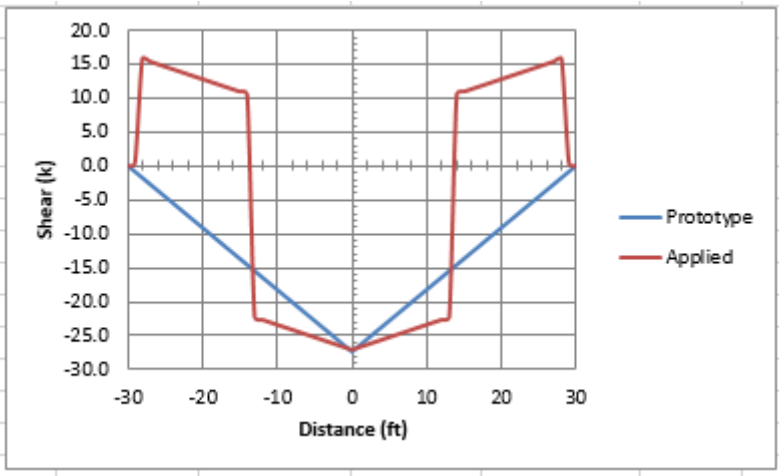

Figure 3.38: Gravity shear along the girders and at the connection

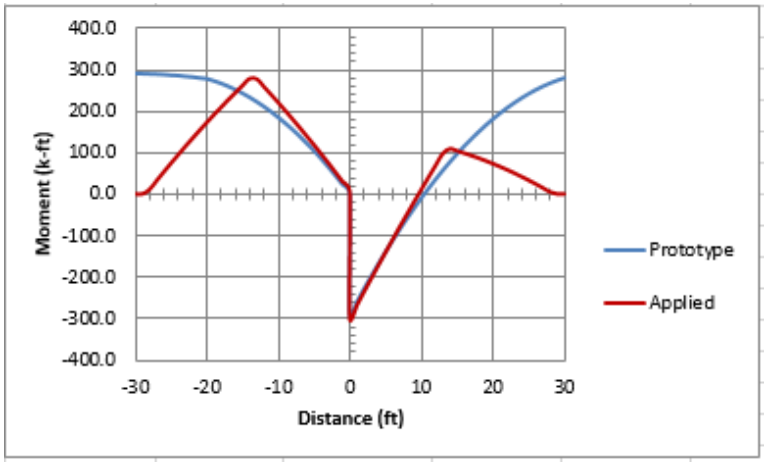

Figure 3.39: Gravity + horizontal moment along the girders and at the connection

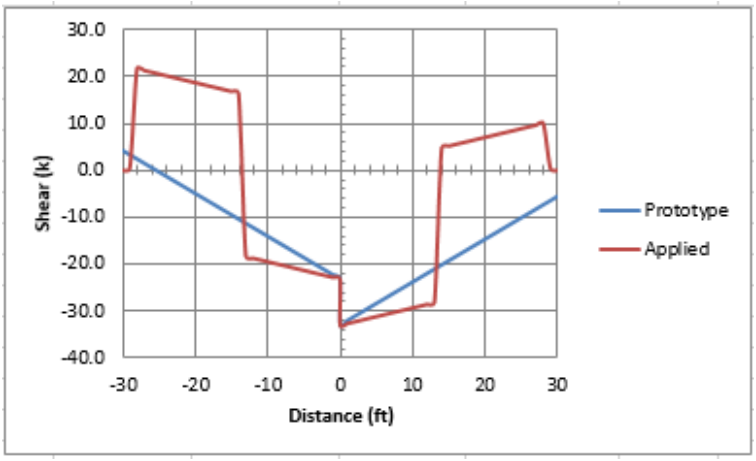

Figure 3.40: Gravity + horizontal shear along the girders and at the connection

www.manaraa.com

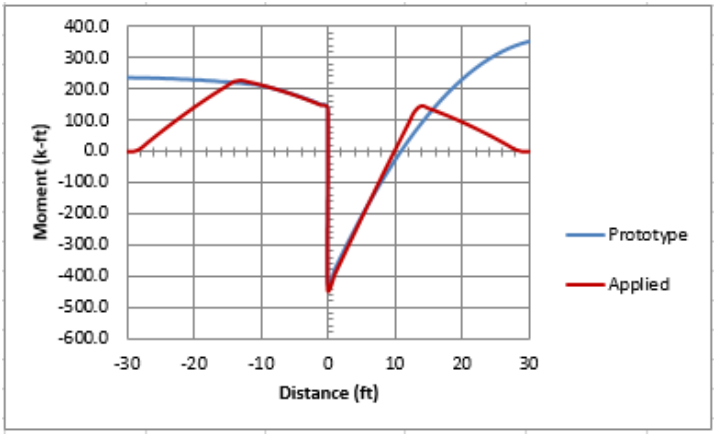

Figure 3.41: Gravity + horizontal + 0.5g vertical moment along the girders and at the connection

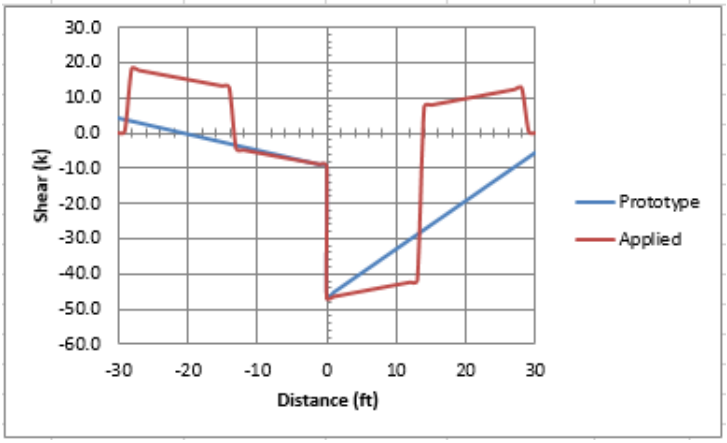

Figure 3.42: Gravity + horizontal + 0.5g vertical shear along the girders and at the connection

Four target moment and shear values are shown in Table 3-4 which represent a gradual increase in force and the target levels of girder performance. The target values, with the exception of the gravity load, each contained values for positive moment, positive shear, negative moment and negative shear in order to accurately simulate the reversal of forces that the prototype structure would experience.

Table 3-4: Target Moment and Shear Values

Target Values	Positive Moment (k-ft)	Positive Shear (k)	Negative Moment (k-ft)	Negative Shear (k)
Gravity (G)	-	-	-130.00	-27.5
G + Horizontal Seismic (H)	23.5	-22.3	-317.50	-33.7
G + H + 0.5g Vertical Seismic (0.5gV)	160.8	-8.6	-454.90	-47.4
G + H + 1.0g Vertical Seismic (1.0gV)	298.1	5.1	-592.20	-61.2

www.manaraa.com

After applying the gravity load, a series of four load steps were exercised as the load was increased to the next target value. Each load step contained both a positive and negative moment value which the girder was cycled between three times. The cycling of actuators was performed in order to simulate seismic activity and fully exercise the connection. The actuators are labeled by color and located along the length of the girder. The blue actuator was located 13.5 ft from the connection interface while the black actuator was located 28.5 ft from the interface. The connection interface was assumed to be located at the end of the girder embedded in the cap beam. An example of the four load steps between gravity and the horizontal seismic target values (G+H) is shown in Table 3-5. For the actuator forces a positive value indicated that the actuator would push down while negative indicated that the actuator would pull up. An extra load step was added between 0.5g and 1.0g vertical acceleration in order to provide more details regarding the connection performance beyond the target value of 0.5g. The loading protocol for the entire testing sequence is included in Appendix C, however a graphical representation is provided in Figure 3.43. In order to fully quantify each connection detail, the actuators would be switched to displacement control when the connections exhibited inelastic behavior. Each connection would then be exercised to failure. A loading sequence for the displacement cycles is shown in Figure 3.44. Negative displacements correspond to an upward displacement of the girder which generated a positive moment.

Table 3-5: Loading protocol example

Force (kips)				
Blue Actuator	Black Actuator	Target	Moment	Shear
32.5	-16.5	Gravity (G)	-134.55	-27.07
32.5	-14.70	Load Step 1		
32.95	-18.20			
32.5	-14.70			
32.95	-18.20			
32.5	-14.70		-185.85	-28.87
32.95	-18.20		-92.18	-25.82

www.manaraa.com

Table 3.5 continued

Force (kips)				
Blue Actuator	Black Actuator	Target	Moment	Shear
32.5	-12.90	Load Step 2		
33.4	-19.90			
32.5	-12.90			
33.4	-19.90			
32.5	-12.90		-237.15	-30.67
33.4	-19.90		-49.8	-32.5
32.5	-11.10	Load Step 3		
33.85	-21.60			
32.5	-11.10			
33.85	-21.60			
32.5	-11.10		-288.45	-32.47
33.85	-21.60		-7.425	-23.32
32.5	-9.3	Load Step 4 Horizontal Seismic (H)		
34.3	-22.3			
32.5	-9.3			
34.3	-22.3			
32.5	-9.3		-339.75	-34.27
34.3	-23.3		34.95	-22.07

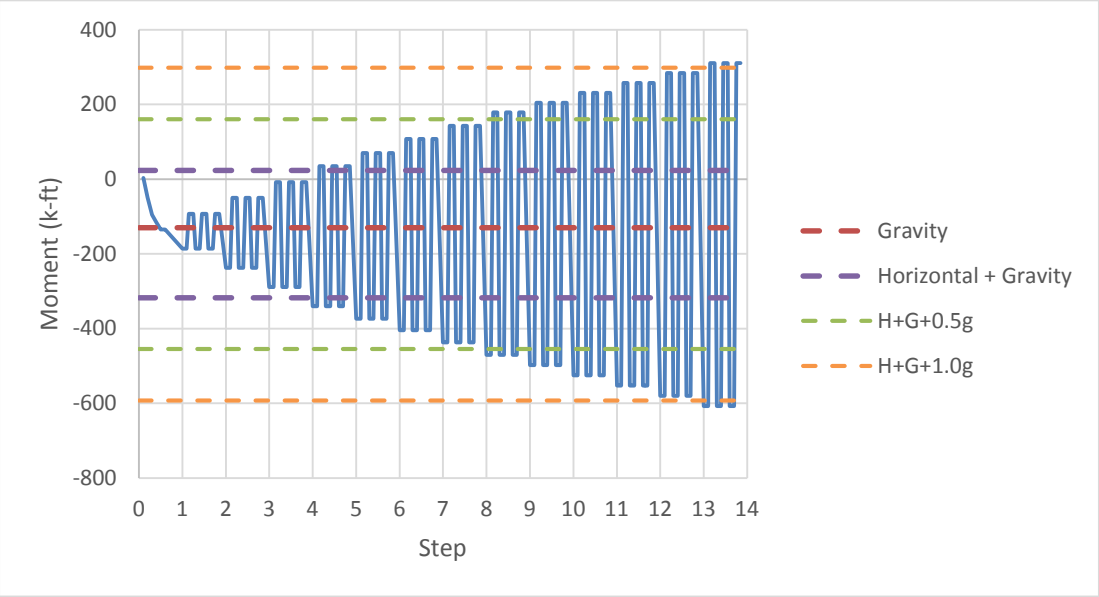

Figure 3.43: Force control loading protocol

www.manaraa.com

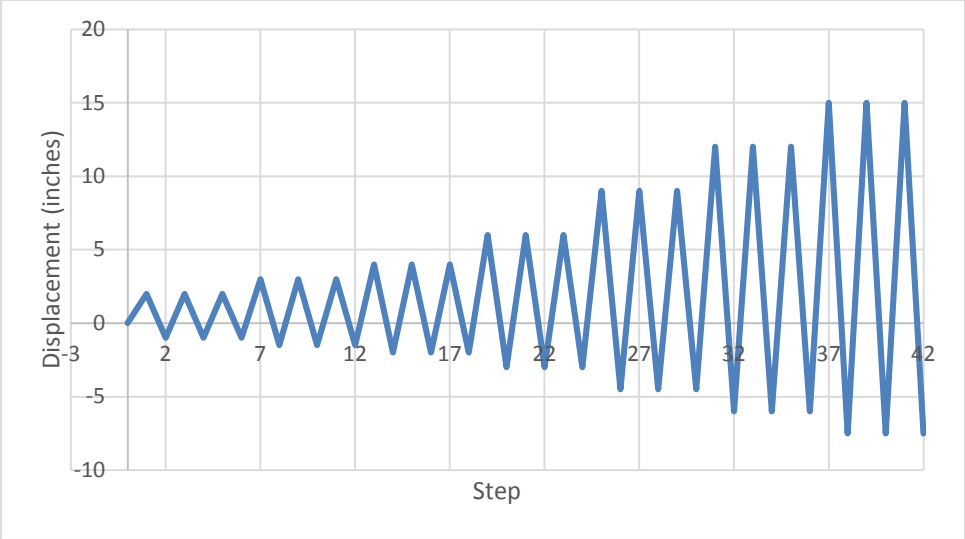

Figure 3.44: Displacement control loading protocol

3.8 Strain Penetration Analysis

3.8.1 Overview

In order to predict the behavior of each connection, a force based design approach was developed for the ESSP and ESBF girder to cap connections. The design approach utilized the relationship between strain penetration of rebar or strand and the corresponding moment applied to the connection. The method was designed to be applicable at both the test unit and prototype level and included application for both positive and negative moments.

3.8.2 Positive moment resistance

For the design of positive moment resistance, a method was developed based on the relationship between horizontal girder displacement and strain penetration in the extended girder strands. The relationship provides a force based approach to predict the displacement of the girder for positive moments and also includes the moment resistance from the dowel action in the connection.

3.8.2.1 Dowel action

For the strain penetration analysis, the moment resistance due to dowel action was quantified. Dowel action includes interaction between the dowel bars and surrounding concrete as well as concrete friction between the cap and girder. The ESBF

www.manaraa.com

and ESSP test unit connections contained three #4 dowel bars positioned as shown in Figure 3.45 and in both connections the girder extends into the cap beam 9 in. To calculate the moment resistance due to the dowel action, the first part of Equation 4.1 from ACI 318-11 was used to first calculate the shear resistance of the dowel bars. The calculated dowel bar shear resistance is assumed to be in the horizontal direction to counteract the tension force developed at the bottom edge of the girder due to positive moments. Calculation of the shear resistance assumed that only the bottom dowel bar and half of the middle dowel would be effective to resist positive moment. The dowel yield stress was assumed to be 66 ksi.

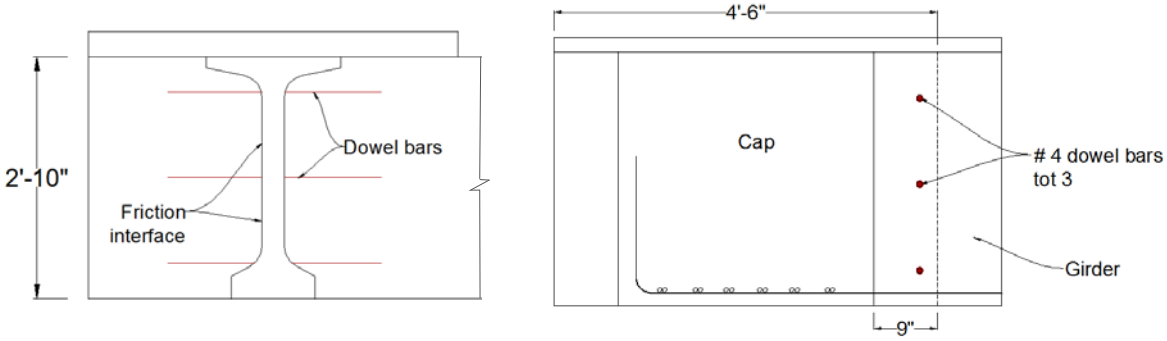

Figure 3.45: Dowel location

$$V = 0.8A_{vf}f_y + A_cK_1 \qquad (4.1)$$

V = shear resistance

A_{vf} = area of steel reinforcement crossing shear interface

f_y = yield strength of steel reinforcement

A_c = area of concrete resisting shear through friction

K_1 = friction coefficient factor

Dowel bar shear friction resistance:

$$V = 0.8 * 0.3in.^2 * 66\ ksi * 2\ sides = 31.68 \text{ kips}$$

To determine the moment resistance of the dowel bars, the calculated shear force was multiplied by the distance from the top edge of the deck to the force location as shown in Figure 3.46. The location of the shear force was assumed to be at the lower dowel bar with the resulting lever arm of 32.25 in. The resulting yield moment

www.manaraa.com

resistance was 85.14 k-ft. The second portion of Equation 4.1, which considers concrete friction, was also originally calculated and combined with the dowel bar moment resistance. However, the resulting moment resistance was not comparable to observed results from the system and GUSC tests, therefore it was decided to use a multiplier to account for the moment contribution of concrete friction. Based on observed system and GUSC test results, the multiplier was determined to be 1.2 which resulted in a dowel action yield moment of 102 k-ft. The ultimate moment resistance due to dowel action was then calculated. It was assumed that the dowel bars would reach a yield stress of 99 ksi and the ultimate moment capacity was calculated to be 153 k-ft.

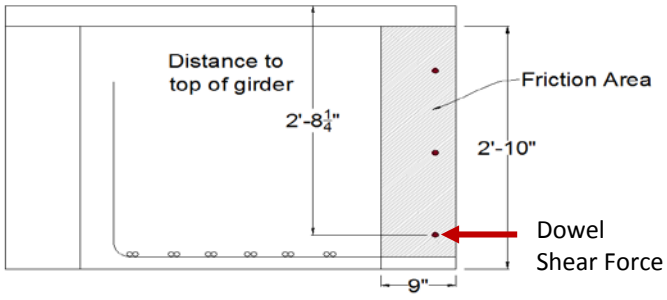

Figure 3.46: Lever arm distances for moment calculations

3.8.2.2 Extended Strands

The moment resistance of the extended strands can be calculated using the equivalent stress block approach and considering the number and location of the extended strands. However, in order to predict the behavior of the connection, strain penetration values were used to predict the horizontal displacement of the girder and subsequent connection rotation.

The first step was to establish a value for the equivalent strain penetration length (L_{eq}) at the test unit level. Equivalent strain penetration length is an approximate length corresponding to an idealized strain distribution that results from a debonding of a strand or reinforcing bar at the interface of two members. Figure 3.47 shows the debonded region of a reinforcing bar, the true strain distribution, and also the resulting idealized strain distribution. The equivalent strain penetration length L_{eq} is equal to $L_{ua}+L_{ui}+L_{ua}$

www.manaraa.com

where L_{ui} is the debonded length of the rebar or strand and l_{ua} is a length of constant strain that is assumed to be equivalent to the actual strain distribution. As the bar or strand debonds, a gap will form between the two connected members. The relationship used to relate the gap length to the strain in the reinforcement is based on the idealized strain distribution length L_{eq} as shown in Equation 4.2:

$$\varepsilon = \delta / L_{eq} \qquad (4.2)$$

ε = strand strain

δ = horizontal displacement or gap opening

L_{eq} = equivalent strain penetration length

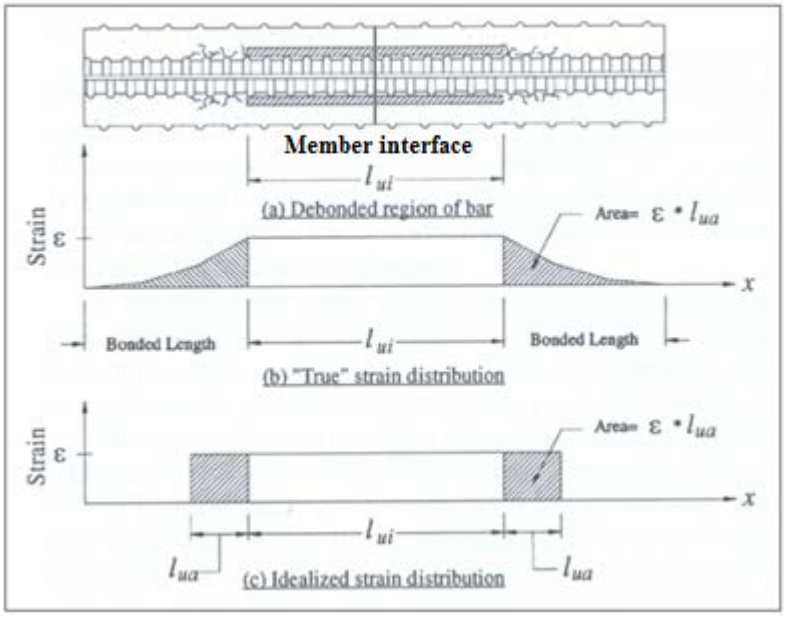

Figure 3.47: Strain penetration strain distribution (Snyder, 2010)

Results from the GUSC test were used to formulate values for L_{eq} for a 3/8 in. strand which were determined to be 17 inches at yield condition and 31 inches at yield condition. Strain values corresponding to the yield and ultimate condition of the strand were then substituted into Equation 4.2 using the formulated L_{eq} values to determine the predicted horizontal displacement values for the ESBF and ESSP connections. The strain values and corresponding horizontal displacements are shown in Table 3-6. To predict the overall behavior of the connections, the moment resistance of the extended strands

www.manaraa.com

and dowel action were combined. The rotation of the connection was calculated by dividing the horizontal displacement from strain penetration by the distance from the top of the deck to the centroid of the bottom strand. It was assumed that the yield and ultimate moments due to dowel action would occur at the same rotation values as the yield and ultimate moments of the extended strands. The resulting moment-rotation behavior of the connection is shown in Figure 3.48.

Table 3-6: Strain and horizontal displacement

Load Condition	Stress (ksi)	Strain	Leq	H. Disp (in.)
Zero	0	0	0	0
Yield	230	0.00793	17	0.133
Ultimate	250	0.0086	31	0.27

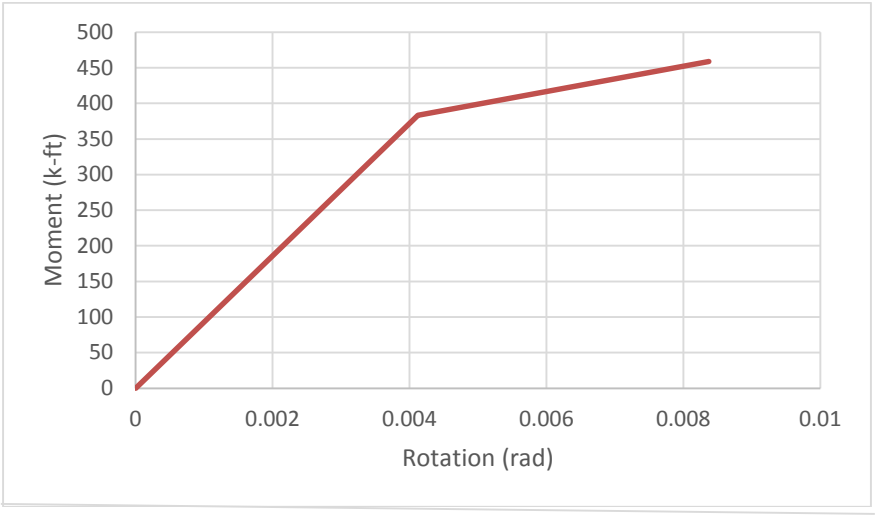

Figure 3.48 Predicted positive moment connection behavior

3.8.3 Negative moment resistance

For the ESBF and ESSP connections, negative moment resistance is provided by the deck steel. It is possible that the dowel bars also contribute some negative moment resistance, however, due to the stiffness of the deck, it is assumed that the contribution of the dowel bars is negligible. The yield and ultimate negative moment capacities were calculated to be 940 k-ft and 1410 k-ft respectively and a curvature was calculated for each moment value using an equivalent stress block approach and Equation 4.3.

www.manaraa.com

$$\varphi = \frac{\epsilon_c}{c} \quad (4.3)$$

φ = curvature

ϵ_c = concrete strain at yield or ultimate condition

c = neutral axis depth of the section

Curvature values were found to be 81.16 x 10^{-6} and 519.3 x 10^{-6} at yield and ultimate conditions respectively and were then used along with strain penetration equations 4.4 and 4.5 to predict the rotation of the connection. The resulting moment-rotation behavior in the negative direction is shown in Figure 3.49.

$$\theta_{yp} = (0.08L + 0.15fydb) * \varphi e \quad (4.4)$$

$$\theta_{up} = 0.15fydb * \varphi e + (0.08L + 0.15fydb) * \varphi p \quad (4.5)$$

θ_{yp} = rotation due strain penetration at yield condition

θ_{up} = rotation due to strain penetration at ultimate condition

L = length of girder

fy = yield stress of deck steel

db = largest diameter of deck steel reinforcement

φe = elastic curvature of girder at connection region

φe = curvature of section at yield for θ_{yp}

$\varphi e = \frac{curvature\ of\ section\ at\ yield}{940\ k-ft} * 1410$ k-ft for θ_{up}

ϕp = plastic curvature of girder at connection region

$\varphi_p = curvature\ of\ section\ at\ ultimate - \varphi_e$

www.manaraa.com

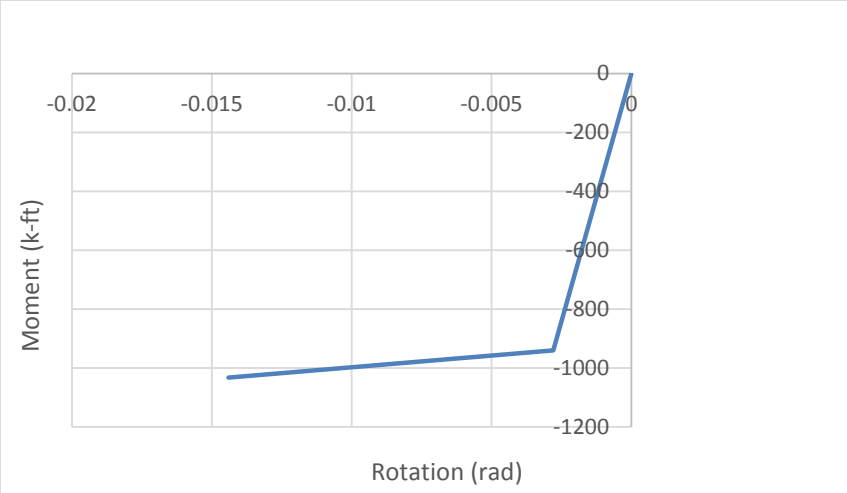

Figure 3.49: Predicted negative moment behavior of connection

www.manaraa.com

CHAPTER 4 – EXPERIMENTAL TESTING AND RESULTS

4.1 Introduction

Following the completion of the test unit construction and analysis, the two loading actuators were attached to frames and secured to the strong floor of the ISU laboratory. The actuators were attached to a single girder and lateral braces were placed between the load frames as shown in Figure 4-1 to prevent out of plane movement. Instrumentation was then connected to external data acquisition systems and a post-tensioning force of 200 kips was applied to each of the twelve column bars in a series of four steps as shown in Table 4-1. The column capacity after post-tensioning was 850 k-ft which would be sufficient for testing until displacement cycles were reached.

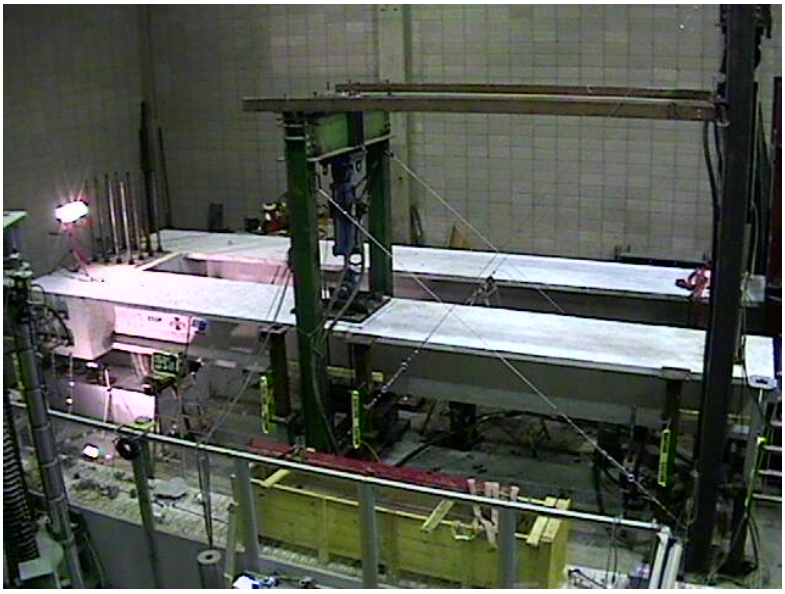

Figure 4.1: Test setup

Table 4-1: Post-tensioning sequence

Step	Post-tensioning force (kips)
1	25
2	75
3	120
4	200

www.manaraa.com

4.2 ESBF Connection Observations

For testing of the connections, the first step of the test was to apply a gravity load. A full gravity load was applied to the ESBF connection and no damage to the test unit was observed, with the exception of a couple small hairline cracks at the top of the deck. The actuator loads were then stepped from gravity to horizontal seismic (G+H). Under negative moment a small amount of cracks appeared in the top and bottom of the deck close to the connection region but the girder did not crack. For positive moments no damage or gap opening was observed.

Loads were then stepped from G+H to G+H+0.5gV as shown in Table 4-2. Girder cracking began under negative moments at step H1. Girder and deck cracking continued as the load increased. The cracking started close to the connection and then gradually extending along the girder toward the blue actuator as shown in Figure 4-2. A small amount of torsional cracks in the cap were also observed under increase of negative moment. For positive moments a hairline gap began to form between the girder and cap at step H2. The crack widened to 1/16" at the last step of 0.5gV. No other damage around the connection was observed under positive moment.

Table 4-2: Load steps from G+H to G+H+0.5gV

	Actuator Forces (k)		Target Values	
Load Step	Blue	Black	Moment (k-ft)	Shear (k)
G+H	32.5	-9.3	-339.75	-34.27
	34.3	-22.3	34.95	-22.07
H1	36.9	-10.2	-373.5	-37.77
	30.4	-22.7	70.5	-18.77
H2	41.3	-11.2	-404.4	-41.17
	26.6	-22.2	107.55	-15.47
H3	45.6	-12.1	-436.8	-44.57
	22.7	-21.6	143.1	-12.17
G+H+0.5gV	50.0	-13.0	-470.55	-48.07
	18.8	-21.0	178.65	-8.87

www.manaraa.com

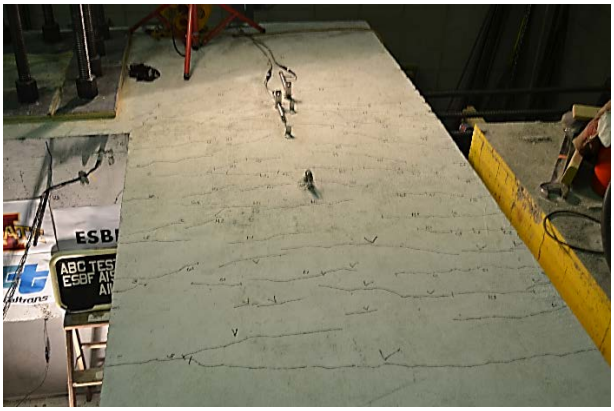

Figure 4.2: Deck cracking extending from connection region

After reaching 0.5gV, the cap was post-tensioned to provide higher torsional capacity before increasing the loads to G+H+1.0gV. Load steps are again provided in Table 4-3. Under negative moments, cracking in the girder and deck increased slowly as the applied moment was increased. As positive moments increased, cracking of the cap cover concrete around the girder occurred at V4 as shown in Figure 4-3. The bottom of the girder next to the connection started to crack at 1.0gV and the gap between the girder and cap increased slightly to 3/32" (Figure 4-4). The connection appeared to still be behaving elastically in both the positive and negative directions at 1.0gV. After G+H+1.0gV was reached, the black actuator was switched to displacement control to further exercise the connection.

Table 4-3: Load steps from 0.5gV to 1.0gV

	Actuator Forces (k)		Target Values	
Load Step	Blue	Black	Moment (k-ft)	Shear (k)
0.5gV	50.0	-13.0	-470.55	-48.07
	18.8	-21.0	178.65	-8.87
V1	53.4	-13.65	-497.93	-50.82
	14.94	-20.1	205.11	-5.91
V2	56.8	-14.3	-525.3	-53.57
	11.08	-19.2	231.57	-2.95
V3	60.2	-14.95	-552.68	-56.32
	7.22	-18.3	258.08	0.01
V4	63.6	-15.6	-580.05	-59.07
	3.36	-17.4	284.49	2.97
1.0gV	67	-16.25	-607.43	-61.82
	-0.5	-16.5	310.95	5.93

www.manaraa.com

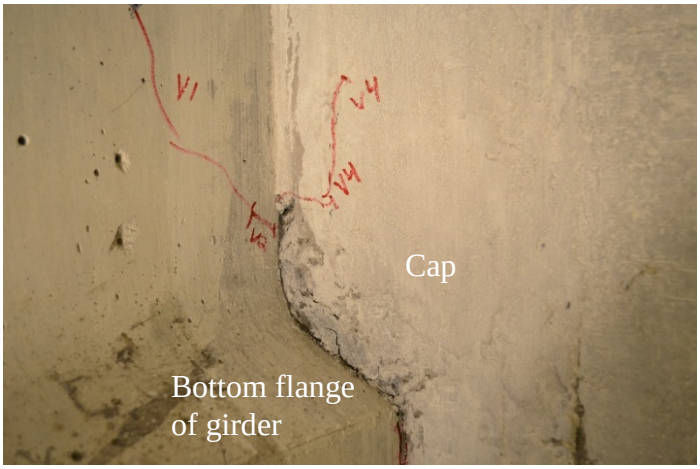

Figure 4.3: Cracking of cap cover concrete

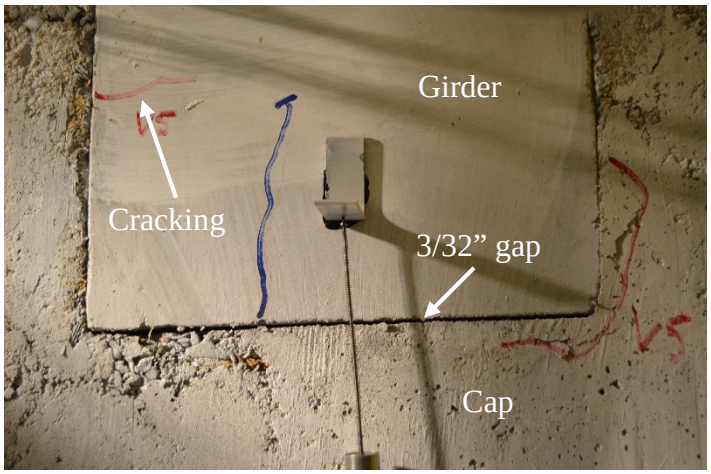

Figure 4.4: Cracking along bottom of girder

For the displacement load steps, positive displacement corresponded to downward movement of the girder and negative moment while negative displacements corresponded to upward movement of the girder and positive moment. The blue actuator was cycled between constant force values in order to apply a consistent shear at the connection interface. The steps of loading for the displacement cycles are shown in Table 4-4. At step D3 in the positive moment direction, the gap between the bottom of the girder and the cap increased to 3/16” and the girder continued to crack across the bottom face as shown in Figure 4-5. After cycling at load step D3, softening was observed in both the positive and negative moment directions and the cracking in the cap cover concrete around the girder increased. At load step D4, under negative moments,

www.manaraa.com

spalling occurred under the cap and cracks extended further along the girder and deck towards the blue actuator as shown in Figure 4-6 and Figure 4-7.

Table 4-4: Displacement load steps

	Constant force (k)	Displacement (in.)
Load Step	Blue Actuator	Black Actuator
D1	40	2
	-22	-1
D2	40	3
	-22	-1.5
D3	40	4
	-22	-2
D4	40	6
	-22	-3
D5	40	9
	-22	-4.5
D6	40	12
	-22	-6
D7	40	15
	-22	-7.5

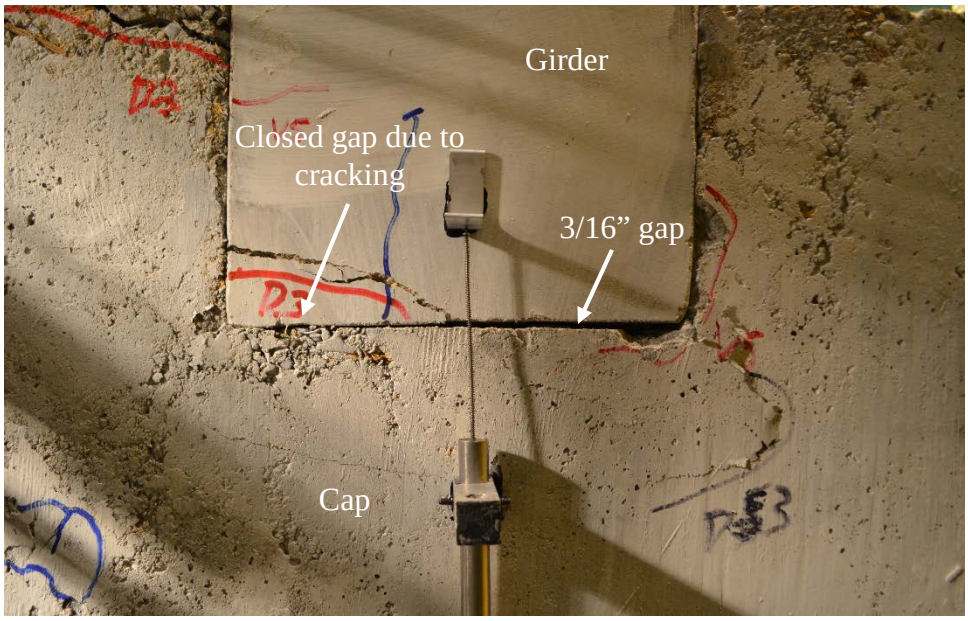

Figure 4.5: Girder gap opening of 3/16"

www.manaraa.com

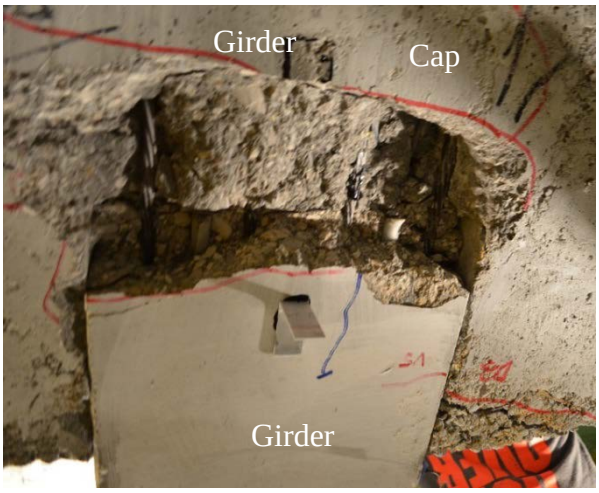

Figure 4.6: Spalling at bottom of girder and cap

Figure 4.7: Extended deck cracking

During load step D5 the girder started to pull away from the deck under negative moment cycles, and a 1/8” gap was observed. As the displacement cycles continued, spalling of the cap cover concrete around and underneath the girder increased. Also, one of the extended strands partially fractured under positive moment as shown in Figure 4-8. The LED’s for the NDI system were removed at this time to prevent damage to the attached wires. At load step D7 spalling continued and the gap due to vertical slip of the girder was 3/8” under negative moments (Figure 4-9). The positive moment at D7 caused two more of the extended strands to fracture. The connection was no longer able to maintain a large positive moment and the negative moment capacity was also decreasing due to the large amount of cap cover concrete spalling around the girder. The

www.manaraa.com

testing was terminated since full capacity of the connection was reached. Figure 4-10 and Figure 4-11 show the final condition of the connection.

Figure 4.8: **Partial extended strand fracture**

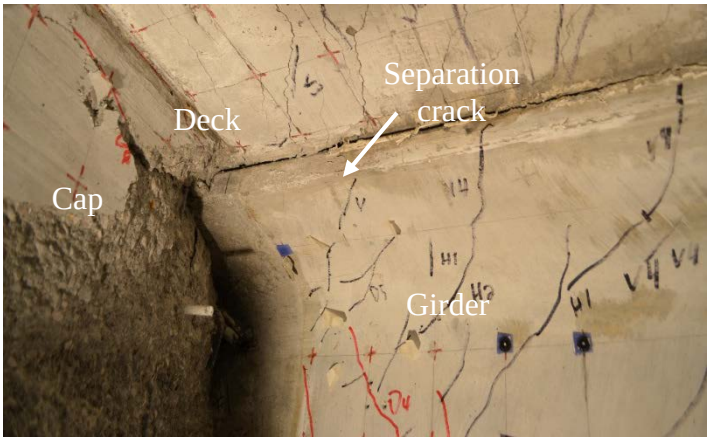

Figure 4.9: Vertical slip of girder and separation from deck

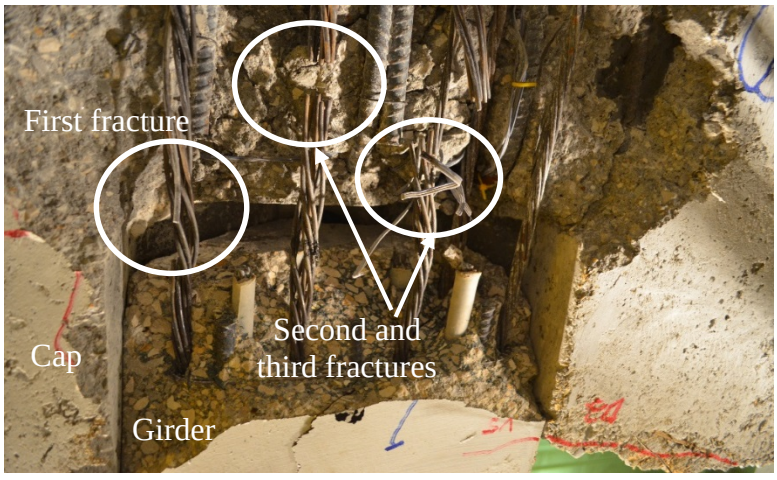

Figure 4.10: Fractured extended strands

www.manaraa.com

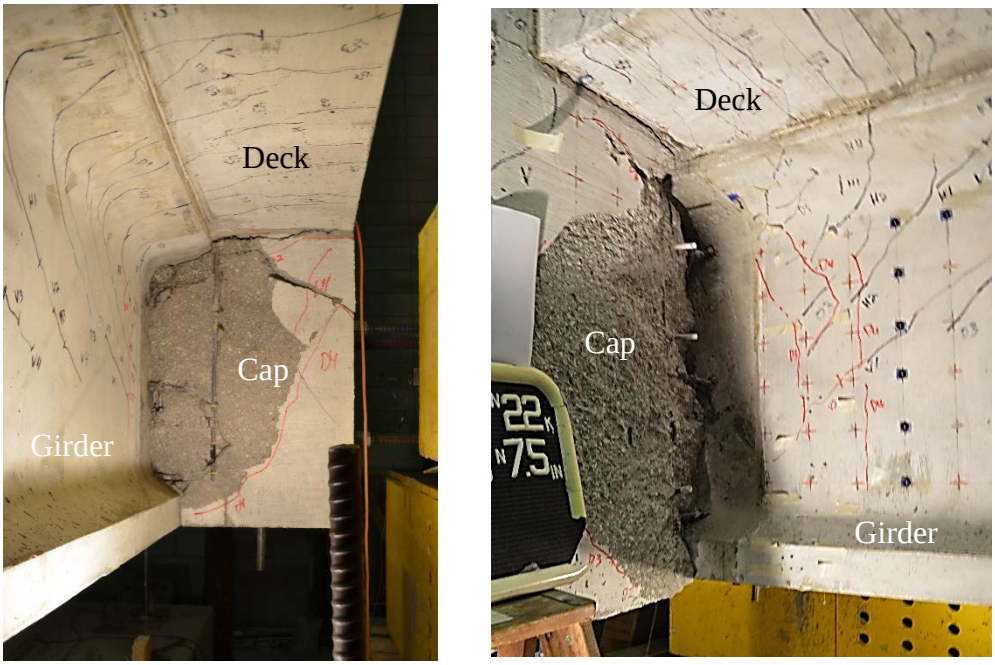

Figure 4.11: Final condition of connection region

4.3 ESSP Connection Observations

The ESSP connection was tested in a similar manner to the ESBF connection. To begin the test, the actuators were placed in force control and a gravity load was applied. However, as the first load steps were applied a large amount of cracks began to appear on the deck and girder. The load was slightly increased and even more cracks appear as shown in Figure 4-12. At this point, the testing was stopped due to the concern that too large of forces were being input into the connection since little to no cracking should have occurred at such a low load level.

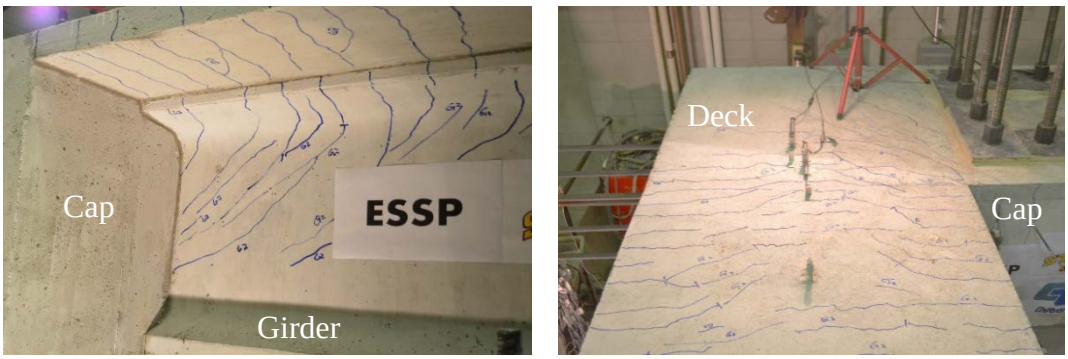

Figure 4.12: Cracking caused by overloading

www.manaraa.com

After checking the loading and test equipment, it was found that the loading pin on the blue actuator was rotated and caused the blue actuator to apply incorrect forces and overload the connection. The overloading was high enough to cause permanent deformation of the test unit including yielding of a small amount of deck steel as well as a displacement near the end of the girder close to 1.0 inch. The extent of the connection damage was not immediately clear but preliminary estimates showed that a 600-700 k-ft negative moment was applied to the connection instead of the gravity moment of 130 k-ft. The loading pin was corrected and the testing resumed. Further details regarding the effects of the overloading will be discussed with the results of the test.

When testing resumed, the connection was subject to gravity (G) loads and then gradually increased up to G + horizontal seismic (H). No new cracks were observed in the negative moment direction since the overloading moment exceeded the gravity plus horizontal seismic moment. The connection did not show any cracking in the positive moment direction. The connection moments were then stepped from G+H, to G+H+0.5g vertical acceleration (0.5gV). For negative moments some new girder and deck cracks appeared at 0.5gV. In the positive moment direction a gap started to open between the end of the girder and the cap beam. At 0.5gV the crack was 1/16” wide as shown in Figure 4-13. In both the positive and negative moment directions the behavior of the connection remained elastic.

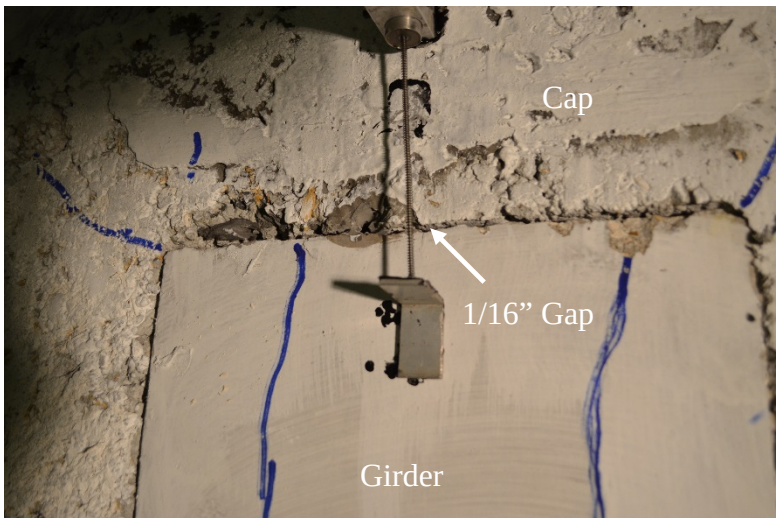

Figure 4.13: Girder to cap gap

www.manaraa.com

After reaching 0.5gV, testing stopped temporarily and the cap was post-tensioned to provide adequate torsional capacity for higher moments. Testing continued and the connection was subject to increasing moments up to G+H+1.0g vertical acceleration (1.0gV). Table 4-5 shows each load step from 0.5gV to 1.0gV and the corresponding moment and shear values.

Table 4-5: Load steps from 0.5gV to 1.0gV

	Actuator Forces (k)		Target Values	
Load Step	Blue	Black	Moment (k-ft)	Shear (k)
0.5gV	50.0	-13.0	-470.55	-48.07
	18.8	-21.0	178.65	-8.87
V1	53.4	-13.65	-497.93	-50.82
	14.94	-20.1	205.11	-5.91
V2	56.8	-14.3	-525.3	-53.57
	11.08	-19.2	231.57	-2.95
V3	60.2	-14.95	-552.68	-56.32
	7.22	-18.3	258.08	0.01
V4	63.6	-15.6	-580.05	-59.07
	3.36	-17.4	284.49	2.97
1.0gV	67	-16.25	-607.43	-61.82
	-0.5	-16.5	310.95	5.93

As the magnitude of the moments increased in the negative direction, deck cracking continued to increase and extend farther from the connection region. The connection still behaved elastically in this direction without showing any signs of strength loss. In the positive moment direction the gap between the girder and cap continued to increase. At step V4 the gap had increased to 1/4" and cracks began to appear in the cap concrete adjacent to the girders (Figure 4-14). The connection was then cycled between positive and negative moments two more times. At the end of the cycle the gap had widened to 5/16" (Figure 4-15) and the cap cover concrete next to the girder began to spall (Figure 4-16). At this time the connection began to soften and behave in an inelastic manner. At this point in the test, the black actuator was switched to displacement control in order to be able to better exercise the inelastic action of the connection. The loading protocol for displacement cycles is shown in Table 4-6. Just as

www.manaraa.com

for force control, each step was cycled between positive and negative displacement three times.

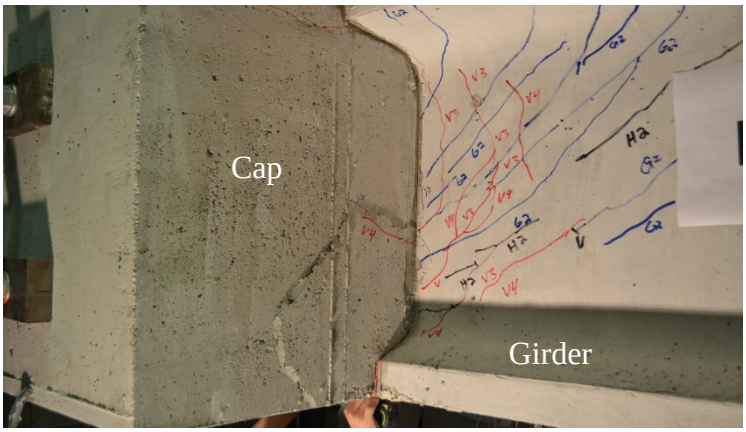

Figure 4.14: Cracking of cap cover concrete adjacent to girder

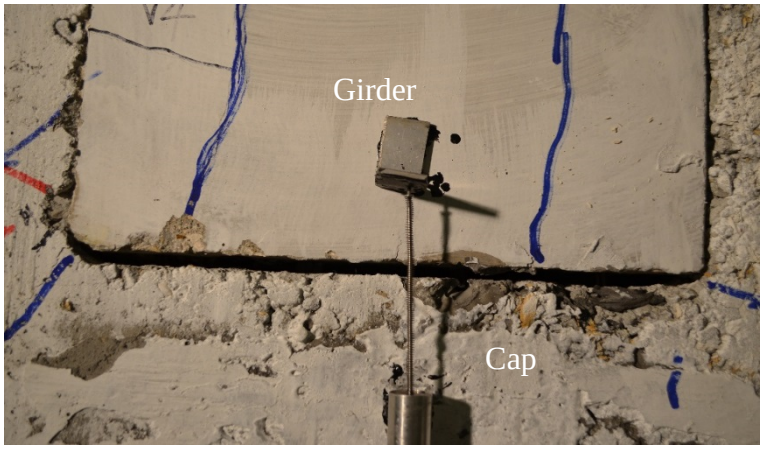

Figure 4.15: Gap (5/16”) between girder and cap beam

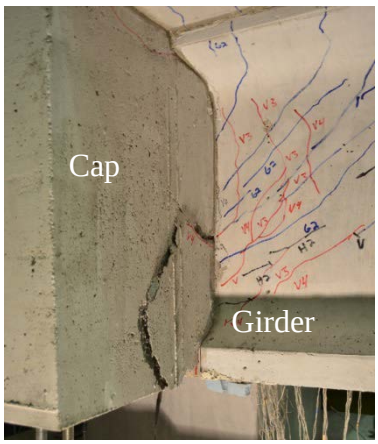

Figure 4.16: Spalling of cap cover concrete

www.manaraa.com

Table 4-6: Displacement load steps

	Constant force (k)	Displacement (in.)
Load Step	**Blue Actuator**	**Black Actuator**
D1	40	3.25
	-22	-1
D2	40	4
	-22	-2
D3	40	6
	-22	-3
D4	40	**9**
	-22	-4.5
D5	40	12
	-22	-6
D6	40	15
	-22	-7.5

As the displacement cycles progressed, the positive moment at step D2 (+4 in./-2 in.) caused cracking at the bottom of the girder near the connection region as shown in Figure 4-17. The cap cover concrete around the girder also continued to spall (Figure 4-18). The LEDs from the NDI system that were positioned on cap were removed at this time to prevent damage due to spalling.

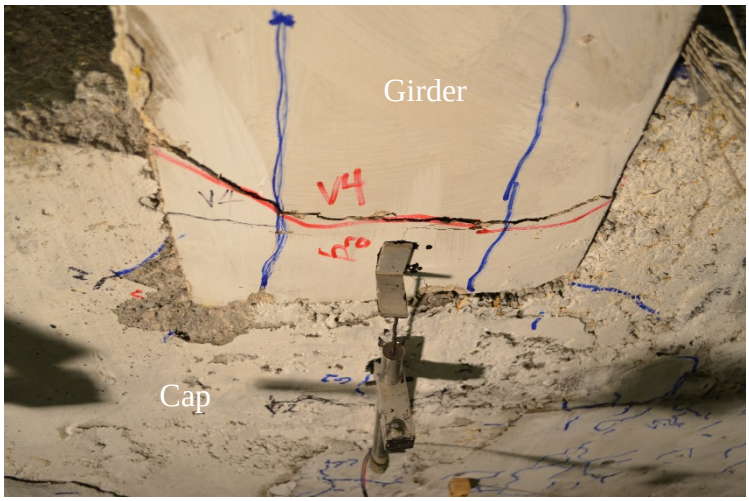

Figure 4.17: Cracking at bottom of girder

www.manaraa.com

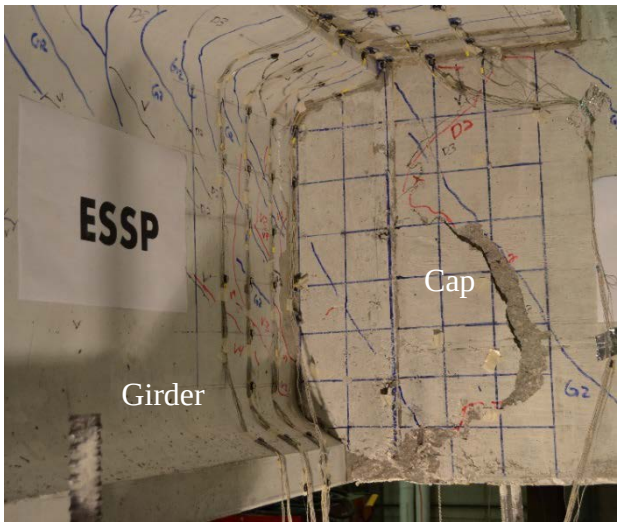

Figure 4.18: Continued spalling of cap cover concrete

At step D3 (+6 in./-3 in.), the bottom of the girder began to spall near the connection region along with the bottom of the cap. The spalling caused a loss of compression area for the girder under negative moment and resulted in the mushrooming of the extended strands as shown in Figure 4-19. The loss of compression area also caused the negative moment capacity to decrease as the lever arm was shortened. In the positive moment direction one extended strand snapped causing a decrease in moment capacity but the other four strands remained intact.

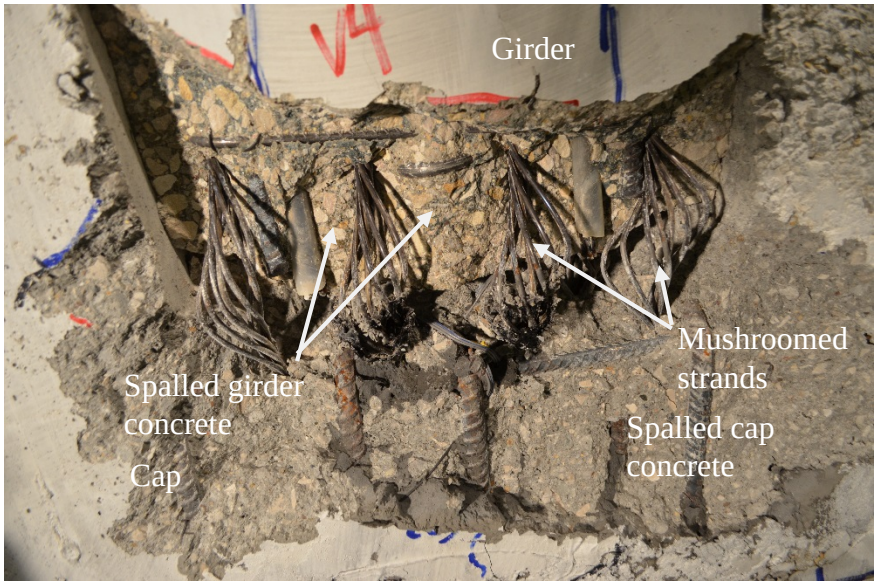

Figure 4.19: Spalling of concrete and mushrooming of strands

www.manaraa.com

In the last three displacement steps, large amounts of spalling occurred in the cover concrete at the girder interface which fully exposed the dowel bars. The moment capacity in both the positive and negative direction continued to decrease and separation between the girder and deck was also observed under negative moment. The girder was able to reach a final displacement step of +15 in./-7.5 in. but the strength of the connection had already significantly decreased. The final condition of the connection is shown in Figure 4-20.

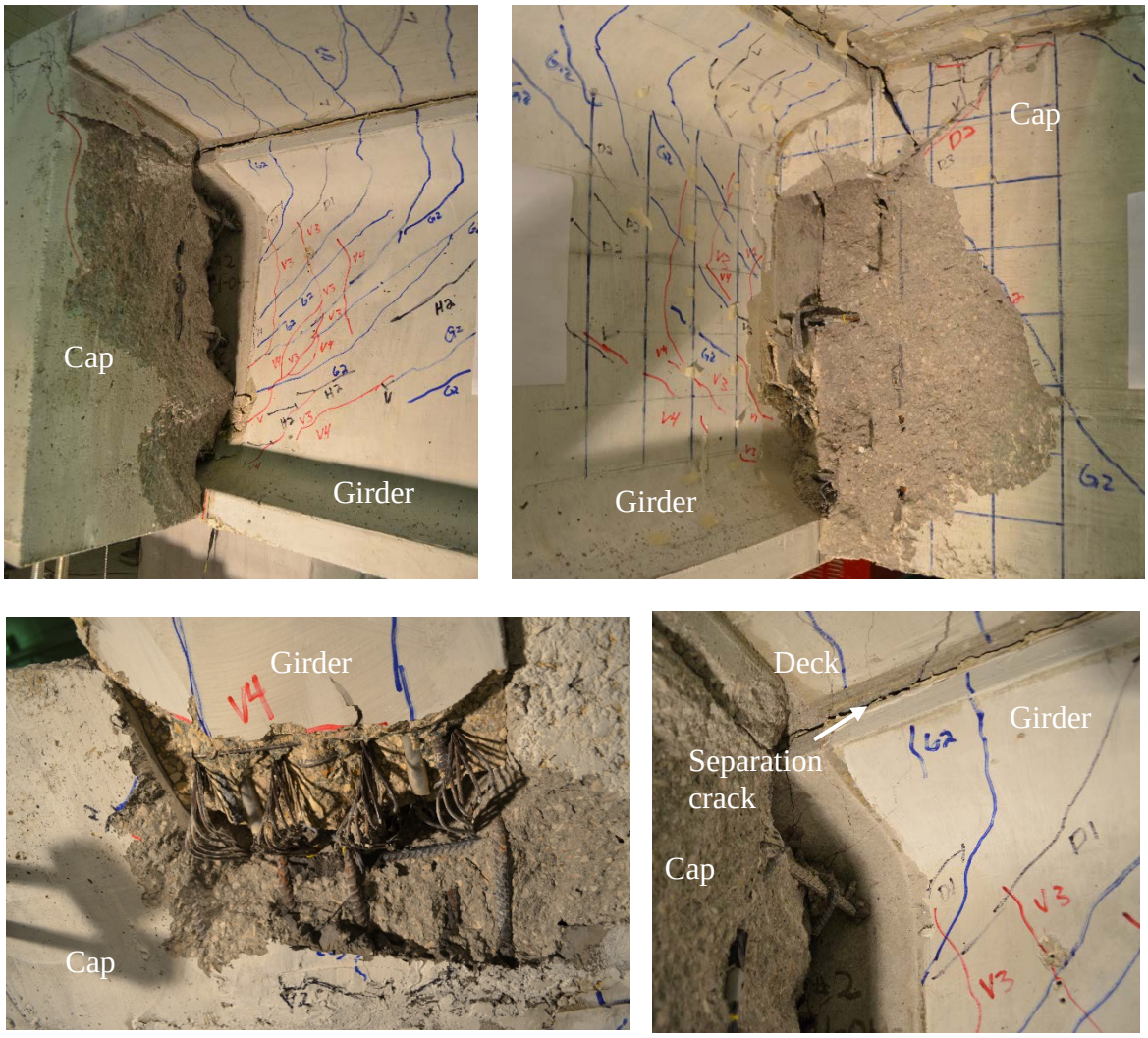

Figure 4.20: Final condition of connection region (upper - cap adjacent to girder; lower left – underside of girder to cap connection; lower right – separation of girder from deck)

www.manaraa.com

4.4 ESBF Test Results

4.4.1 General

Results and behavior of the ESBF and ESSP connections will be summarized in the following sections according to positive and negative moments. During processing of data from the test results, it was found that the self-weight of the prototype wearing surface had not been correctly calculated which resulted in an underestimation of moments for the loading protocol. It was found that the moments applied to the test unit were on average 15% smaller than the actual prototype loads. The shear values were on average 3% smaller than the actual prototype loads. The results summarized in the following sections will be reported with regard to the corrected loading protocol which is also included in Appendix C. In the following sections, behavior of specific connection details will be discussed along with failure mechanisms of both details. Comparisons to predicted responses will be provided as well as recommendations for improving the performance of the connections.

4.4.2 Positive Moment Response

The ESBF connection performed well under positive moment and remained elastic up to the combined loads of gravity, horizontal seismic corresponding to the column overstrength moment, and 0.72g vertical acceleration. Figure 4-21 shows the moment-rotation behavior of the connection as well as moments corresponding to different loading levels. The maximum positive moment capacity reached by the connection was 416 k-ft.

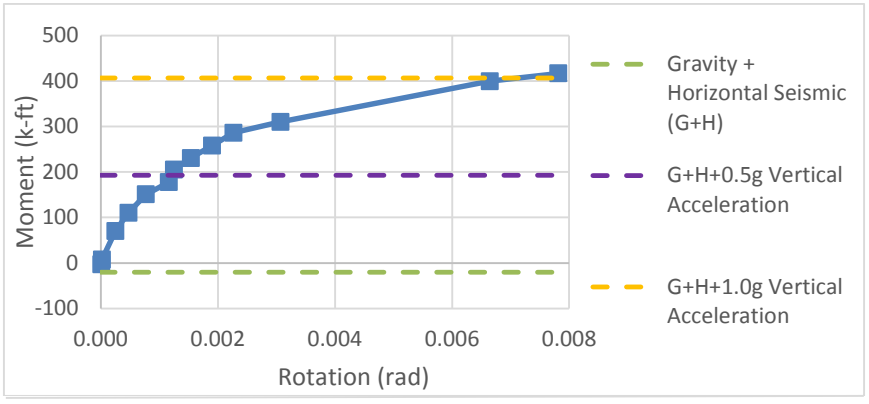

Figure 4.21: Positive moment vs. rotation response of ESBF connection

www.manaraa.com

4.4.3 Behavior of Strands and Dowel Action

The response of the extended strands and dowel action was examined to further understand the behavior of the connection during positive moments. The yield moment of the connection was defined as the moment at which inelastic behavior began and was found to be 286 k-ft. At this moment value, the strain in the extended strands at the connection interface was 3100 με and the dowel bar strain was 1800 με as shown in Figure 4.22. These strain values were then converted to stresses and moment resistance using Equation 4.1 and an equivalent stress block approach. It was found at the yielding of the connection that the moment resistance of the strands was 111 k-ft and the moment resistance due to dowel action was 175 k-ft.

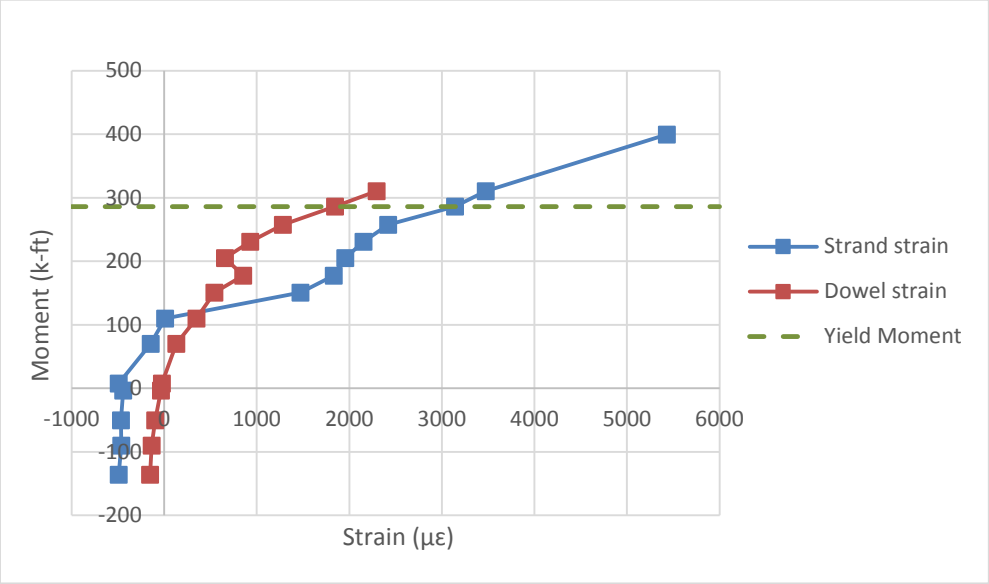

Figure 4.22: Strand strain and dowel bar response

Observing the moment resistance provided by each mechanism at the connection yield point, it appears that the concrete friction and dowel bars actively resist the majority of the connection moment (61%). However, Figure 4.22 shows that the extended strands consistently were subject to higher strain values than the dowel bars after the connection moment exceeded 100 k-ft. The dowel action resists a large percentage of the overall moment through friction and concrete adhesion between the end of the girder and the cap beam as well as dowel bar strain. The yield point of the

www.manaraa.com

connection is very close to the yield point of the dowel bars. After the connection yields and the connection loads continue to rise, the strain in the strand increases due to the diminishing capacity of the dowel action. To validate this explanation, the calculation process performed for the yield point was repeated for the moment values listed in Table 4-7. The table shows that concrete friction and dowel action account for an average of 65% of the moment resistance until the dowel bars reach yield stress. Once the dowel bars reach yield, the cover concrete around the dowel bars began to crack and the strain in the strand increased until the ultimate moment value of the connection was reached. Based on strain measured in the extended strands, 70% of the positive moment resistance at the connection was carried by the strand at ultimate condition.

Table 4-7: Mechanism moment values for connection moments approaching yield strength

Strand Moment (k-ft)	Dowel bar Moment (k-ft)	Concrete Friction Moment (k-ft)	Dowel Action (D+C)	Dowel Action Moment Percentage	Connection Moment (k-ft)
52.1	18.3	80.4	98.6	65%	150.8
64.9	28.7	84.1	112.8	63%	177.7
69.3	22.1	113.6	135.7	66%	205.1
76.3	31.3	123.3	154.6	67%	230.8
85.8	43.1	128.9	172.0	67%	257.7
111.3	62.1	112.8	175.0	61%	286.3
123.1	77.2	110.11	187.3	60%	310.4
192.4	75.0	132.3	207.3	52%	399.8
292.4	128.6	-4.11	124.53	30%	416.9

The ESBF connection reached ultimate condition in the positive direction with a displacement at the black actuator of -3 inches. The girder was then cycled through displacement of -4.5, 6, and -7.5 inches. The strand strain continued to increase and the concrete adjacent to the girders began to spall. At each displacement cycle beyond -3 in. the positive moment capacity of the girder decreased as shown in Figure 4.23. The decrease in moment at the displacement of -4.5 in. occurred due to cracking of the concrete adjacent to the girder around the lower dowel bar as well as the partial fracture of one of the extended strands. At -6 in. of displacement the moment loss was due to the continued loss of concrete adjacent to the girder which caused the moment capacity of

www.manaraa.com

the dowel bars and concrete friction to decrease. At a displacement of -7.5 inches a large drop in capacity was caused by the fracture of a second and third strands.

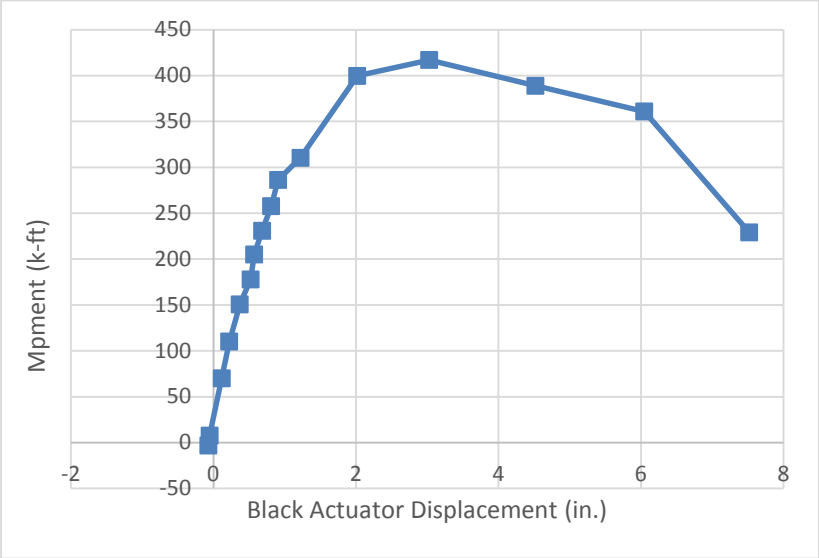

Figure 4.23: Moment decrease in ESBF connection after ultimate

4.4.3.1 Strand Anchorage Length

The strain in the extended strands was examined to better understand the transfer of strain along the length of the strand. Strain gages were located at the connection interface, 15 in. from the interface, and 45 in. from the interface. Table 4-8 shows the strain values for each gage along with the corresponding applied moment. Strain values in the table that are listed as 99999 indicate that the gage was no longer reading values due to overly high strand strains or damage to the gage. The table shows that strain was transferred to the 15 in. gage at relatively low moment values but the 45 in. gage did not experience noticeable strains until the strand approached fracture. The fracture of the strand shows that the development length of 60 in. was sufficient for anchorage, and the data in Table 4-8 indicates that an anchorage length of at least 45 inches is needed to prevent slipping of the strand.

www.manaraa.com

Table 4-8: Transfer of strain in extended strands

Strains (με)			Connection Moment (k-ft)
Interface	15 in.	45 in.	
-147	-66	2	70.2
11	-35	2	110.1
1471	-7	3	150.8
1831	525	5	177.7
1957	720	22	205.1
2152	1123	22	230.8
2420	1628	22	257.7
3141	2164	22	286.3
2256	2873	23	310.4
5431	5285	33	399.8
99999	8251	198	416.9
99999	3900	1662	388.9
99999	99999	99999	360.9
Fracture of Strand			229.0

4.4.3.2 Spalling of Cover Concrete

The spalling of the cap cover concrete during positive moment cycles occurred due to the location of the cap stirrups. Stirrups were placed adjacent to the top flange of the girder; however, no stirrups were placed under the top flange as shown in Figure 4.24. Lack of stirrups under the top flange resulted in a six inch gap of unreinforced cover concrete adjacent to the girder web. The dowel bars were located in this region of cover concrete. Movement of the girder and subsequent displacement of the dowel bars caused cracking in the unreinforced region which led to spalling of the cover concrete as shown in Figure 4.25. This problem could be avoided in the field or in future tests by ensuring that the cap stirrups extend all the way under the top flange of the girder and are also adjacent to the girder web as indicated in Figure 4.24.

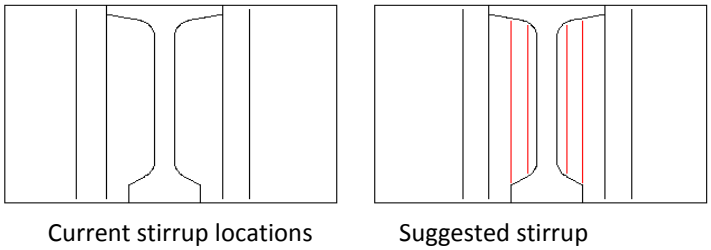

Figure 4.24: Cap stirrup locations

www.manaraa.com

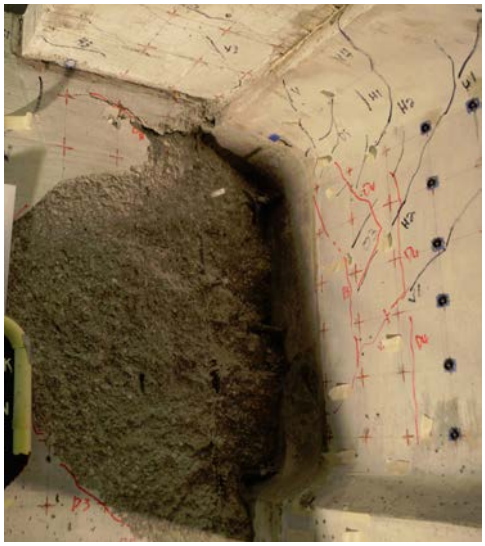

Figure 4.25: Spalling of cap cover concrete adjacent to girder

4.4.4 Negative Moment Response

The ESBF connection had considerable negative moment capacity and remained elastic up to the combined loads of gravity, horizontal seismic corresponding to the column overstrength moment, and 0.71g vertical acceleration. The moment capacity of the connection corresponding to the displacement at the black actuator, which was located close to the end of the girder, is shown in Figure 4.26 along with lines indicating specific load values. The connection reached an ultimate negative moment capacity of 1032 k-ft.

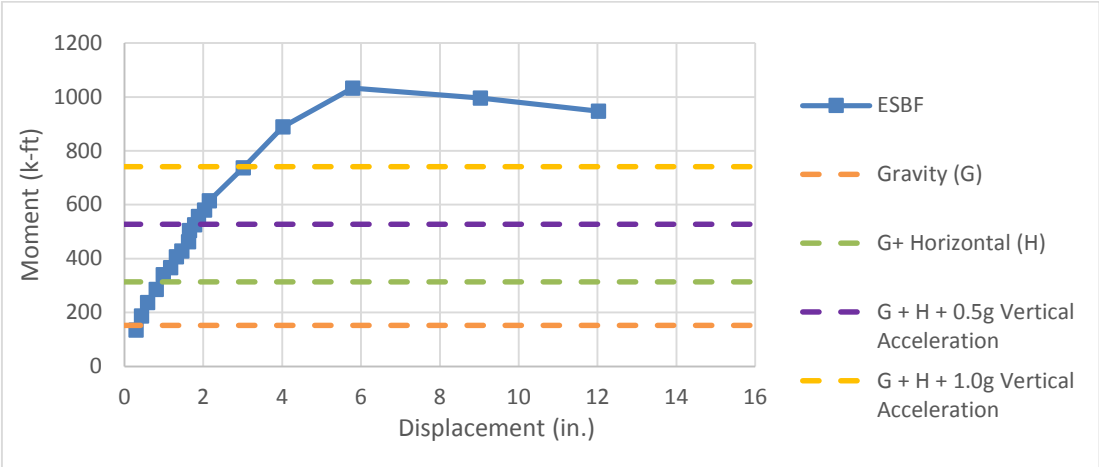

Figure 4.26: Negative moment vs. displacement of black actuator

www.manaraa.com

4.4.4.1 Deck Steel Behavior

The ultimate capacity of the connection in the negative direction was less than originally expected. The yield moment for the deck steel was originally calculated to be 940 k-ft, however, the yield moment of the test was around 615 k-ft. The predicted yield moment of 940 k-ft assumed that all the deck steel yielded simultaneously. The strains recorded in the deck steel during the test indicated that the rebar in the center of the deck reached yield sooner than rebar near the edge of the deck as shown in Figure 4.27 where zero position represents the center of the deck. The rebar in the middle of the deck began to exhibit inelastic behavior before yielding of the outer deck steel which caused the connection to behave in an inelastic manner at a lower than predicted moment value of 615 k-ft.

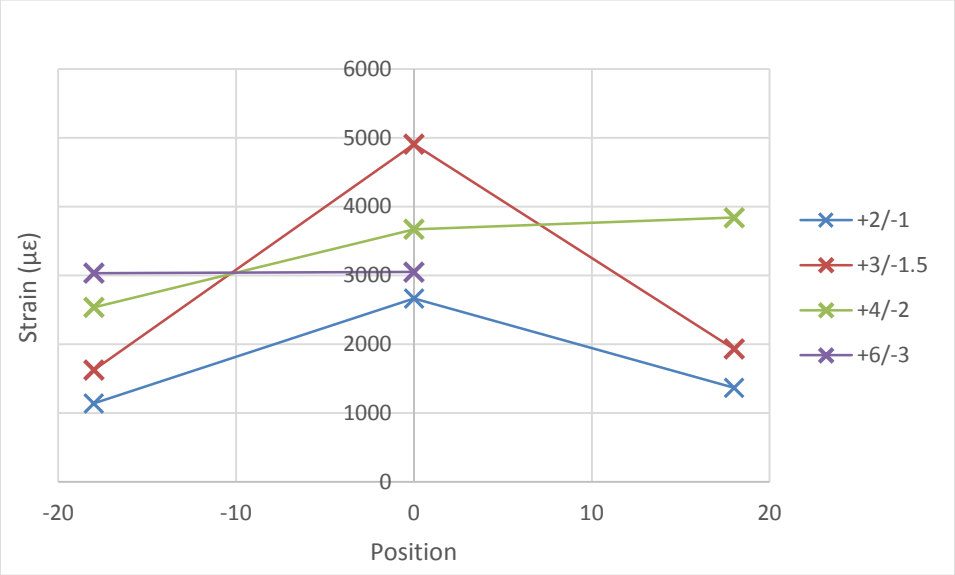

Figure 4.27: Strain profile of deck steel

The connection did continue to gain a considerable amount of strength after the initial yield moment of 615 k-ft and reached the ultimate moment capacity of 1032 k-ft. It is possible that the moment capacity of the connection would have continued to increase beyond 1032 k-ft but was prevented due to the damage at the connection interface. First, the bottom of the girder and cap began to spall (Figure 4.28) which reduced the compressive area and lever arm for negative moment. Second, due to spalling of cover concrete adjacent to the girder interface, the girder began to separate

www.manaraa.com

from the deck and slip vertically. The vertical slip prevented the girder and deck from behaving as a fully composite section and reduced the moment resistance in the negative moment direction.

Figure 4.28: Spalling at bottom of girder to cap interface

4.4.5 ESBF Overall Response

The ESBF connection remained elastic for positive and negative moments up to values equivalent to the combined loads of gravity, horizontal seismic corresponding to the column overstrength moment, and vertical acceleration of 0.71g. The connection reached a maximum positive moment of 416 k-ft and a maximum negative moment of 1032 k-ft. The overall moment versus displacement response of the connection is shown in Figure 4.29.

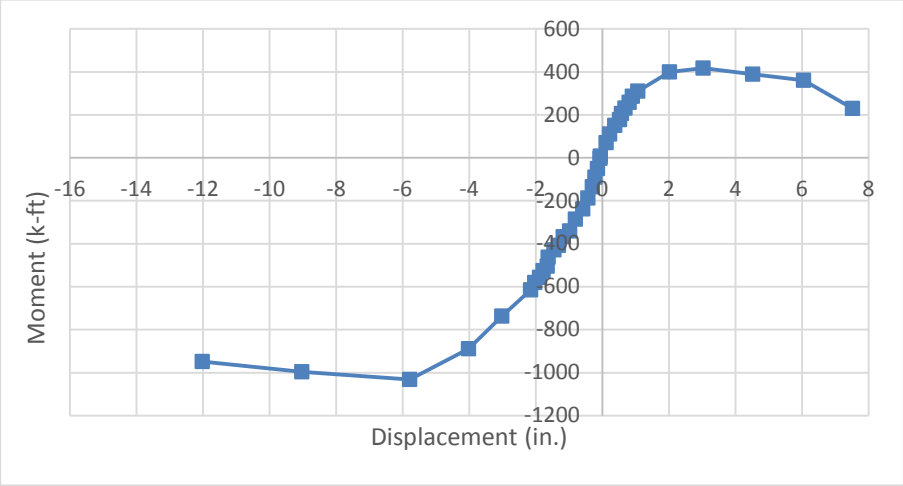

Figure 4.29: Moment vs. black actuator displacement of the ESBF connection

www.manaraa.com

4.5 ESSP Test Results

4.5.1.1 General

The ESSP connection behaved in a similar manner to ESBF connection. However, the effects of overloading adversely affected the connection in both the positive and negative directions. The overall response of the connection, along with behavior in the positive and negative moment directions, will be summarized in a manner similar to the ESBF connection.

4.5.1.2 Positive Moment Response

The ESSP connection remained elastic in the positive moment direction up to a combined load equivalent to gravity, horizontal seismic corresponding to the column overstrength moment, and 0.77g vertical acceleration. Figure 5.33 shows the moment verses rotation response of the connection as well as specific load levels. The maximum moment reached by the connection was 287 k-ft which corresponds to a vertical acceleration value of 0.72g vertical acceleration.

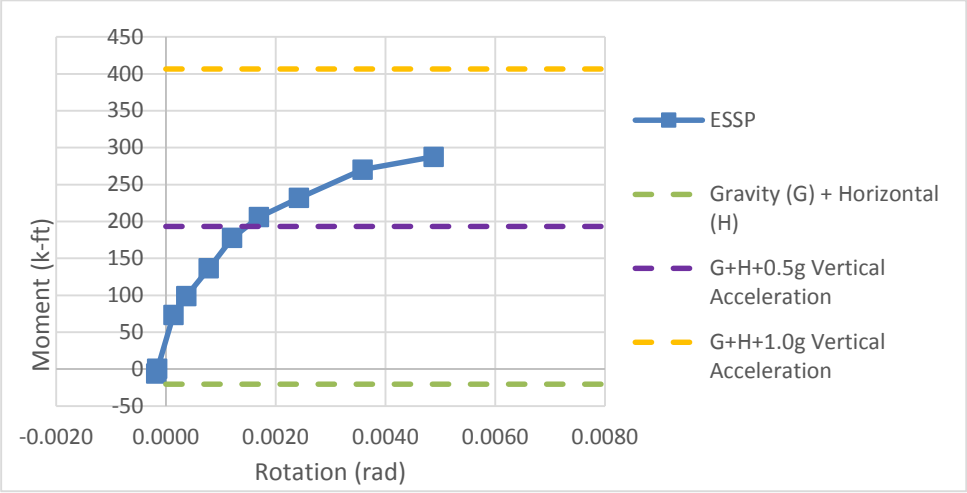

Figure 4.30: Moment vs. rotation behavior of ESSP connection

The positive moment behavior of ESSP connection was very similar to the ESBF connection except for smaller moment capacity at yield and ultimate. The difference in moment between the two connections is most likely due to the overloading of the ESSP connection. Strain data from the ESSP test shows that the overloading caused a permanent downward deflection of the girder. As a result, when testing resumed

www.manaraa.com

following the overloading, a strain was present in the dowel bars of approximately 500-600 με. This caused a slight softening of the connection as well as lower overall moment capacity. The lower dowel bar capacity resulted in the bars reaching yield strain at a lower moment value. Similar to the ESBF connection, when the dowel bars reach yield strain, the concrete surrounding the dowel bars began to crack which resulted in a loss of dowel action and an increase in strand strain. The connection behaved similar to the ESBF and as the moment increased, the loss of dowel bar strength continued, and the concrete began to spall which led to the crushing of the girder concrete in the positive moment compression region (Figure 4.31). Crushing of the girder concrete prevented the strands from being exercised to full capacity and resulted in a lower ultimate positive moment. Comparison of the positive moment response between the two connections is shown in Figure 4.32.

Figure 4.31: Crushing of girder concrete

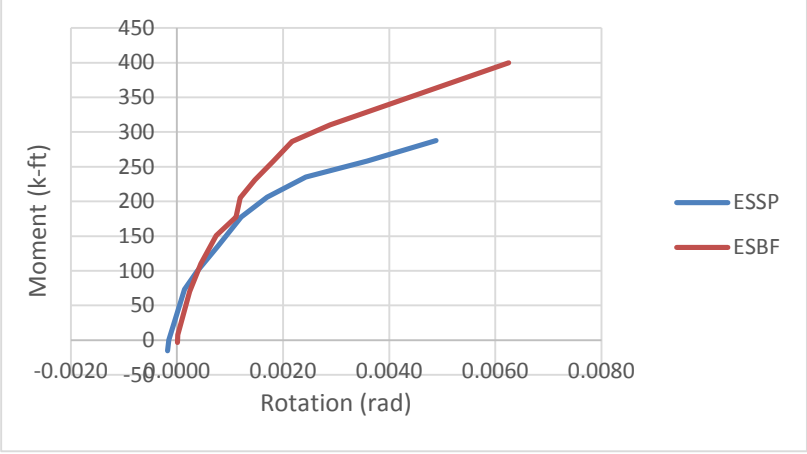

Figure 4.32: Connection behavior comparison of ESBF and ESSP connections

www.manaraa.com

Even though the ultimate moment capacity of the strands was not developed, strain values of the extended strands and strand ties were compared to validate the transfer of force between the two strand members. It was found that the strand ties did not experience strain values comparable to the extended strands. In fact, the strain values in the strand ties remained constant throughout the test at values ranging from approximately 10-50 με. It is possible that the strain transferred to the cap reinforcement or that the plate and chuck attached to the extended strand was sufficient for anchorage.

4.5.1.3 Negative Moment Response

The negative moment response of the ESSP connection was also very similar to the ESBF connection. The overloading at the beginning of the test resulted in yielding of some of the deck reinforcement and residual strains ranging from 300-900 με which resulted in a lower overall moment capacity. A comparison of the ESSP connection behavior to that of the ESBF connection is shown in Figure 4.33 along with target load levels. The connection remained elastic up to a load value equivalent to gravity, horizontal acceleration corresponding to the column overstrength moment, and vertical acceleration of 0.71g. The connection negative yield moment of 615 k-ft was the same as the ESBF connection but occurred at a larger vertical displacement due to the overloading. The maximum negative moment capacity of the ESSP connection was 936 k-ft.

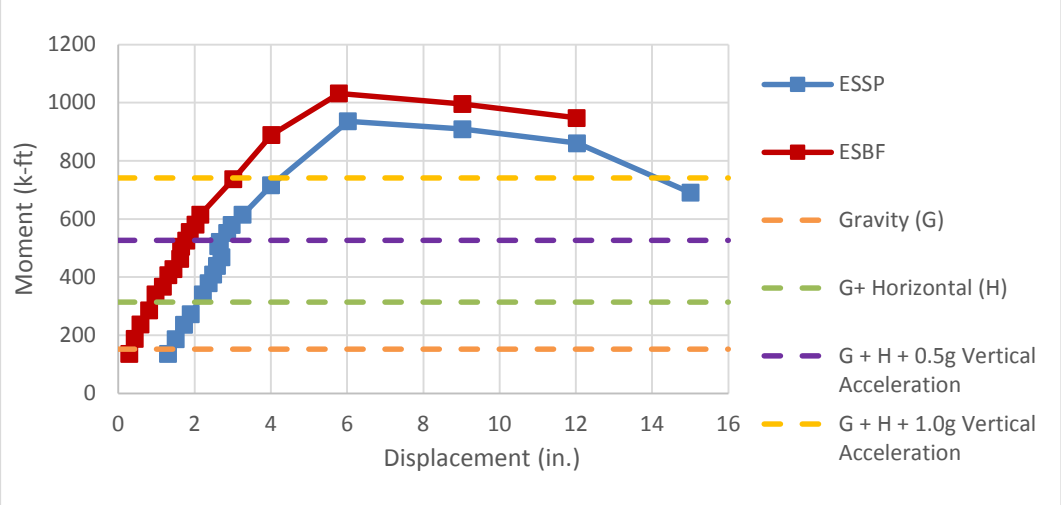

Figure 4.33: Negative moment vs. displacement comparison

www.manaraa.com

4.5.1.4 Overall Connection Response

The connection performed reasonably well by remaining elastic to positive moment capacity corresponding to 0.72g of vertical acceleration and a negative moment capacity corresponding to 0.71g. The maximum capacity of the connection was 286 k-ft in the positive moment direction and 936 k-ft in the negative moment direction. The connection did rotate more than the ESBF connection as a result of softening due to the initial overloading of the connection. The overall behavior of both connection is shown in Figure 4.34.

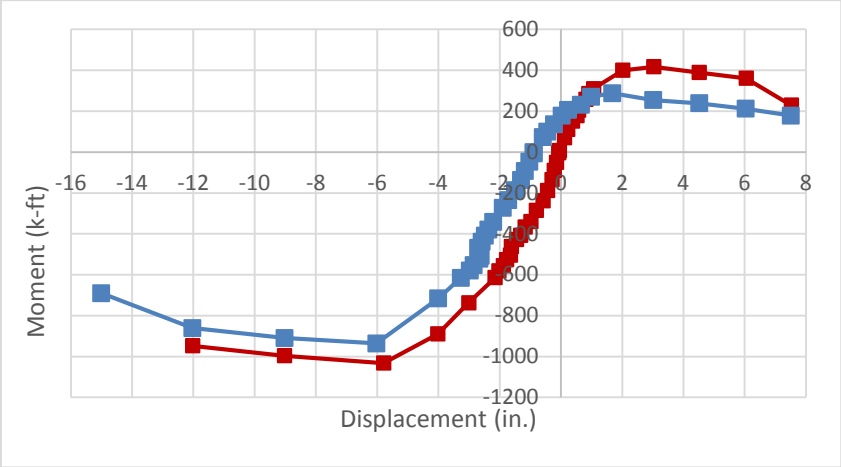

Figure 4.34: Moment vs. black actuator displacement comparison of ESSP and ESBF connections

4.6 Comparison to Prediction Models

4.6.1 General

The results of the ESBF and ESSP connections were compared to the behavior predicted by the strain penetration model in both the positive and negative moment directions. The following sections discuss how the test results compare with the predicted behavior and changes that can be made to the prediction models to more accurately represent the connection behavior.

4.6.2 Positive Moment Response

The positive moment response of both connections is compared to the predicted response in Figure 4.35. The predicted model method did not accurately represent the

www.manaraa.com

initial stiffness of the connection region. The connection was stiffer than predicted and also had smaller yield and ultimate moments than indicated by the model.

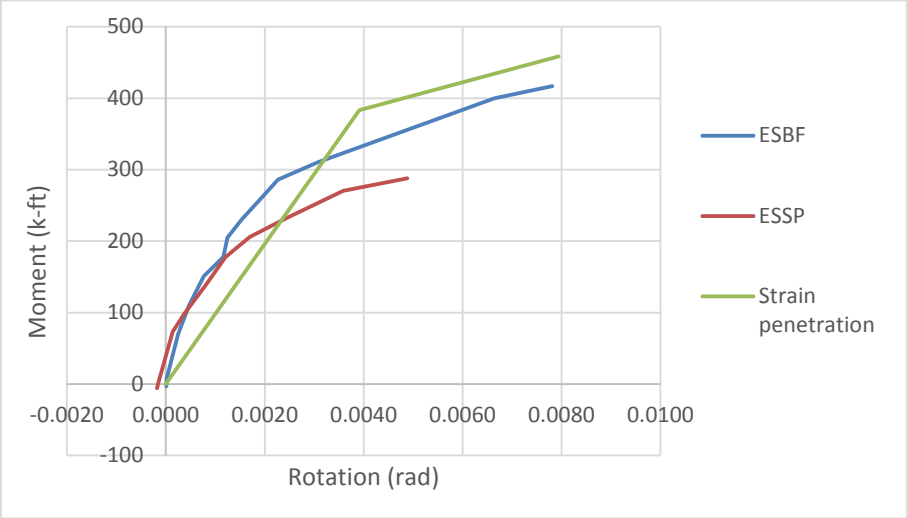

Figure 4.35: ESBF vs. predicted positive moment response

It is possible that the difference in the initial stiffness that occurred in the prediction models is due to the choice to utilize the GUSC connection data for comparison when the models were formulated. The GUSC connection utilized a dapped end with a longer embedment length of the girders into the cap beam. The larger girder embedment length provided more surface area for concrete friction resistance and also increased the distance between the dowel bars and connection interface as shown in Figure 4.36.

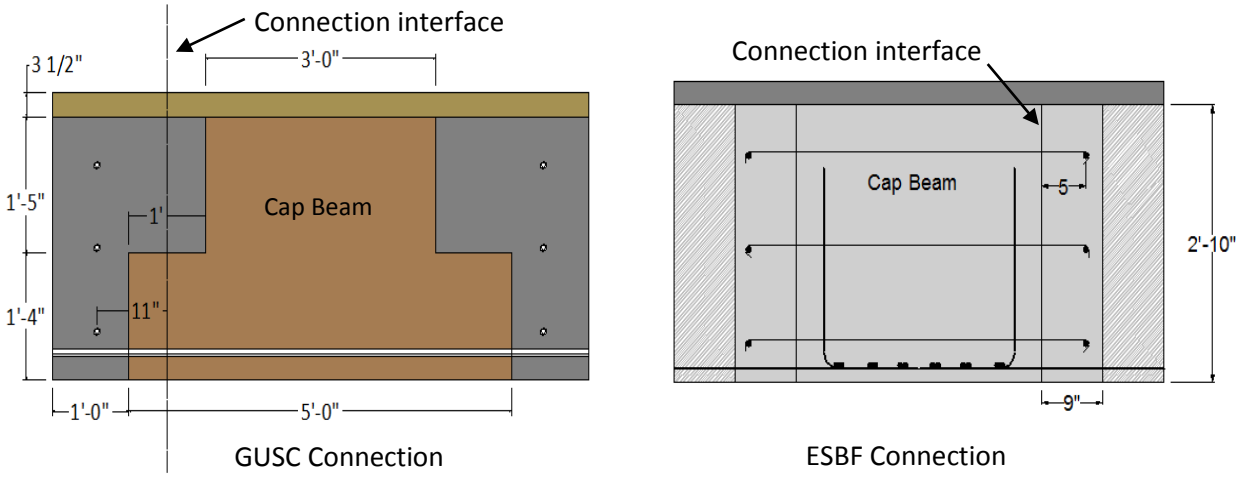

Figure 4.36: Comparison of GUSC and ESBF connections

www.manaraa.com

The stiffness difference between the GUSC and ESBF connection was likely due to dowel action resulting from the concrete friction area of each connection and the location of the dowel bars. The dowel bars in the ESBF connection are located closer to the connection interface as well as in the center of a smaller concrete friction area. Shear friction equations from ACI 308-11 were originally used to calculate the resistance of the two mechanisms. The shear friction mechanism as defined by ACI assumes that the steel rebar acts as a clamping force which enables the frictional resistance between the two concrete surfaces (ACI, 2011). The clamping force provided by the dowel bars in the ESBF connection is distributed over a smaller area which provides a stiffer connection region than the GUSC connection. Also the closer dowel bar location and smaller concrete friction resistance of the ESBF connection results in the dowel bars experiencing larger amounts of strain at lower rotation values which causing the connection to yield under lower loads.

After further examining the positive behavior of both connections two observations were made. The first, as discussed earlier, was that the yield point of the connection corresponded to the yielding of the dowel bars. The prediction model based the yield point of the connection on the yielding of the extended strands. This difference explains the lower yield moment and also partly explains the difference in initial stiffness between the two models. The second observation was that the concrete interface between the cap and girder provides a significant amount of moment resistance which results in a higher moment and stiffer initial stiffness due to dowel action than originally predicted. The prediction model was adjusted to include the concrete shear friction resistance from Equation 4.1 instead of the multiplication factor of 1.2. In Equation 4.1, K_1 values of 0.15 and 0.075 and steel stress values of 60 ksi and 90 ksi were used respectively at yield and ultimate conditions. The model as was changed to account for yielding of the dowel bars as the connection yield point with the distribution of the force between the strands and dowel bars calculated according to Table 4-7. The new prediction model is shown in Figure 4.37. The model is slightly conservative in regard to

www.manaraa.com

rotation and ultimate moment values to prevent predicting a smaller rotation or larger moment than what the connection would experience.

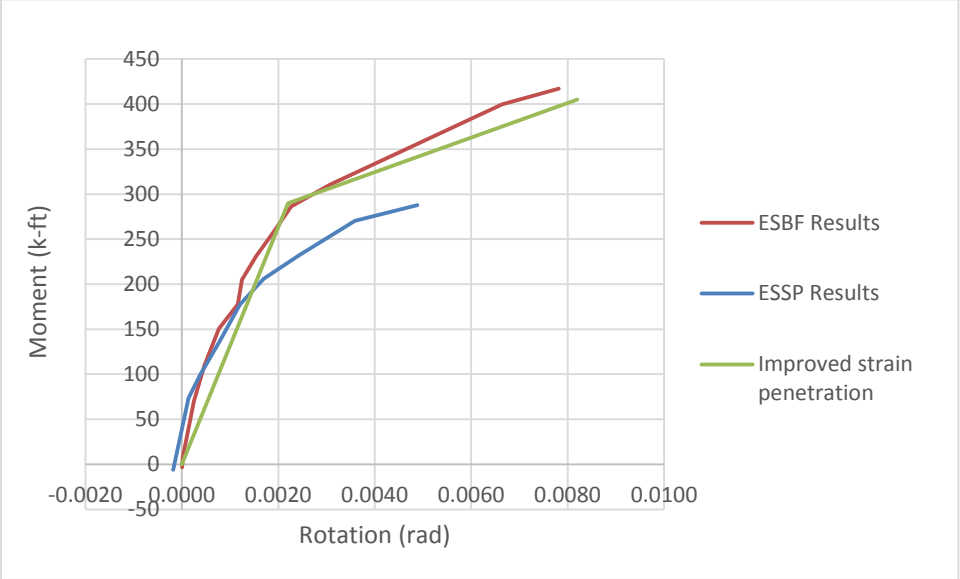

Figure 4.37: Improved connection model

4.6.3 Negative Moment Response

The ESBF connection negative moment response was stiffer than the predicted behavior of the connection as shown in Figure 4.38. The increase in stiffness could be due to the way the girders were loaded. For negative moments the blue actuator pushed down while the black actuator pulled up. The strain penetration equations assume that the girder is loaded by one load in a single direction. To better predict the rotation of the connection it was decided to use the distance from the connection to the blue actuator for the variable 'L'. This would result in only one load on the girder in a single direction. The test unit also showed an early yielding of the deck steel as mentioned earlier which needed to be accounted for in the prediction model.

www.manaraa.com

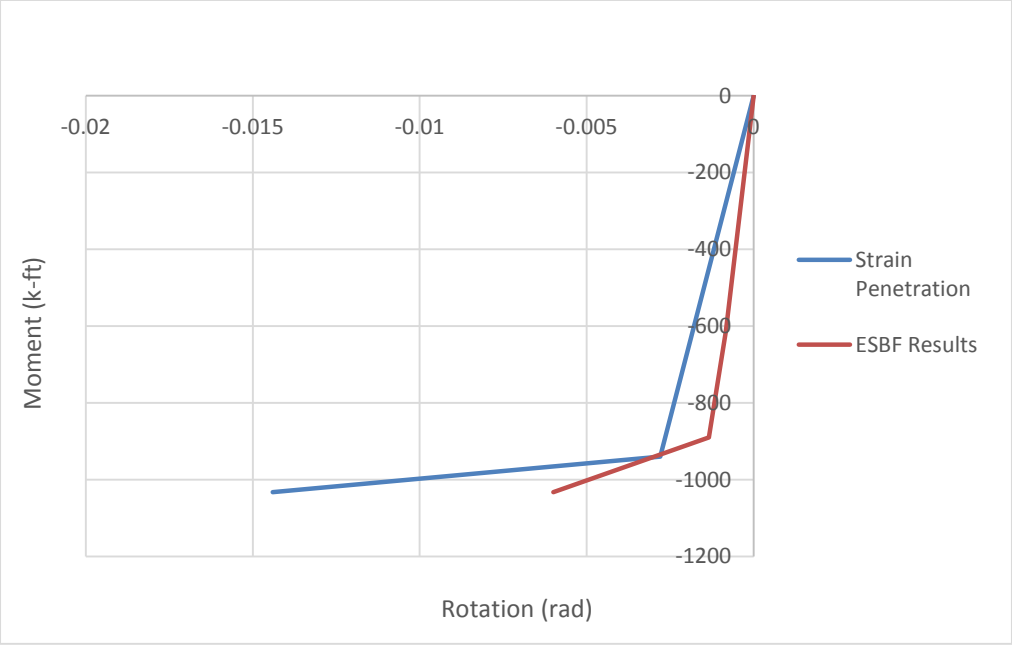

Figure 4.38: Strain penetration vs. negative moment response

To account for the early yielding of the deck steel due to an uneven distribution of strain, an initial yield point was added to the prediction model. It was assumed that the strain would vary linearly across each half of the deck width. Higher strains would occur at the center of the deck above the girder, while lower strains would occur near the edge of the deck. The strain distribution was modeled with a linear strain rate of 49.3 μϵ/inch. Therefore the initial yield point was determined to be the point at which the steel above the girder reached a yield stress of 60 ksi. The resulting moment was calculated to be 611 k-ft. The second yield point was then taken to be 890 k-ft which was the point at which the steel above the girder reached 90 ksi. The ultimate moment achieved in the test of 1032 k-ft was used to calculate the curvature at ultimate condition. Equations 4.3 and 4.4 were then used to the predict connection behavior using the length of 13.5 ft for 'L'. The resulting rotation prediction is shown in Figure 4-39. The predicted rotation is larger than the actual rotation at the ultimate condition, however testing was stopped before the predicted ultimate rotation values were reached due to displacement limits of the test unit.

www.manaraa.com

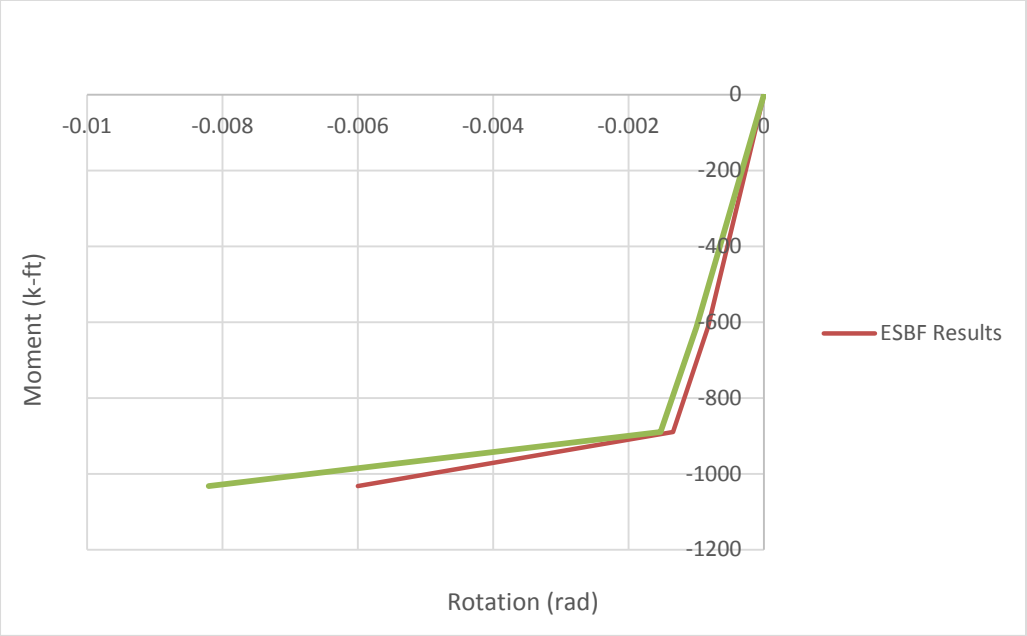

Figure 4.39: Improved negative moment prediction

www.manaraa.com

CHAPTER 5 - CONCLUSION

5.1 Project Overview

Current Caltrans SDC guidelines specify that bridges designed to use ABC methods with precast girders are assumed to be pinned at the girder to cap connection due to historically poor performance of the connections when subject to high seismic forces. A pinned girder to cap connection only allows a single plastic hinge to form as opposed to a fixed girder to cap connection where an additional plastic hinge forms at the top of the column. The additional plastic hinge allows a smaller column cross-section and footing to be used in design of the bridge. The economy provided by the fixed connection is lost when ABC methods are used in accordance with SDC guidelines. To recover the benefits provided by ABC construction, two connection details were designed to create fixed girder to cap connections using precast girders. Fixed connections require the capacity to resist both positive and negative moments. Negative moments will be resisted by traditional deck reinforcement placed in the concrete slab which runs continuously over the girders and cap beam. For positive moment resistance, the two designed connections will use prestressing strands extended from precast girders combined with dowel bars placed transversely through the web of each girder.

A separate SDC requirement states that if vertical acceleration is considered in the design of a bridge due to site conditions, additional side longitudinal reinforcement must be placed in the girder with the capacity to withstand 125% of the dead load shear. The side reinforcement must extended into the cap beam a length of 2.5 times the depth of the superstructure which results in congestion and increased labor costs when using precast members. One solution to meet this requirement is for precast girders connections to have a large enough capacity to resist 125% of the dead load shear and thereby eliminate the need for the additional reinforcement. To further increase the advantages of using precast ABC methods, the two girder to cap connections designed to remain fixed were also designed to withstand moment and shear values corresponding to 150% dead load (0.5g vertical acceleration).

www.manaraa.com

The two connections were designed for a prototype bridge with a 150 ft span utilizing CA-BT85 girders. The CA-BT85 girder is the largest bulb-tee girder currently used by Caltrans and has a maximum span length of 150 ft. The largest girder and longest span provided the maximum possible moment at the connection region. After completion of the prototype design, a 40% scale test unit was designed, constructed, and tested in the ISU structural laboratory. The test unit consisted of a footing, column, cap beam, and two bulb-tee girders with individual decks. One girder was connected to the cap beam with the detail known as the ESBF connection. The ESBF connection utilized extended strands that were bent at 90 degrees with a development length of 60 in. to provide sufficient anchorage. Three dowel bars were also placed transversely through the girder web to provide additional moment resistance at the connection interface. The second girder connection, known as the ESSP connection detail, incorporated design details used by WSDOT. Extended strands extended a short distance into the cap beam and then are spliced to transfer forces. Lengths of strands known as strand ties overlapped the extended strands to create the splices and both the strand ties and extended were anchored by steel plates and anchor chucks. The ESSP connection also used three dowel bars for additional positive moment resistance.

Once the construction of the test unit was completed, each connection was tested individually by applying loads in a series of steps to reach target values. Each step was cycled three times to simulate seismic behavior. The target values were: gravity loads (G), G + horizontal ground acceleration corresponding to the column overstrength moment (H), G + H + 0.5g vertical acceleration, and G + H + 1.0g vertical acceleration. Each girder was then subject to displacement cycles until the capacity of the connection was reached. The displacement values corresponded to a point of load application 28.5 feet from the connection. The values were +2/-1, +3/-1.5, +4/-2, +6/-3, +9/-4.5, +12/-6, and -15/-7.5 inches and each value was cycled three times.

Two prediction models for the behavior of the connection were formulated. One model examined the strain values in extended strands, dowel bars, and deck steel and related those strain values to horizontal girder displacement by using linear rates. The

www.manaraa.com

linear rates for each material were then combined to form a predictive model. The second method used strain penetration values corresponding to the extended strands along with projected strain in the dowel bars to predict the connection behavior. For both methods, data from the previously performed GUSC test was used to correctly formulate the predictive calculations. Upon completion of testing, the measured response of each connection was compared to the predicted behavior in order to verify the accuracy of each model and identify any necessary modifications.

5.2 Summary of Test Results

5.2.1 General

Both the ESBF and ESSP connections performed well and each connection was able to resist the moment and shear values corresponding to a combined load of gravity, horizontal seismic corresponding to the column overstrength moment, and 0.5g vertical acceleration loads. The moment resistance of the connection showed that precast girder connections have adequate capacity to resist high seismic forces and can be designed as fixed connections. Additionally, both connections had sufficient shear and moment capacity at vertical acceleration values above 0.25g which eliminates the need for the additional longitudinal reinforcement required by Caltrans SDC.

5.2.2 ESBF Connection

The ESBF connection which incorporated the extended strands bent at 90 degrees with a development length of 60 in. remained elastic up to a combined load of gravity (G), horizontal seismic corresponding to the column overstrength moment (H), and 0.96g vertical acceleration. The ultimate capacity of the connection was well over values corresponding to G + H + 1.0g vertical acceleration. The failure mechanism of the ESBF connection was fracture of the extended strands which validated that for a 3/8 in diameter bent strand a development length of 60 in. was sufficient.

www.manaraa.com

5.2.3 ESSP Connection

The ESSP connection which consisted of the spliced strands anchored with plates and chucks, had slightly less capacity than the ESBF connection. It is thought that the difference in capacity is likely due to the mechanical malfunction at the beginning of the test which resulted in overloading of the connection. The connection remained elastic up to a combined load of gravity (G), horizontal seismic corresponding to the column overstrength moment (H), and 0.77g of vertical acceleration. The ultimate capacity of connection in the positive moment direction was G + H + 0.96g with a negative moment ultimate capacity well over G + H + 1.0g. The failure of the connection was due to a combination of two mechanisms. First, spalling of the cap beam cover concrete occurred adjacent to the girder due to the absence of cap stirrups under the top flange of the girder. The absence of stirrups resulted in a concrete thickness around the dowel bars that was larger than what is normally used for cover concrete. The thick cover concrete eventually spalled which exposed the dowel bars and reduced the capacity of the connection. Second, crushing of concrete at the end of the girder occurred which reduced the lever arm needed to develop adequate moment resistance in the strands and deck steel.

The behavior of the strand splices was examined throughout the test, and it was observed that the extended strands did not transfer force to the strand ties as was previously purposed but instead experienced very low strains. It appeared that the force in the extended strands either transferred to the cap reinforcement or was sufficiently anchored by the attached plate and chuck. Therefore, the strand ties which form the splices with the extended strands, are not necessary to include in the connection design.

5.3 Conclusions

Based on current Caltrans SDC requirements, along with test observations and results, the following conclusions have been made:

- Precast girders used with ABC methods are able to form fixed connections to resist high seismic forces contrary to current Caltrans SDC guidelines as evidenced by the performance of the ESBF and ESSP connections

www.manaraa.com

- Additional longitudinal reinforcement to resist vertical acceleration as specified by Caltrans SDC is not necessary when adequate shear and moment capacity can be provided by fixed precast girder to cap connections. This was demonstrated by the extended strand, ESBF and ESSP connections which provided adequate moment and shear capacities up to a combined load of gravity, horizontal seismic corresponding to the column overstrength moment, and 0.5g vertical acceleration.
- For a 3/8 in. strand bent at 90 degree, a development length of 60 in. is sufficient to for anchorage as evidenced in the ESBF connection
- The shortened extended strands in the ESSP connection (14 in. length) were adequately anchored with a plate and chuck without transferring forces through the strand splices
- Dowel action in both connections affects the initial stiffness of the connection and provides 60% of the connection positive moment capacity until yielding of the dowel bars after which the capacity of the dowel action decreases
- Both connection details can be improved by the addition of stirrups under the top flange of the girders to prevent spalling of cap cover concrete

5.4 Recommendations for Future Work

The results of the ESBF and ESSP connection tests show that ABC methods using precast girder to cap connections are economical due to fixed connection behavior and the additional capacity to withstand seismic forces corresponding to 0.5g vertical acceleration. The results also provide opportunities for future work in area of precast girder connections, specifically extended strand connections. It is recommended that a test be conducted using the ESSP detail but excluding the strand ties to provide information regarding the required embedment length for plate and chuck anchorage. During testing, some spalling occurred at the bottom of the connection region at the connection interface near the extended strands. In order to reduce damage to the bridge and ensure the integrity of the connection, methods of confinement for the extended strands at the connection region in both the girder and cap beam could be investigated.

www.manaraa.com

As recommended, stirrups should also be added under the top flange of the girder to decrease spalling of the cap cover concrete. Finally, new methods for anchorage of extended strands in bridge cap beams should be explored to provide more options for design and construction of precast girder connections. Overall, the performance of the test ESBF and ESSP connections strongly supports the use of ABC methods as a cost-effective solution for bridge construction in high seismic regions.

www.manaraa.com

REFERENCES

ACI, A. C. (2011). *Building Code Requirements for Structural Concrete (ACI 318-11).*

ASCE. (2014). *2013 Report Card on America's Infrastructure*. Retrieved March 21, 2014, from American Society of Civil Engineers: http://www.infrastructurereportcard.org/bridges/

California Department of Transportation, C. (2013). Preliminary Plan Drawings.

Caltans, C. D. (2012). *Bridge Design Aids.* Caltrans.

Caltrans, C. D. (2010). *Seismic Design Criteria (SDC).*

Culmo, M. P. (2011). *Accelerated Bridge Construction Manual.* McLean, Virginia: U.S. Federal Highway Administration.

Federal Highway Administration. (2013, April). *Fully Prestessed Bridge System used in Washington State Highways for Life Project, Part 2*. Retrieved March 14, 2014, from Concrete Bridge Views: http://www.concretebridgeviews.com/i70/Article2.php

Holombo, G. J. (1999). *Seismic Design of Precast Girder Bridges.* San Diego, CA: University of California, San Diego.

Interior, U. D. (2012, July 24). *Earthquake Facts*. Retrieved January 21, 2014, from U.S. Geological Survey: http://earthquake.usgs.gov/learn/facts.php

Khaleghi, B. (2012, July 4). Design Memorandum on Extended Strand Continuity Design. Washington: Washington State Department of Transportation.

NCHRP, N. C. (2004). *Connection of Simple-Span Precast Concrete Girders for Continuity.* Washington D.C.: Transportation Research Board.

Office of Operations. (2013, October 17). *Work Zone Mobility and Safety Program.* Retrieved January 21, 2014, from U.S. Department of Transportation : http://ops.fhwa.dot.gov/wz/construction/accelerated/

Phares, W. B. (2009). *Precast Concrete Elements for Accelerated Bridge Construction.* Ames, IA: Iowa Highway Research Board.

Priestley, S. C. (1996). *Seismic Design and Retrofit of Bridges.* New York: John Wiley & Sons Inc.

www.manaraa.com

R. Snyder, J. V. (2011). *Seismic Performance of an I-Girder to Inverted-T Bent Cap Connection.* Ames, IA: Iowa State University.

Salmons, J. R. (1974). *End Connections of Pretensioned I-Beam Bridges Study 72-2.* Jefferson City, Missouri: Missouri State of Highway Department.

Snyder, R. (2010). *Seismic performance of an I-girder to inverted-t bent cap bridge connection.* Ames, IA: Iowa State University.

Thiemann, Z. J.-W. (2009). *Pretest 3-D finite element analysis of the girder-to-cap-beam connection of an inverted-tee cap beam designed for seismic loadings.* Ames, IA: Iowa State University.

USGS. (1999, November). *The October 17,1989, Loma Prieta, California Earthquake*. Retrieved February 2014, from United States Geological Survey: http://pubs.usgs.gov/dds/dds-29/

USGS. (2010, November). *Historic Earthquakes: Northridge, California*. Retrieved February 2014, from United States Geological Survey: http://earthquake.usgs.gov/earthquakes/states/events/1994_01_17.php

Vander Werff, J., & Sritharan, S. (2014). Girder Load Distribution for Seismic Design of Integral Bridges. *ASCE Journal of Bridge Engineering*.

www.manaraa.com

APPENDIX A – EQUATIONS AND CALCULATIONS

Deck steel equations:

For calculation purposes the bottom flange of the girder was treated as a rectangular flange with a height of 10.8 inches. The girder deck is 8” thick with the centroid of deck steel located 4” above the top of the girder.

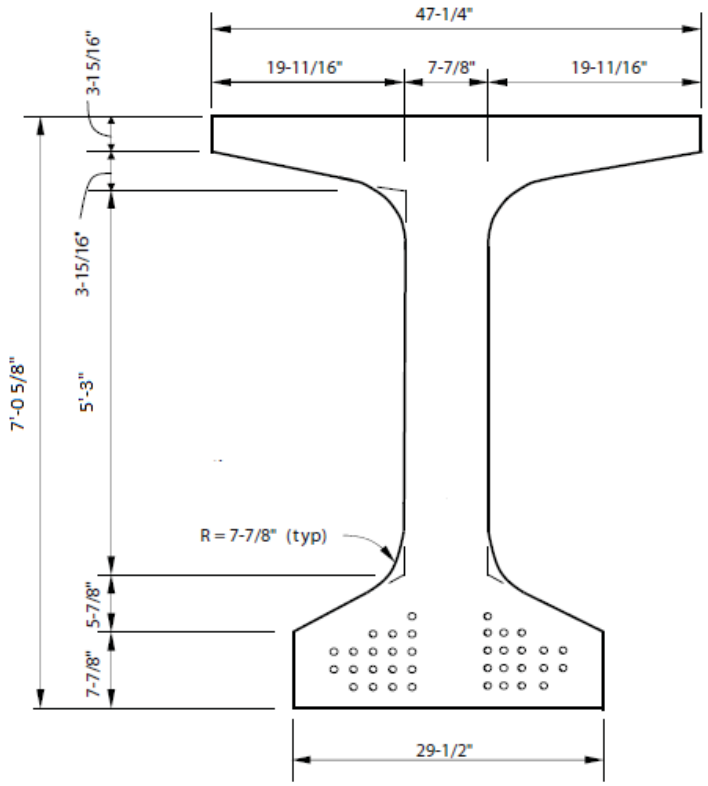

Equation 3.3:

$$M_{neg} = A_s f_y \left(d - \frac{a}{2}\right)$$

M_{neg} = Negative design moment

A_s = Area of steel

f_y = yield strength of steel

d = depth from center of deck steel to bottom of girder

a = depth of compressive block

www.manaraa.com

$$7150 * 12\frac{in}{ft} = A_s * 66\ ksi * \left(88.625 - \frac{a}{2}\right)$$

$$85800 = A_s * 66\ ksi * \left(88.625 - \frac{a}{2}\right)$$

$$A_s = \frac{85800}{66\ ksi * \left(88.625 - \frac{a}{2}\right)}$$

Equation 3.4:

$$A_s f_y = 0.85 f'_c a b_f$$

f'_c = compressive strength of concrete

b_f = width of lower flange

$$A_s * 66\ ksi = 0.85 * 4\ ksi * a * 29.5$$

$$A_s * 66\ ksi = 100.3$$

$$A_s = 1.52a$$

Set Equations 3.3 and 3.4 equal to each other and solve:

$$1.52a = \frac{85800}{66\ ksi * \left(88.625 - \frac{a}{2}\right)}$$

Solved using online solver:

$$A_s = 15.56 \text{ in.}^2$$

a = 10.24 in

Extended strand equations:

Centroid of strands is located 4 inches from bottom of girder. The effective girder width was calculated based using the same distribution factor of 0.24 with a total deck with of 34.5 feet.

Derivation of Equation 3.5:

$$M_{tot} = A_s f_{ys} \left(d_s - \frac{a}{2}\right)$$

M_{tot} = total positive moment

f_{ys} = yield strength of strand

A_s = area of prestressing strands

d_s = depth from top of deck to centroid of strands

www.manaraa.com

a = depth of compression block

$$M_{tot} = M_{pos} - M_{DA}$$

M_{pos} = positive design moment

M_{DA} = moment resistance of dowel action

$$A_s = N_s * A_{strand}$$

N_s = number of strands

A_{strand} = area of a single 0.6 in. diameter prestressing strand

$$M_{pos} - M_{DA} = N_s * A_{strand} * f_{ys} * (d_s - \frac{a}{2})$$

$$N_s = (M_{pos} - M_{DA})/(f_{ys} * A_{strand} * (d_s - \frac{a}{2}))$$

Equation 3.6:

$$a = \frac{A_s f_{ys}}{0.85 * f'_c * b_d}$$

b_d = effective width of deck

$$a = \frac{N_s * A_{strand} * f_{ys}}{0.85\, f'_c b_d}$$

$$N_s = \frac{0.85\, f'_c b_d * a}{A_{strand} * f_{ys}}$$

Solution of equations:

$$\frac{0.85 * 4\ ksi * 100\ in.* a}{0.217 * 230} = ((3065 - 1280) * 12\ in./ft)/(230\ ksi * 0.217\ in.^2 * (88.625 - (a/2))$$

$$6.812a = 21402/(49.91 * (88.625 - \frac{a}{2}))$$

Solved using online solver:

a = 0.714

Ns = 5 strands

www.manaraa.com

APPENDIX B - TEST UNIT DRAWINGS

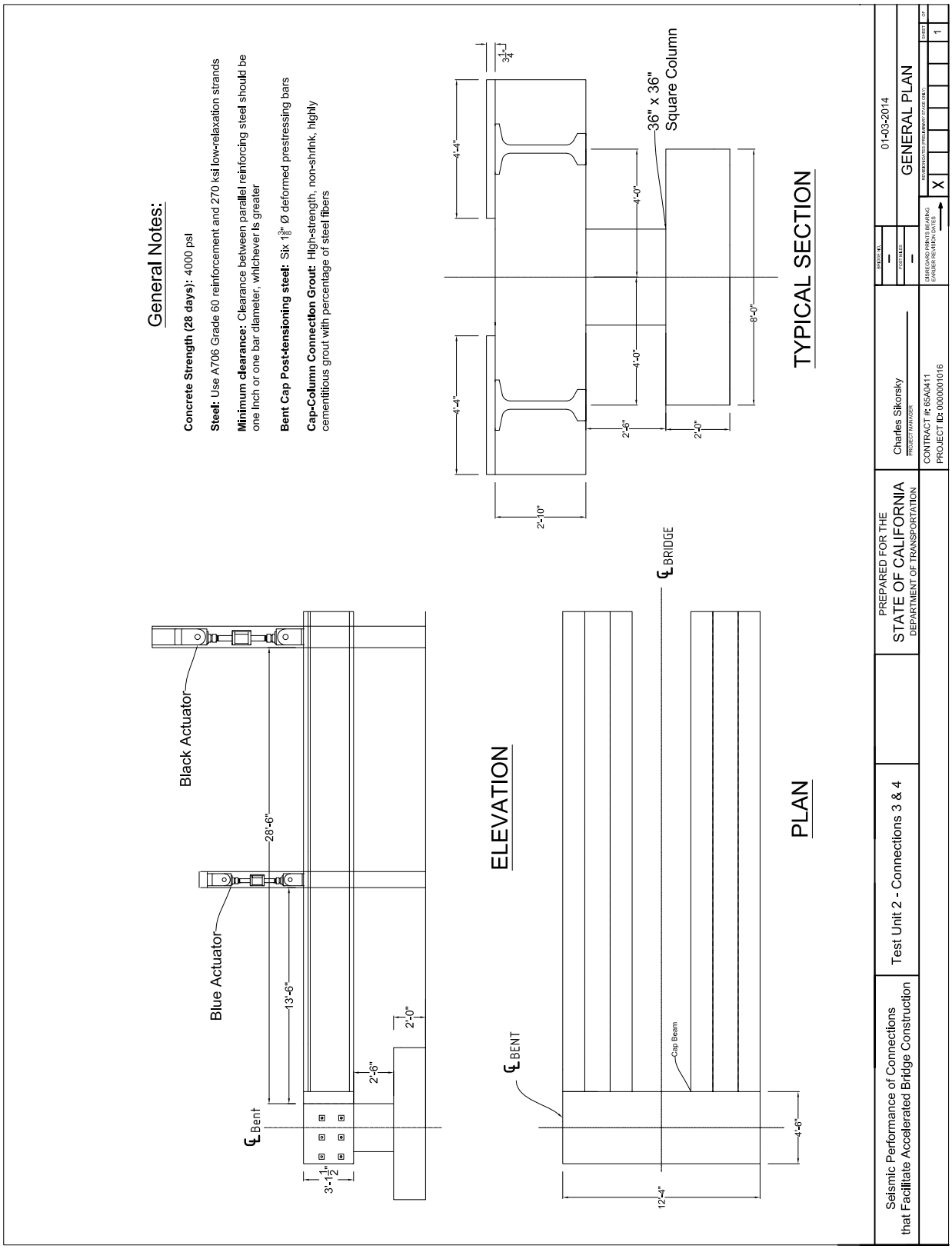

www.manaraa.com

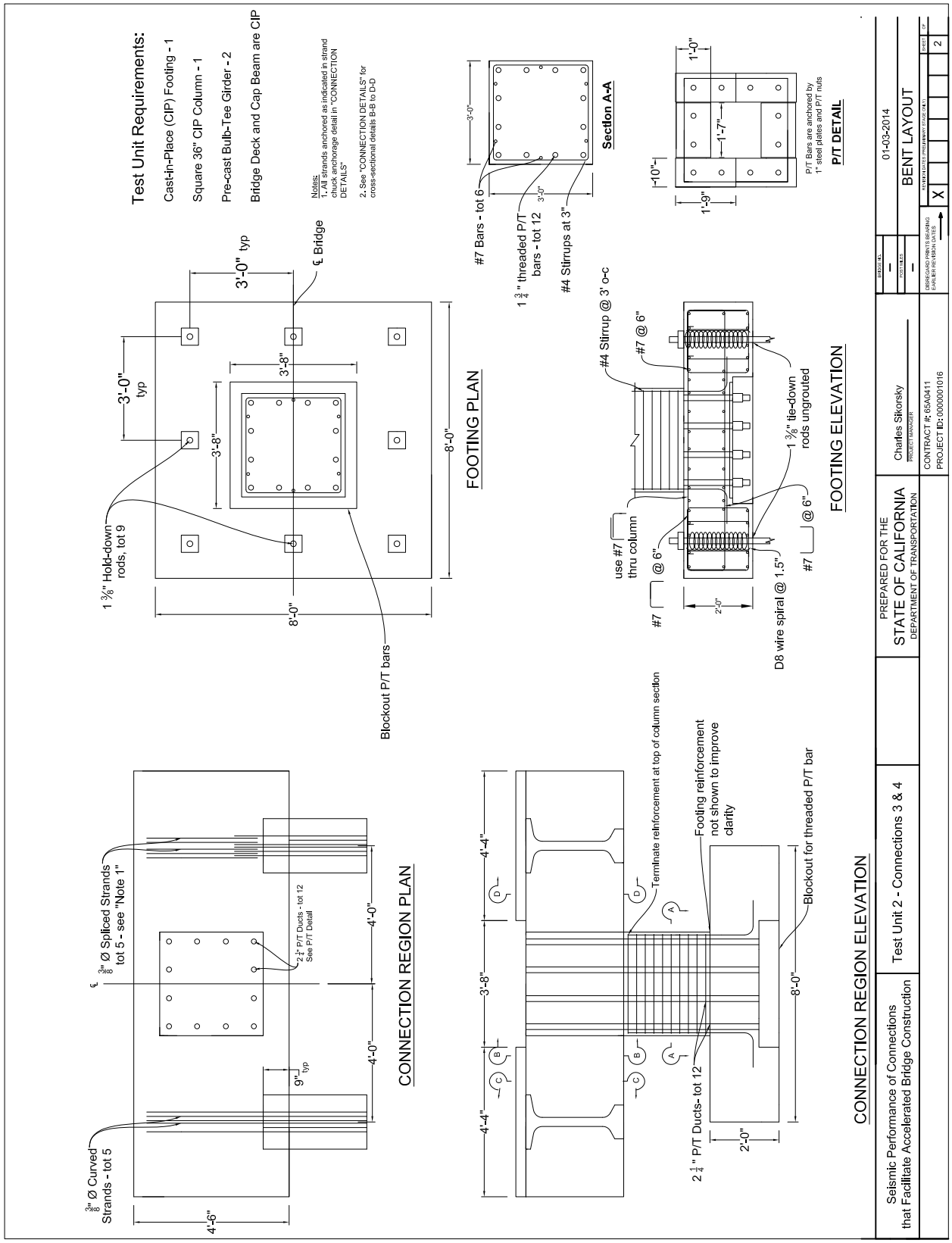

www.manaraa.com

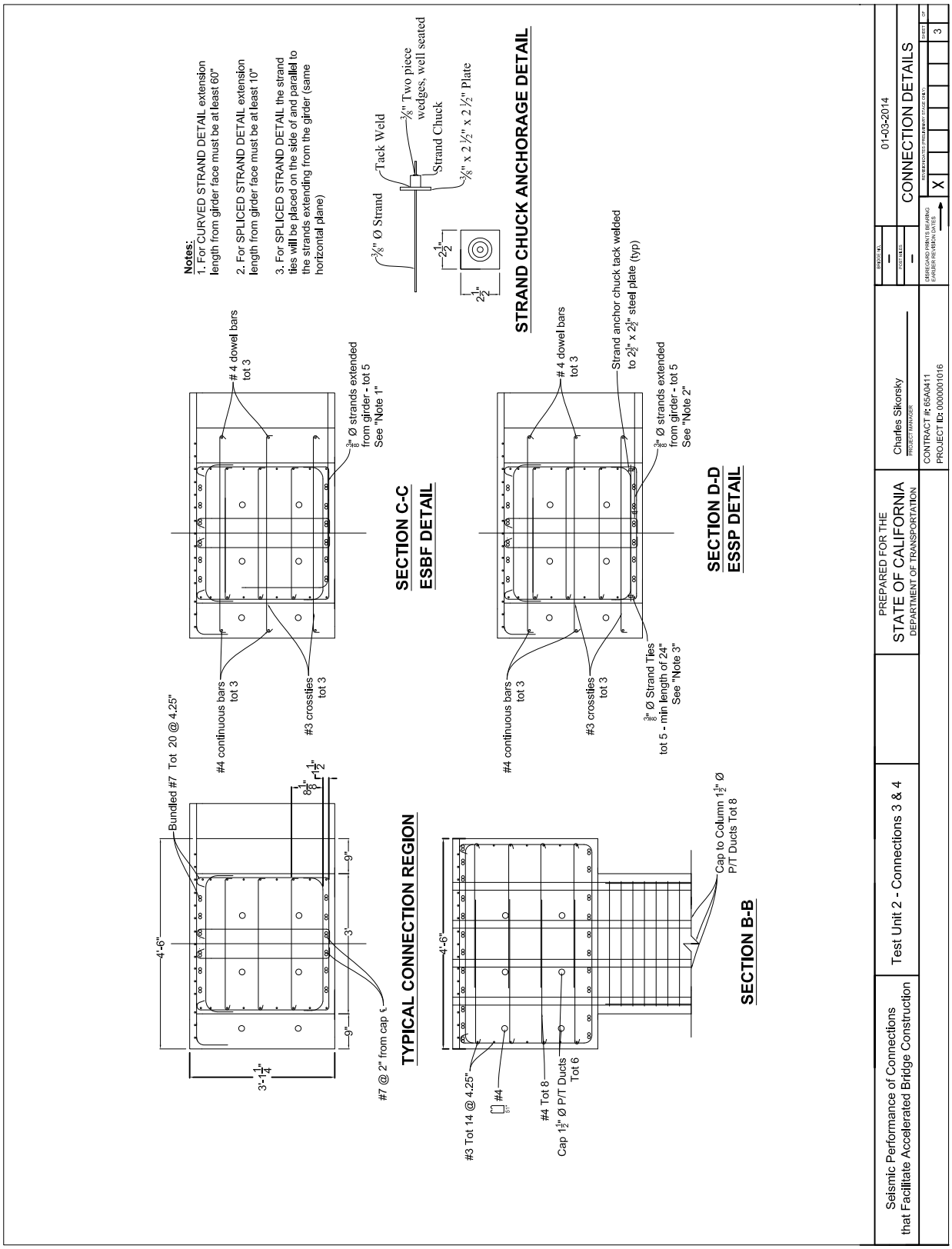

www.manaraa.com

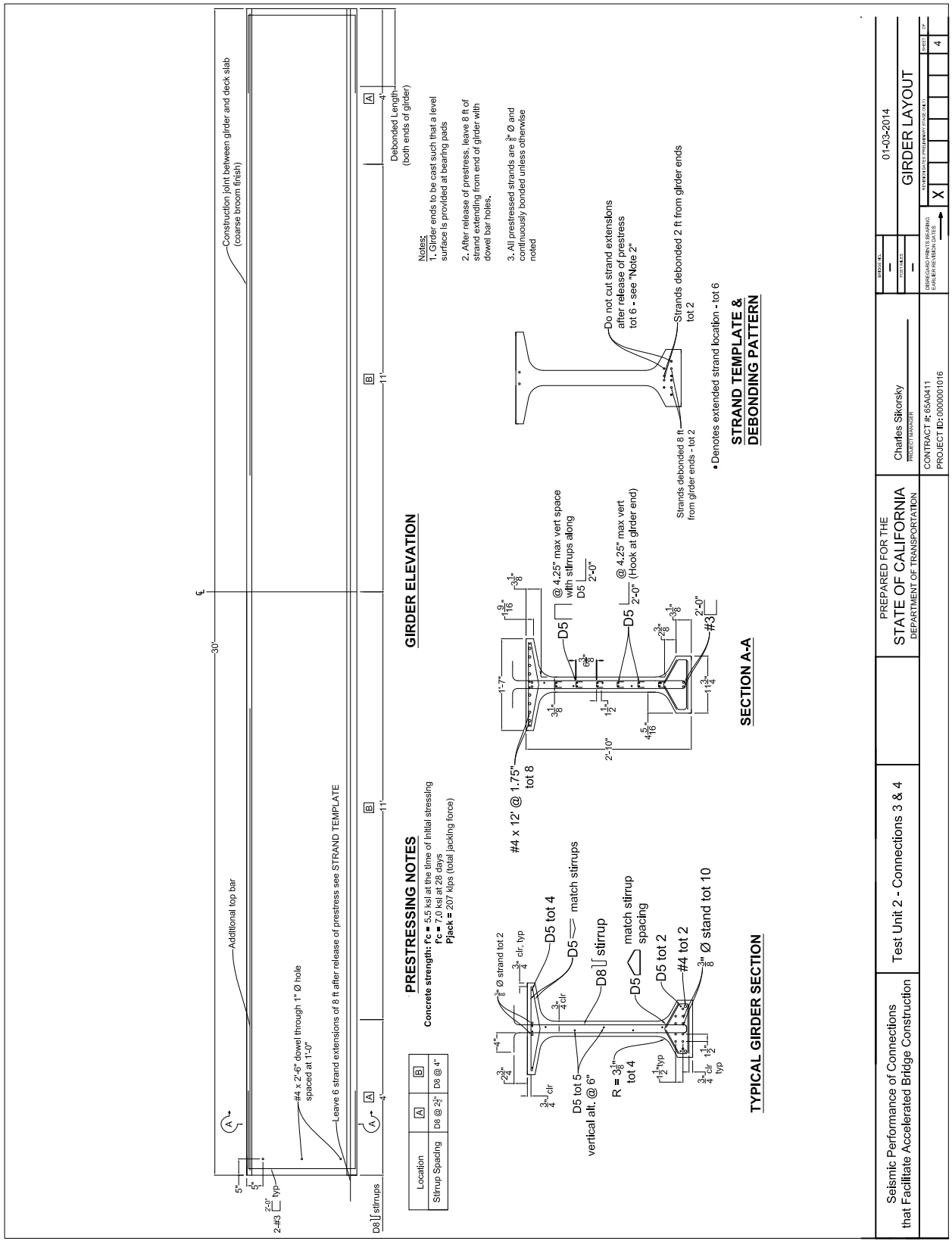

www.manaraa.com

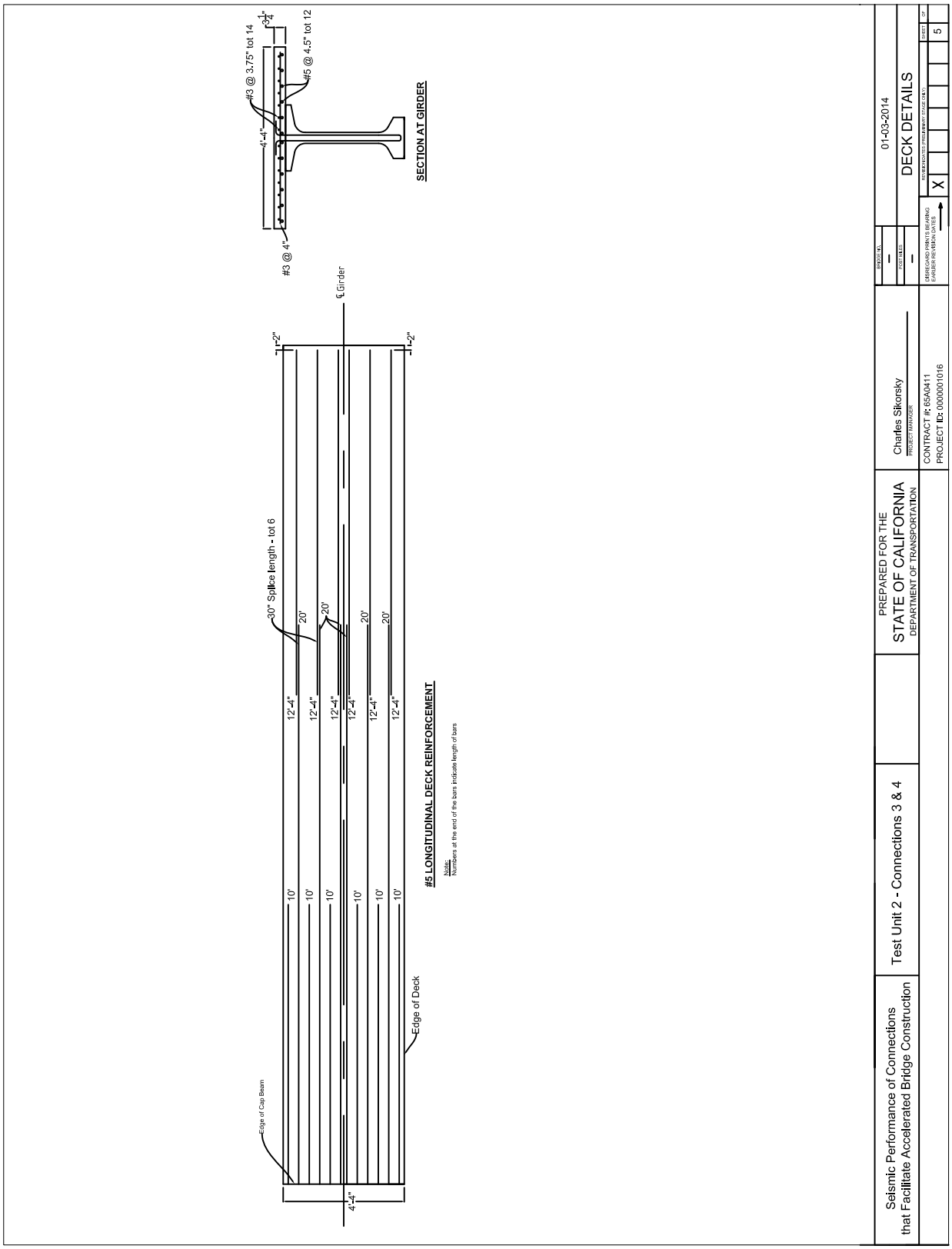

www.manaraa.com

APPENDIX C – LOADING PROTOCOLS

Original Loading Protocol – Force Control

	Force (kips)				
Cycle	Blue Actuator	Black Actuator	Stage	Moment	Shear
0	0	0	0		
1	-2.0	-5.0		3.45	-4.07
	0.0	-4.1		-49.2	-7
	12.3	-8.3		-95.55	-15.07
	22.4	-12.4		-115.05	-21.07
	32.5	-16.5	Gravity	-134.55	-27.07
2	32.5	-14.70			
	32.95	-18.20			
3	32.5	-14.70			
	32.95	-18.20			
4	32.5	-14.70		-185.85	-28.87
	32.95	-18.20		-92.18	-25.82
5	32.5	-12.90			
	33.4	-19.90			
6	32.5	-12.90			
	33.4	-19.90			
7	32.5	-12.90		-237.15	-30.67
	33.4	-19.90		-49.8	-32.5
8	32.5	-11.10			
	33.85	-21.60			
9	32.5	-11.10			
	33.85	-21.60			
10	32.5	-11.10		-288.45	-32.47
	33.85	-21.60		-7.425	-23.32
11	32.5	-9.3			
	34.3	-22.3			
12	32.5	-9.3			
	34.3	-22.3			
13	32.5	-9.3		-339.75	-34.27
	34.3	-23.3	Ultimate (Δμ = 10)	34.95	-22.07
14	36.9	-10.2			
	30.4	-22.7			
15	36.9	-10.2			
	30.4	-22.7			
16	36.9	-10.2		-373.5	-37.77
	30.4	-22.7		70.5	-18.77
17	41.3	-11.2			
	26.6	-22.2			

www.manaraa.com

	Force (kips)				
Cycle	Blue Actuator	Black Actuator	Stage	Moment	Shear
18	41.3	-11.2			
	26.6	-22.2			
19	41.3	-11.2		-404.4	-41.17
	26.6	-22.2		107.55	-15.47
20	45.6	-12.1			
	22.7	-21.6			
21	45.6	-12.1			
	22.7	-21.6			
22	45.6	-12.1		-436.8	-44.57
	22.7	-21.6		143.1	-12.17
23	50.0	-13.0			
	18.8	-21.0			
24	50.0	-13.0			
	18.8	-21.0			
25	50.0	-13.0		-470.55	-48.07
	18.8	-21.0	0.5 g	178.65	-8.87
26	-2.0	-5.0			
	0.0	-4.1			
	12.3	-8.3			
	22.4	-12.4			
	32.5	-16.5	Gravity		
27	50.0	-13.0			
	18.8	-21.0			
28	50.0	-13.0			
	18.8	-21.0			
29	50.0	-13.0		-470.55	-48.07
	18.8	-21.0	0.5 g	178.65	-8.87
30	53.4	-13.65			
	14.94	-20.1			
31	53.4	-13.65			
	14.94	-20.1			
32	53.4	-13.65		-497.93	-50.82
	14.94	-20.1		205.11	-5.91
33	56.8	-14.3			
	11.08	-19.2			
34	56.8	-14.3			
	11.08	-19.2			
35	56.8	-14.3		-525.3	-53.57
	11.08	-19.2		231.57	-2.95

المنارة للاستشارات
www.manaraa.com

	Force (kips)				
Cycle	Blue Actuator	Black Actuator	Stage	Moment	Shear
36	60.2	-14.95			
	7.22	-18.3			
37	60.2	-14.95			
	7.22	-18.3			
38	60.2	-14.95		-552.68	-56.32
	7.22	-18.3		258.08	0.01
39	63.6	-15.6			
	3.36	-17.4			
40	63.6	-15.6			
	3.36	-17.4			
41	63.6	-15.6		-580.05	-59.07
	3.36	-17.4		284.49	2.97
42	67	-16.25			
	-0.5	-16.5			
43	67 -0.5	-16.25 -16.5			
44	67	-16.25		-607.43	-61.82
	-0.5	-16.5	1.0 g	310.95	5.93

www.manaraa.com

Original Loading Protocol – Displacement Control

	Force (k)	Disp (in)	
	Blue Actuator	Black Actuator	
Force	-2	-5	
Control	32.5	-16.5	
Disp	10	0.5	
Control	-5	-0.25	
	20	1	
	-10	-0.5	
	30	1.5	
	-15	-0.75	
	40	2	D1
	-22	-1	
	40	2	
	-22	-1	
	40	2	
	-22	-1	
	40	3	D2
	-22	-1.5	
	40	3	
	-22	-1.5	
	40	3	
	-22	-1.5	
	40	4	D3
	-22	-2	
	40	4	
	-22	-2	
	40	4	
	-22	-2	
	40	6	D4
	-22	-3	
	40	6	
	-22	-3	
	40	6	
	-22	-3	

www.manaraa.com

	Force (k)	Disp (in)	
	Blue Actuator	Black Actuator	
	40	9	D5
	-22	-4.5	
	40	9	
	-22	-4.5	
	40	9	
	-22	-4.5	
	40	12	D6
	-22	-6	
	40	12	
	-22	-6	
	40	12	
	-22	-6	
	40	15	D7
	-22	-7.5	
	40	15	
	-22	-7.5	
	40	15	
	-22	-7.5	

www.manaraa.com

Corrected Loading Protocol – Force Control

	Force (kips)				
Cycle	Blue Actuator	Black Actuator	Stage	Moment	Shear
0	0	0	0		
1	-2.0	-5.0		3.45	-4.07
	0.0	-4.1		-38.1	-6.88
	12.3	-8.3		-76.2	-13.75
	22.4	-12.4		-114.3	-20.63
	32.5	-16.5	Gravity	-152.4	-27.5
2	32.5	-14.70			
	32.95	-18.20			
3	32.5	-14.70			
	32.95	-18.20			
4	32.5	-14.70		-192.73	-28.825
	32.95	-18.20		-119.98	-26.4
5	32.5	-12.90			
	33.4	-19.90			
6	32.5	-12.90			
	33.4	-19.90			
7	32.5	-12.90		-233.05	-30.15
	33.4	-19.90		-87.55	-25.3
8	32.5	-11.10			
	33.85	-21.60			
9	32.5	-11.10			
	33.85	-21.60			
10	32.5	-11.10		-273.375	-31.475
	33.85	-21.60		-55.125	-24.2
11	32.5	-9.3			
	34.3	-22.3			
12	32.5	-9.3			
	34.3	-22.3			
13	32.5	-9.3		-313.7	-32.8
	34.3	-23.3	Ultimate (Δμ = 10)	-22.7	-23.1
14	36.9	-10.2			
	30.4	-22.7			
15	36.9	-10.2			
	30.4	-22.7			
16	36.9	-10.2		-363.05	-36.25
	30.4	-22.7		27.23	-19.65
17	41.3	-11.2			
	26.6	-22.2			

www.manaraa.com

	Force (kips)				
Cycle	Blue Actuator	Black Actuator	Stage	Moment	Shear
18	41.3	-11.2			
	26.6	-22.2			
19	41.3	-11.2		-412.4	-39.7
	26.6	-22.2		77.15	-16.2
20	45.6	-12.1			
	22.7	-21.6			
21	45.6	-12.1			
	22.7	-21.6			
22	45.6	-12.1		-461.75	-43.15
	22.7	-21.6		127.075	-12.75
23	50.0	-13.0			
	18.8	-21.0			
24	50.0	-13.0			
	18.8	-21.0			
25	50.0	-13.0		-511.1	-46.6
	18.8	-21.0	0.5 g	177	-9.3
26	-2.0	-5.0			
	0.0	-4.1			
	12.3	-8.3			
	22.4	-12.4			
	32.5	-16.5	Gravity		
27	50.0	-13.0			
	18.8	-21.0			
28	50.0	-13.0			
	18.8	-21.0			
29	50.0	-13.0		-511.1	-46.6
	18.8	-21.0	0.5 g	177	-9.3
30	53.4	-13.65			
	14.94	-20.1			
31	53.4	-13.65			
	14.94	-20.1			
32	53.4	-13.65		-550.58	-49.34
	14.94	-20.1		216.48	-6.56
33	56.8	-14.3			
	11.08	-19.2			
34	56.8	-14.3			
	11.08	-19.2			
35	56.8	-14.3		-590.06	-52.08
	11.08	-19.2		255.95	-3.82

www.manaraa.com

	Force (kips)				
Cycle	Blue Actuator	Black Actuator	Stage	Moment	Shear
36	60.2	-14.95			
	7.22	-18.3			
37	60.2	-14.95			
	7.22	-18.3			
38	60.2	-14.95		-629.54	-54.82
	7.22	-18.3		295.44	-1.08
39	63.6	-15.6			
	3.36	-17.4			
40	63.6	-15.6			
	3.36	-17.4			
41	63.6	-15.6		-669.02	-57.56
	3.36	-17.4		334.92	1.66
42	67	-16.25			
	-0.5	-16.5			
43	67 -0.5	-16.25 -16.5			
44	67	-16.25		-708.5	-60.3
	-0.5	-16.5	1.0 g	374.4	4.4

*Note: The displacement loading protocol did not require correction

Comparison of loading protocols:

	Negative Moment (k-ft)		Negative Shear (kips)		Positive Moment (k-ft)		Positive Shear (kips)	
	Tested	Adjusted	Tested	Adjusted	Tested	Adjusted	Tested	Adjusted
Gravity	-134.55	-152.4	-27.07	-27.5	-	-	-	-
H+G	-339.75	-313.7	-34.27	-32.8	34.95	-20.4	-22.07	-23.1
H+G+0.5gV	-470.55	-511.1	-48.07	-46.6	178.65	177	-8.87	-9.3
H+G+1.0gV	-607.43	-708.5	-61.82	-60.3	310.95	374.4	5.93	4.4

www.manaraa.com